



The effects of mechanical stretch on the immunological and anti-inflammatory properties of skeletal muscle cells: An *in vitro* study of potential mechanisms that affect response to exercise therapy

Thesis submitted for the degree of

Doctor of Philosophy

at the University of Leicester

by

Ziyad Mohammed Aldosari

Department of Infection, Immunity and Inflammation

College of Life Sciences

School of Medicine

University of Leicester

2020

The effects of mechanical stretch on the immunological and anti-inflammatory properties of skeletal muscle cells: An *in vitro* study of potential mechanisms that affect response to exercise therapy

Ziyad Mohammed Aldosari

Abstract

The contraction of skeletal muscle during exercise that occurs in the absence of muscle damage has been demonstrated to yield a significant increase in the release of potentially anti-inflammatory myokine interleukin-6 (IL-6). Increased generation of IL-6 may be valuable in managing inflammatory states, such as chronic kidney disease (CKD). However, the IL-6 output of CKD patients during muscular exercise may be unusually weak, due to factors such as metabolic acidosis.

In CKD, physical exertion has been reported to lower levels of amino acids in muscles *in vivo*. This effect may be attributable to uraemic metabolic acidosis and exercise-induced acidosis impairing mitogen-activated protein kinases (MAPKs) such as p38, which normally activate the amino acid transporter SNAT2. The SNAT2 transporter protein is also known to be directly and rapidly inhibited by low pH. The resulting intracellular amino acid depletion could, in turn, result in inhibited protein synthesis, and hence reduced production of IL-6.

This study sought to test the following hypotheses: (1) higher levels of IL-6 expression occur in mechanically stressed skeletal muscle cells following *in vitro* mechanical stretch, arising from the activation of MAPKs, followed by activation of SNAT2; and (2) low pH blocks this process.

Experiments on L6 rat skeletal muscle cells showed that drug inhibition of MAPKs inhibited SNAT2 transport activity, confirming that MAPKs play a role in the regulation of SNAT2 and, by extension, in the availability of amino acids for protein synthesis.

Interestingly, while P-p38 and P-JNK activation significantly increased after cyclic stretching of 1-10 minutes duration, SNAT2 activity significantly increased only transiently i.e. after periods of stretching lasting 1 minute, suggesting that this transporter may paradoxically be inhibited by prolonged stretching. In addition, mRNA of IL-6 was increased after 30 minutes of intermittent stretching and, (as previously reported elsewhere) by 6 hours of Ca²⁺ loading of the cells with ionomycin which activates p38.

The siRNA silencing of SNAT2 in L6 myoblasts decreased gene expression of the mRNA of IL-6, suggesting that SNAT2 can influence IL-6 expression. As SNAT2 and MAPKs, particularly p38 and JNK, are inhibited at low pH, it would be predicted that low pH (pH 7.1) would decrease IL-6 expression. However, both with and without ionomycin, low pH failed to decrease IL-6 mRNA; indeed with ionomycin low pH strongly activated IL-6 expression.

It is concluded that even though the acidosis-sensing amino acid transporter SNAT2 may play some role in regulating IL-6 expression (as previously hypothesised), a distinct and novel stimulatory effect of low pH over-rides this and maybe a more important regulator of IL-6 expression in L6 skeletal muscle cells.

Acknowledgments

I would like to express my profound appreciation to my supervisors, Dr Alan Bevington and Dr Emma Watson, for their help and support throughout the entirety of my PhD. My sincere thanks to Dr Bevington for his encouragement and constant support. It was a pleasure and an honour to be mentored by such a remarkable scientist. Dr Watson has always been available to provide support and useful insights, for which I am eternally grateful. I would also like to express my gratitude to the members of my progress review panel, Professor Jonathan Barratt and Professor James Burton, for their invaluable advice and guidance in our annual meetings.

I would like extend my gratitude and heartfelt appreciation to Mr Jeremy Brown for his assistance during my PhD. When I started my PhD, he trained me in the techniques that I used in early experiments and he was very cooperative and extremely helpful. My sincere thanks to Dr Nima Abbasian and Dr Ravinder Chana for assistance with the mycoplasma screening testing of L6 cells. I would like to thank Professor Gary Willars and Mr Heider Qassam for their support, their assistance with the calcium experiments, and for graciously allowing access to their lab equipment. My thanks to Dr Jonathon Willets for his help and for giving access to his Flexercell Strain Unit (FX-4000) machine for the purpose of stretching L6 cells. My profound thanks also to Dr Alan Bevington for his help with the experiments presented in Figures 3.6, 3.1B and 3.2B. My sincere gratitude to BSc project student Mr Toramaru Sugawara who performed (under my supervision) the 5 minute stretching experiments that contributed to the data displayed in Figures 4.3A, 4.5A and 4.6.

Very special thanks to the people in the renal lab for all of their help and support, and for helping to create a positive, healthy environment inside the lab: Safia Balbas, Violeta Diez Beltran, Abdullah Alruwaili, Douglas Gould, Tom O'Sullivan, Patricia Higgins, Katherine Robinson, Soteris Xenophontos, and Luke Baker.

I would like to thank Shaqra University for supporting my studies in the UK.

I would like to take this opportunity to thank all my family members and friends for their support. I would like to thank my mother and father for their unceasing help and for providing enormous and invaluable emotional support.

I would like to express my deepest gratitude towards my children, Rawan, Mohammed and Deena, for their emotional support, for making me happy and for being my sanctuary every time I returned home from the lab.

Finally, I wish to express my deepest thanks to my wife, Rana, for her encouragement and unending support along every step of the way. I could not have completed this PhD without her.

Table of contents

Abstract.....	i
Acknowledgments.....	iii
Table of contents	iv
List of figures.....	viii
List of tables	x
List of abbreviations.....	xi
Chapter 1 General introduction.....	1
1.1 Overview	1
1.2 Protein energy wasting	2
1.3 Physical exercise and chronic inflammation	3
1.4 Effect of exercise training on chronic inflammation.....	6
1.5 Direct evidence for anti-inflammatory effects of physical exercise	6
1.6 Skeletal muscle as an endocrine organ.....	7
1.7 The biosynthesis of IL-6.....	9
1.7.1 Transcriptional regulation of IL-6.....	9
1.7.2 Protein synthesis.....	10
1.8 Mammalian target of rapamycin (mTOR)	12
1.9 The SNAT2 amino acid transporter	14
1.10 Mechanotransduction.....	17
1.11 The effect of mechanical stress on MAP kinases and System A / SNAT2	22
1.12 Mitogen-activated protein kinases (MAPKs)	22
1.12.1 ERKs.....	23
1.12.2 JNKs.....	23
1.12.3 p38 isoforms	24
1.13 <i>In vitro</i> cell stretching.....	25
1.14 The choice of the <i>in vitro</i> model of skeletal muscle used in this project.....	28
1.15 Hypothesis.....	29
Chapter 2: Materials and Methods.....	32
2.1 General materials and reagents.....	32
2.2 Cell culture models	32
2.2.1 L6 cells.....	32
2.2.2 Screening cultures for mycoplasma contamination	32
2.2.3 L6-cells, maintenance and passaging.....	33

2.2.4 Preparing L6 myoblasts for experiments	34
2.2.5 L6-myotube formation	34
2.3 Passive continuous stretch technique	35
2.4 Cyclic stretch by vacuum suction – the “pull” technique	36
2.5 Cyclic stretch by motor-driven pistons – the “push” technique	38
2.6 Medium for experimental incubations	40
2.7 Protein assays	41
2.7.1 Lowry Protein Assay	41
2.7.2 Bio-Rad detergent-compatible (DC) protein assay	41
2.8 Enzyme-linked Immunosorbent assay (ELISA) for IL-6	42
2.9 Creatine phosphokinase activity	42
2.10 Transport activity assay (¹⁴ C MeAIB uptake measurement)	43
2.10.1 Preparation of cell lysates for counting the radio-activity	44
2.11 Measuring ¹⁴ C-urea as an intracellular water space marker	44
2.12 Sodium Dodecyl Sulphate Polyacrylamide Gel Electrophoresis (SDS-PAGE)	45
2.12.1 Preparing the samples for SDS-PAGE	45
2.12.2 Running the gel	45
2.12.3 Immunoblotting	45
2.12.4 Quantification and data analysis	46
2.13 RNA techniques	48
2.13.1 RNA extraction	48
2.13.2 Reverse transcription	48
2.13.3 Real time qPCR for detailed studies of IL6 and SNAT2 mRNA expression using Taqman assays	50
2.13.4 SNAT2 silencing in L6 myoblasts with small interfering RNAs (siRNAs)	51
2.14 Measurement of intracellular Ca ²⁺ using Fluo-4 fluorescence	52
2.15 Statistical analysis	53
Chapter 3 Regulation of MAPK activation in L6 cells	54
3.1 Introduction	54
3.2 Results	55
3.2.1 Dependence of System A / SNAT2 transporter activity in L6-G8C5 cells on MAP kinase activity	55
3.2.2 The effect of low pH on MAPKs in L6 Myotubes	58
3.2.3 The role of JNK in the inhibition of System A by low pH	61
3.2.4 The role of cell swelling	62

3.2.5 The acute effect of cyclic stretching on the phosphorylation of MAPKs in L6-G8C5 myotubes	64
3.3 Discussion.....	68
3.3.1 Inhibition of MAP kinases inhibits System A / SNAT2 activity in L6-G8C5 myotubes.....	68
3.3.2 pH sensitivity of MAP kinases	68
3.3.3 Sensing of pH by MAP kinases	69
3.4 Conclusion	70
Chapter 4 Characterisation of experimental systems for studying mechanical stretch effects on System A in L6 cells	72
4.1 Introduction	72
4.2 Results	73
4.2.1 Positive control for MAPK response in stretched cells	73
4.2.2 Monitoring of pH drift.....	75
4.2.3 Effect of continuous stretching of L6-G8C5 myotubes on System A (SNAT2) amino acid transport activity.....	75
4.2.4 The effect of cyclic stretch on the activity of System A (SNAT2) on L6-G8C5 myotubes	76
4.2.5 The effect of cyclic stretch on the activity of System A (SNAT2) in L6 myoblasts	78
4.3 Discussion.....	81
4.3.1. The effect of stretch on System A (SNAT2) transporters.....	81
4.3.2. Technical artifacts	81
4.3.4. Rapid inactivation of the effect of stretch on System A (SNAT2) transport	82
4.3.5. Implications of this negative result.....	83
Chapter 5 Regulation of expression of Interleukin-6 (IL-6) in L6 cells	84
5.1 Introduction	84
5.2 Results	85
5.2.1 The effect of stimulation with ionomycin and p38 MAP kinase inhibition on IL-6 gene expression in L6-G8C5 myotubes.....	85
5.2.2 The effect of low pH on IL-6 mRNA and protein expression in L6-G8C5 myotubes	86
5.2.3 The effect of p38 inhibitor, JNK inhibitor and MeAIB on the stimulatory effect of ionomycin on IL-6 gene expression in L6-G8C5 myotubes	88
5.2.4 The effect of low pH with JNK inhibitor and MeAIB on the stimulation by ionomycin of IL-6 gene expression in L6-G8C5 myotubes.....	90
5.2.5 Measurement of intracellular Ca ²⁺	91
5.2.6 The effect of siRNA silencing of SNAT2 on the stimulation of IL-6 gene expression in L6-G8C5 myoblasts	93
5.2.7 A revised model for regulation of IL-6 expression	95
5.2.8 The effect of short periods of cyclic stretching on IL-6 mRNA expression in L6-G8C5 myotubes	96

5.2.9 The effect of blockade of Focal Adhesion Kinase (FAK) with selective inhibitor (PF-573228) and p38 inhibitor (SB202190) on the effect of mechanical stretch on IL-6 expression in L6-G8C5 myotubes	99
5.3 Discussion.....	102
5.3.1 Ionomycin or cyclic stretch increase expression of IL-6 mRNA but not IL-6 protein	102
5.3.2 Low pH exerts an unexpected stimulatory effect on ionomycin-induced IL-6 mRNA expression	102
5.3.3 Coupling between System A/SNAT2 and IL-6 expression	103
5.3.4 A revised model for regulation of IL-6 expression in L6G8-C5 myotubes	104
5.3.5 Conclusion from the experimental work	105
Chapter 6 General Discussion and Future Work.....	106
6.1 General discussion	106
6.1.1 The physiological significance of the findings in this thesis.....	106
6.1.2 The complex relationships between MAPKs, SNAT2, IL-6 and pH.....	108
6.1.3 The physiological significance of System A/SNAT2 during exercise	109
6.1.4 The role of ionomycin in IL-6 expression <i>in vitro</i>	109
6.2 Future work.....	110
6.2 Conclusion	112
Appendixes.....	113
References	123

List of figures

Figure 1.1. The effect of IL-6 from contracting muscle in different organs.....	4
Figure 1.2. Schematic comparison of sepsis-induced verses exercise-induced increases in circulating cytokines in plasma.....	5
Figure 1.3. Schematic representation of the promoter region of the human interleukin-6 (IL-6) gene showing possible cis-regulatory elements.....	9
Figure 1.5. Relationship between mTORC1 activation and muscle hypertrophy.....	14
Figure 1.7. Schematic diagram showing how SNAT2, mechanical stretch and MAPK activation may be linked, and impaired by low pH, in L6-G8C5 cells.....	31
Figure 2.1. PCR gel electrophoresis to screen for mycoplasma contamination in cultures of L6-G8C5 cells.....	33
Figure 2.2. Photographs of L6-G8C5 cells.....	34
Figure 2.3. The in vitro model of continuous mechanical stretch comprising.....	35
Figure 2.5. An illustration of the FX-4000 cell stretching system.....	37
Figure 3.1. The effect of pre-incubation with MAPK inhibitors on the activity of System A transporters in L6-G8C5 myotubes.....	56
Figure 3.2. The acute effect of MAPK inhibitors on the activity of System A transporters in L6-G8C5 myotubes.....	57
Figure 3.3. The effect of different pH media on p-JNK in L6-G8C5 myotubes.....	59
Figure 3.4. The effect of different pH media on p-p38 in L6-G8C5 myotubes.....	60
Figure 3.5. The effect of different pH media on p-ERK-1 in L6-G8C5 myotubes.....	61
Figure 3.7. Effect of 1 min or 5 min or 10 min of cyclic stretch on P-p38 activity.....	65
Figure 3.8. Effect of 10 min of cyclic stretch on P-JNK activity.....	66
Figure 3.9. Effect of 10 min of cyclic stretch on p-ERK-1/2 activity.....	67
Figure 4.1. Effect of 5 minutes of cyclic stretch on p-p38 activity.....	74
Figure 4.2. Images showing stable phenol red colour following 5 minutes of cyclic stretching in the culture incubator.....	75
Figure 4.3. Time course of the effect of passive continuous stretch on System A (SNAT2) transporter activity in L6-G8C5 myotubes.....	76
Figure 4.4. Time course of the effect of vacuum-induced cyclic stretch on System A (SNAT2) transport activity in L6-G8C5 myotubes.....	77
Figure 4.5. Time course of the effect of cyclic stretch induced by mechanical pushing on System A (SNAT2) transport activity in L6-G8C5 myotubes.....	78
Figure 4.6. Time course of the effect of vacuum-induced cyclic stretch on System A (SNAT2) transport activity in L6-G8C5 myoblasts.....	79
Figure 4.7. Effect of 1 hour of cyclic vacuum-induced stretch and 1 hour of post-stretch incubation on System A (SNAT2) transport activity in L6-G8C5 myoblasts.....	80
Figure 5.1. The effect of ionomycin and p38 MAP kinase inhibition on IL-6 gene expression in L6-G8C5 myotubes and myoblasts.....	86
Figure 5.2. The effect of low pH on the stimulation by ionomycin of IL-6 gene expression in L6-G8C5 myotubes.....	87
Figure 5.3. The effect of low pH and of ionomycin on IL-6 protein secretion in L6-G8C5 myotubes.....	88
Figure 5.4. The effect of JNK inhibition and MeAIB on the stimulation by ionomycin of IL-6 gene expression in L6-G8C5 myotubes.....	89
Figure 5.5. The effect of JNK inhibition and MeAIB on the stimulatory effect of low pH and ionomycin on IL-6 gene expression in L6-G8C5 myotubes.....	90

Figure 5.6. The effect of pH and MeAIB with or without ionomycin on intracellular calcium levels of L6 myoblasts.	92
Figure 5.7. Testing the effect of anti-SNAT2 siRNA reagent on SNAT2 mRNA expression.	94
Figure 5.8. Effect SNAT2 silencing on the expression of IL-6 mRNA in absence of ionomycin.....	95
Figure 5.9. Effect of 30 minutes of cyclic stretch on the expression of IL-6 mRNA.	97
Figure 5.10. Effect of 30 minutes of cyclic stretch on the secretion of IL-6 protein.....	98
Figure 5.11. The effect of 30 minutes of cyclic stretch on creatine phosphokinase (CPK) released into the medium from L6-G8C5 myotubes.	99
Figure 5.12. Testing the effectiveness of FAK inhibitor (PF-573228) on phosphorylation of phospho-FAK (Tyr576/577) in L6-G8C5 myotubes.....	100
Figure 5.13. The effect of blockade of Focal Adhesion Kinase (FAK) with selective inhibitor (PF-573228) and p38 inhibitor (SB202190) on the effect of mechanical stretch on IL-6 Expression in L6-G8C5 myotubes.....	101
Figure 5.14. Schematic diagram showing pathways investigated in this chapter that may contribute to increased IL-6 mRNA expression in L6-G8C5 cells.	104
Figure 6.1 The 2002 model proposed for the transcriptional regulation of IL-6 in skeletal muscle in Febbraio, MA and Pedersen, BK (Febbraio and Pedersen, 2002).....	106

List of tables

Table 2.1 Details of antibodies.....	47
Table 2.2 RT- Reaction	49
Table 2.3 Real time qPCR thermal cycle	50
Table 2.4. siRNA transfection mixture for L6 transfection.	52

List of abbreviations

IL-6	Interleukin-6
CKD	Chronic Kidney Disease
MAPKs	Mitogen-activated protein kinases
SNAT2	Sodium-coupled neutral amino acid transporter
PEW	Protein Energy Wasting
ESRD	End-Stage Renal Disease
GFR	Glomerular filtration rate
ATP	Adenosine triphosphate
PI3K	Phosphoinositide 3-kinase
IGF1	Insulin-like Growth Factor-1
ERK	Extracellular Signal-Regulated Kinase
JNK	c-Jun NH ₂ -terminal kinase
IRS-1	Insulin receptor substrate-1
AKT	Protein kinase B (PKB)
WHO	World Health Organization
CRP	C-reactive protein
IL-1	Interleukin-1
TNF- α	Tumor necrosis factor alpha
IL-1ra	IL-1 receptor antagonist
IL-10	Interleukin-10
CRF	Cardiorespiratory fitness
COPD	Chronic obstructive pulmonary disease
CVD	Cardiovascular disease
AMPK	AMP-activated protein kinase
4E-BP1	Eukaryotic translation initiation factor 4E binding protein 1
mTOR	Mechanistic or mammalian target of rapamycin
DFBS	Dialysed foetal bovine serum
DMEM	Dulbecco's Modified Eagle's Medium
DMSO	Dimethyl sulfoxide
HBS	Hepes Buffered Saline

HBSS	Hanks' Balanced Salt Solution
HIA-FBS	Heat inactivated foetal bovine serum
MeAIB	Methylaminoisobutyric acid
MEM	Minimum Essential Medium
PIP2	Phosphatidylinositol 4,5-Biphosphate
TSC	Tuberous sclerosis complex proteins
FAK	Focal adhesion kinase
EIMD	Exercise-induced muscle damage
ELISA	Enzyme-linked Immunosorbent assay
CPK	Creatine phosphokinase
PSS	Physiological Salt Solution

Chapter 1 General introduction

1.1 Overview

Chronic kidney disease (CKD) patients suffer from complications resulting from the defect in their kidney functions, one of which is metabolic acidosis, which arises as a result of the accumulation of acid in blood and tissue interstitial fluid, resulting in a low pH (Raphael, 2018). CKD, acidosis and their accompanying metabolic defects lead to a range of problems, including protein energy wasting (PEW) and cachexia (Wing et al., 2015), and chronic inflammation (Viana et al., 2014). This can lead to a very complicated condition in which different aspects of the immune response might be activated. CKD also results in a continuous state of chronic inflammation, resulting in increased risk of cardiovascular disease (CVD) (Descamps-Latscha et al., 2002) and protein energy wasting (PEW) (Wing et al., 2014, Deger et al., 2017). These disorders eventually increase the chance of morbidity and mortality among CKD patients (Block et al., 2004). There is a strong association in CKD with increased levels of C-reactive protein (CRP) and pro-inflammatory cytokines, mostly IL-6 whose level is dependent on the stimulation of TNF- α and IL-1, which reflect a pro-inflammatory state in CKD patients (Cheung et al., 2010). Most inflammatory conditions are characterised by increased levels of TNF- α , IL-6 and IL-1 (Scheller et al., 2011). Therefore, numerous investigations (Hauser et al., 2008, Kato et al., 2008, Yeo et al., 2010) have examined immunity dysfunction and the associated chronic inflammatory complications and PEW among CKD patients.

Multiple studies (Viana et al., 2014, Steensberg et al., 2002, Starkie et al., 2003) have shown that moderate exercise can exert beneficial effects on PEW/cachexia and on the immune system by producing anti-inflammatory cytokines that assist in the reduction of inflammation. IL-6 can be produced by muscle fibers through a TNF-independent pathway during exercise (Petersen and Pedersen, 2005b). It was seen that the levels of anti-inflammatory cytokines such as IL-10 and IL-1ra were increased following the acute increases in levels of IL-6 after prolonged running exercise (Ostrowski et al., 1998b). However, TNF- α production can be inhibited by strenuous exercise and IL-6 infusion in healthy individuals (Starkie et al., 2003). Therefore, IL-6 can play anti-inflammatory roles in the context of exercise, or inflammatory roles along with CRP, TNF- α and IL-1 in chronic inflammatory states such as CKD.

This thesis investigates, using a cultured skeletal muscle cell model *in vitro*, the regulation of the expression of a key cytokine expressed in muscle (interleukin 6 (IL-6)) which may play a central role in the anti-inflammatory and metabolic effects of exercise.

1.2 Protein energy wasting

The term ‘protein energy wasting’ (PEW) describes a dysfunctional metabolic state that is common in inflammatory conditions. PEW is characterised by profound depletion of energy reserves and the loss of protein mass in the body leading to cachexia (Wing et al., 2014, Deger et al., 2017). PEW typically has a profound impact on the quality of life of patients, resulting in limited mobility, increased frailty, and even psychological side effects. Unlike malnutrition, which occurs as a result of insufficient nutrient intake, PEW is a maladaptive metabolic state that cannot be treated effectively through nutritional supplementation. PEW occurs in patients with chronic kidney disease (CKD) and end-stage renal disease (ESRD), as well as in 20-70% of adults treated by dialysis. The prevalence of both inflammatory markers and PEW increases in response to falls in the glomerular filtration rate (GFR) (Wing et al., 2014).

PEW is associated with numerous factors, including inflammation (Gupta et al., 2012), insulin resistance (Bailey et al., 2006), and metabolic acidosis (Mitch, 1998). Metabolic acidosis is a particularly important factor in PEW, as it contributes to muscle wasting by accelerating protein catabolism (Wing et al., 2014). Even moderate levels of acidosis (20 mmol/L bicarbonate) result in the breakdown of proteins, through activation of the adenosine triphosphate (ATP)-dependent pathway involving ubiquitin and proteasomes (Chiu et al., 2009, Mitch et al., 1994). This has been demonstrated clearly in classical studies, where the muscle protein was shown to preferentially waste in rats with metabolic acidosis and renal failure (May et al., 1987). Metabolic acidosis may also contribute to muscle degradation through multiple defects associated with the condition, including: insulin resistance (Mak, 2008); inflammation and abnormal muscle signalling especially dysregulation of IGF-1 signalling (Abramowitz et al., 2013); and the reduction in serum levels of essential branched-chain amino acids, with the corresponding impact on muscle development and operation (Carrero et al., 2013); and through accelerated proteolysis arising from impairment of the IRS/PI3K/Akt pathway (Bailey et al., 2006). The importance of insulin and IGF-1 signalling in muscle protein studies has been demonstrated through the correction of metabolic acidosis in rats, which yielded a corresponding rise in IRS-associated PI3K activity, in turn led to the reduction in the levels of muscle catabolism (Bailey et al., 2006).

The issue of protein degradation has been investigated through a variety of experimental approaches. For example, using sodium bicarbonate as a pre-dialysis treatment for CKD patients has been shown to lessen protein catabolism (Papadoyannakis et al., 1984, Reaich et al., 1993). Furthermore, this approach also decreased amino acid oxidation and the levels of plasma urea (Papadoyannakis et al., 1984, Reaich et al., 1993). However, comparatively few studies of CKD have examined the viability of exercise in improving the health outcomes in terms of PEW, despite evidence suggesting that patients with CKD benefit from resistance training in terms of muscle repair and development (Balakrishnan et al., 2010, Johansen and Painter, 2012). Kosmadakis *et al.* studied forty CKD patients (stage 4 and 5) on a 6-month walking programme. At 1 month, they found short-term improvement of body composition, with the reduction of fat mass by 0.71 ± 0.62 kg ($P = 0.001$) and corresponding marginally significant increase in lean mass by 0.56 ± 0.98 kg ($P = 0.060$) (Kosmadakis et al., 2012). Balakrishnan *et al.* conducted a 12-week trial on CKD patients (stage 3 and 4) to test the efficacy of high intensity resistance training. In addition to changes in types I and II muscle fibres, the mitochondrial DNA copy numbers of patients increased, indicating increased muscle mass. It was suggested that resistance training is effective in the treatment of metabolic catabolism and the treatment of muscle wasting in CKD (Castaneda et al., 2004, Balakrishnan et al., 2010). The present study further expands upon these outcomes, investigating the effect of low pH in stretched skeletal muscle (L6 cells) (*in vitro*), in an attempt to mimic some aspects of what happens in exercised skeletal muscle (eccentric muscle contractions) in CKD patients.

1.3 Physical exercise and chronic inflammation

The WHO Global Burden of Disease study has shown that chronic non-communicable diseases (such as cardiovascular disease, cancer, chronic lung disease, CKD and type 2 diabetes mellitus) are now the major cause of death worldwide, accounting for 72% of deaths in 2016 (World Health Organization, 2014, Lancet, 2017). These diseases affect not just developed but also developing countries (de-Graft Aikins, 2007). Mounting evidence over the past 20 years has shown that regular physical exercise is a promising tool for the preventive therapy of complications arising from a number of different types of chronic diseases, such as type 2 diabetes, colon cancer, breast cancer, and atherosclerosis (Blair et al., 2001, Taylor et al., 2004, Boulé et al., 2001, Fiuza-Luces et al., 2018, Winzer et al., 2018, Fletcher et al., 2018). Physical exercise has also demonstrated the ability to be an effective treatment for complications arising from other diseases that include heart failure (Swedberg et al., 2005), ischemic heart disease

(Pedersen and Saltin, 2015a) and chronic obstructive pulmonary disease (Lacasse et al., 2001) and, more recently, CKD (Watson et al., 2013b, Viana et al., 2014).

Two key factors linking many of these diseases are obesity (Lancet, 2017) and chronic inflammation, for example in the insulin resistance of type 2 diabetes patients (Dandona et al., 2004) and in atherosclerosis, which is characterised by an accumulation of fibrotic tissue and lipids in large arteries (Petersen and Pedersen, 2005b). Numerous studies (Pedersen and Saltin, 2015a, Lacasse et al., 2001, Mallat et al., 1999, Hansson et al., 2002) have suggested that inflammation plays an important role in the pathogenesis of atherosclerosis in CKD. Low-grade chronic inflammation can be detected by measuring C-reactive protein (CRP) and other acute phase proteins, and some pro-inflammatory cytokines, such as TNF- α and IL-1. There may be a link between chronic inflammation, ageing and obesity, arising at least partly from release of pro-inflammatory adipokines from adipose tissue (Fantuzzi, 2005). However, many studies have noted that chronic physical exercise can also lead to a reduction in inflammation by enhancing the ability of the immune system and of skeletal muscle cells to produce anti-inflammatory cytokines like IL-10 (Figure 1.1) (Petersen and Pedersen, 2005a).

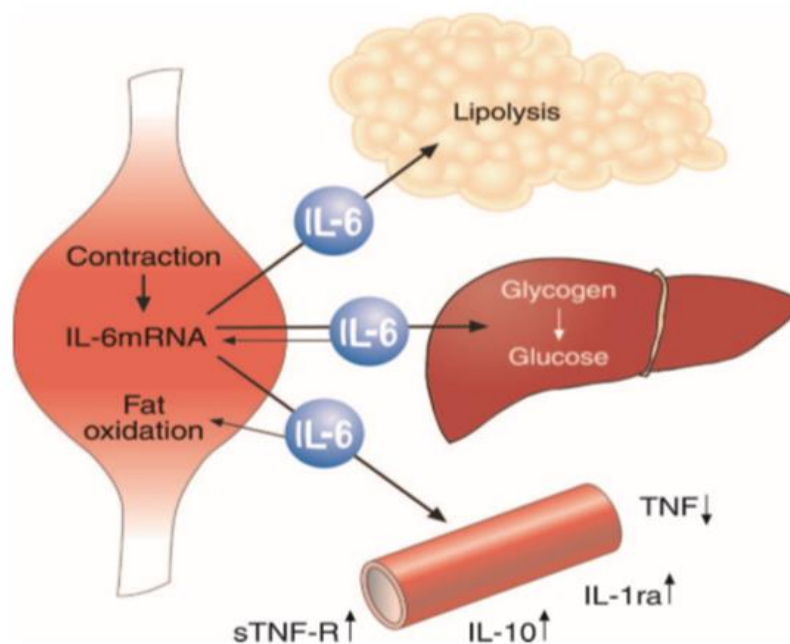


Figure 1.1. The effect of IL-6 from contracting muscle in different organs.

IL-6 enhances the systemic levels of IL-1 receptor antagonist (IL-1ra), soluble TNF receptor (TNF-R), and IL-10. Taken from (Petersen and Pedersen, 2005a).

Interestingly, it has been demonstrated in predialysis CKD that systemic anti-inflammatory status can be developed after acute aerobic physical exercise, due to the increased level of plasma IL-10 just one hour post-exercise (Viana et al., 2014). Paradoxically this may be linked to the increased level of plasma IL-6 just after exercise (Steensberg et al., 2001a, Viana et al., 2014). It has been shown that the level of IL-6 mRNA derived directly from the contracting skeletal muscle (Section 1.6) significantly increases during resistance exercise without muscle damage (Steensberg et al., 2002). However, this was not observed with regard to the level of TNF- α mRNA, which showed no significant increases in skeletal muscle (Steensberg et al., 2002).

The plasma levels of TNF- α were shown to increase following infection and followed by increases in IL-6 production as an indication of inflammatory status (Pedersen and Febbraio, 2008b). However, the levels of IL-6 in exercise are significantly higher compared to TNF- α and are followed by an increase of anti-inflammatory cytokines such as IL-10, which results in an anti-inflammatory state under exercise conditions in general. An exception however is highly strenuous, prolonged exercise such as marathon running which can result in a small detectable increase in the plasma concentration of TNF- α (Figure 1.2) (Pedersen and Febbraio, 2008b).

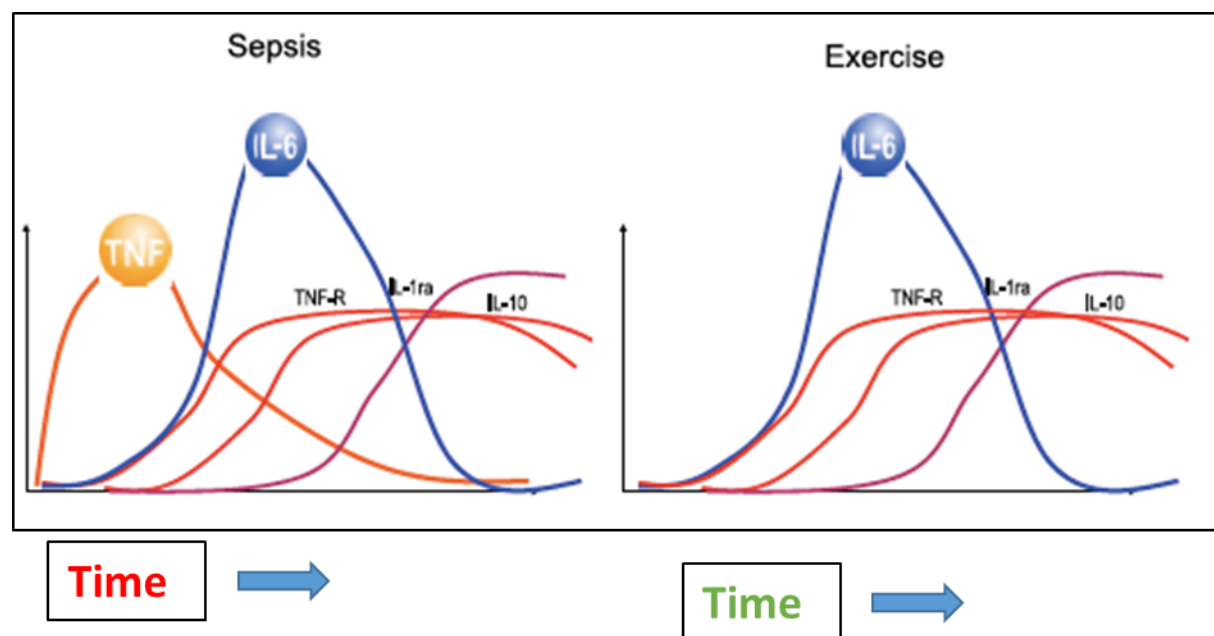


Figure 1.2. Schematic comparison of sepsis-induced versus exercise-induced increases in circulating cytokines in plasma.

The level of circulating tumor necrosis factor (TNF- α) increases rapidly during sepsis and is followed by a marked increase in muscle-derived interleukin-6 (IL-6). However, while IL-6 levels increase during exercise, there is no preceding increase in TNF- α . Taken from (Pedersen and Febbraio, 2008b).

1.4 Effect of exercise training on chronic inflammation

Data from cohort studies suggest the existence of a link between physical exercise and inflammation (Beavers et al., 2010, Pedersen and Saltin, 2015a). People who partake in regular exercise activity tend to show lower inflammatory biomarkers (Pedersen and Saltin, 2006). Physical exercise also seems to have a regulatory effect on the immune response in a way that encourages the production of anti-inflammatory cytokines and even eventually reduces the onset of inflammation (Astrom et al., 2010). This suggested that physical exercise could help in the treatment of some chronic diseases (Pedersen and Saltin, 2015a). This conclusion was supported by a Danish study that showed that physical exercise improved cardiorespiratory fitness (CRF) in patients with chronic obstructive pulmonary disease (COPD) (Pedersen and Saltin, 2015a). As patients with COPD produce a high level of TNF- α , this can affect myocyte differentiation and induce cachexia, thereby leading to reduced muscle strength (Pedersen and Saltin, 2015a). Chronic exercise may exert an indirect beneficial effect on muscle by reducing the production of pro-inflammatory cytokines including TNF- α (Pedersen and Saltin, 2015a). Exercise may increase muscle strength among COPD patients and could eventually lead to improved quality of life compared with patients with a more sedentary lifestyle (Pedersen and Saltin, 2015b).

1.5 Direct evidence for anti-inflammatory effects of physical exercise

To investigate further the observation that physical exercise could reduce systemic low-grade inflammation (Petersen and Pedersen, 2005b), a model of “low-grade inflammation” was developed to see if acute exercise can reduce inflammation under defined laboratory conditions (Starkie et al., 2003). In this laboratory experiment, the level of TNF- α was increased among healthy volunteers by injecting them with a low dose of *Escherichia coli* endotoxin. The level of TNF- α was subsequently found to be decreased when the volunteers performed endurance physical exercise (riding a bicycle for 3 hours). However, the levels of the TNF- α remained higher in control subjects who had received endotoxin but did not perform exercise, suggesting that physical exercise could play an important role in the regulation of the immune response. Interestingly, it has also been shown that a remarkable increase in IL-6 production occurs among people who partake in regular moderate exercise without any inflammatory damage to their muscles, suggesting that IL-6 is a myokine that is secreted from exercising muscles (Section 1.6) (Petersen and Pedersen, 2005b). IL-6 is normally regarded as a pro-inflammatory

cytokine, but the release of IL-6 that occurs during exercise exerts an overall anti-inflammatory effect (Munoz-Canoves et al., 2013). It was seen in functional studies that were done in rodents that IL-6 can play an important role in terms of regeneration of skeletal muscles after injury and that IL-6 has a stimulatory effect on satellite cell proliferation (Munoz-Canoves et al., 2013). Ablation of IL-6 expression with specific siRNA inhibited myoblast differentiation and fusion in cultured myoblasts (Munoz-Canoves et al., 2013). Acute increase of IL-6 after exercise has a role in the activation of satellite cells; however, prolonged activation of systemic IL-6 has a harmful role in terms of catabolic effects and muscle wasting (Munoz-Canoves et al., 2013).

1.6 Skeletal muscle as an endocrine organ

As the largest organ in the human body, skeletal muscle is an endocrine organ that serves a number of key roles. The contraction of skeletal muscle stimulates the production, expression and release cytokines or peptides called ‘myokines’, which have a paracrine or endocrine effect (Pedersen et al., 2007). These myokines can then, in turn, affect organ and tissue metabolism in other parts of the body (Pedersen and Febbraio, 2008a). The ability to increase cytokine production in response to exercise suggests evidence for the long-sought link between immune changes and muscle contraction, opening up the possibility of inducing beneficial metabolic responses in organs like the liver.

The homeostatic state of the human body involves the contribution of the nervous, endocrine, and immune systems, which have a degree of inter-dependence for their normal function and development (Pedersen and Febbraio, 2008a). IL-6 is part of the IL-6 family of cytokines, which includes IL-11, oncostatin M, leukaemia inhibitory factor, ciliary neurotrophic factor, cardiotrophin-1, and cardiotrophin-like cytokine. The common targets of the IL-6 family of cytokines are the gp130 (IL-6R β /CD130) and the gp80 (IL-6R α /CD126) receptors, which are type I cytokine receptors (Kamimura et al., 2003). Levels of IL-6 in plasma increase after protracted periods of exercise, rising exponentially during activity and declining rapidly once exercise terminates (Febbraio and Pedersen, 2002, Suzuki et al., 2002), irrespective of levels of muscle damage involved (Pedersen et al., 2007). Increases in circulating IL-6 are affected by the duration and intensity of the exercise, and the mass and endurance capacity of the muscle involved. IL-6 mRNA is upregulated in skeletal muscle as it contracts (Ostrowski et al., 1998b, Steensberg et al., 2001a), with the transcriptional rate of the IL-6 gene being enhanced by exercise, particularly at low muscle glycogen levels (Keller et al., 2001). IL-6 is released from

skeletal muscle during exercise (Steensberg et al., 2002, Steensberg et al., 2000) and is expressed in muscle fibres in the post-exercise phase (Hiscock et al., 2004), with increased IL-6 receptor production occurring in skeletal muscle in response to physical activity, suggesting the presence of a co-ordinated biological mechanism (Keller et al., 2005).

Although commonly perceived as a pro-inflammatory cytokine, there is some evidence to suggest that IL-6 also may have context-sensitive anti-inflammatory properties (Petersen and Pedersen, 2005b). When circulating levels of IL-6 increase, there is a corresponding rise in levels of anti-inflammatory cytokines like IL-10 and IL-1ra (Ostrowski et al., 2000, Ostrowski et al., 1999). Blood infusion of IL-6 to healthy donors has the same effect on these cytokines as exercise, as well as increasing levels of cortisol in the body (Steensberg et al., 2003). In addition, studies have shown that TNF- α production can be suppressed by exercise and IL-6 infusion (Starkie et al., 2003). A link might also exist between IL-6 and AMP-activated protein kinase (AMPK), which plays an important role in modulating glucose uptake and the stimulation of fatty acid oxidation (Kahn et al., 2005). IL-6 enhances adipose and muscular AMPK activity (Kelly et al., 2004), and its positive effects on glucose uptake and fatty acid oxidation are halted by the presence of dominant-negative AMPK constructs (Carey et al., 2006). In some senses, muscle-derived IL-6 is a myokine with endocrine effects and can be thought of as an ‘exercise factor’ (Pedersen et al., 2007), as it is quickly activated in response to muscle contractions and has a faster transcription rate than other muscle genes. Additionally, the availability of carbohydrates in skeletal muscles strongly influences IL-6 production, suggesting that it is produced in response to variation in energy levels.

In summary, the contraction of human skeletal muscle causes the expression and release of IL-6, which has numerous metabolic effects, such as the activation of AMPK, which influences fatty acid oxidation and insulin-stimulated glucose disposal *in vivo*. IL-6 may have beneficial effects in serious inflammatory states especially when secreted without other pro-inflammatory cytokines, such as TNF- α . Even though acutely secretion of IL-6 has ‘anti-inflammatory’ properties, chronic elevated levels promote atrophy via protein degradation, shown both *in-vitro* and *in-vivo*, and IL-6 is chronically elevated in muscle of elderly individuals with sarcopenia and the increase is associated with earlier morbidity and mortality (Munoz-Canoves et al., 2013).

1.7 The biosynthesis of IL-6

For an understanding of the IL-6 myokine response in exercising skeletal muscle, it is necessary to consider the steps involved in IL-6 biosynthesis: i.e. transcription of the IL-6 gene (Luo and Zheng, 2016), translation of the IL-6 mRNA, and subsequent post-translational modification to generate a mature biologically active IL-6 protein.

1.7.1 Transcriptional regulation of IL-6

In muscle biopsies from exercising human volunteers an increase in IL-6 mRNA expression was found to correlate with increased phosphorylation of a nuclear pool of the MAP kinases JNK and p38 (Chan et al., 2004b) which may be activated in response to muscle contraction (see Section 1.11 and 1.12 below). A similar p38 response was observed *in vitro* in cultured L6 rat myotubes when the intracellular Ca^{2+} concentration was elevated by incubation with the ionophore ionomycin (Chan et al., 2004b). The transcription factors involved in the increased expression of IL-6 in muscle following exercise are still not fully understood, but the promoter region of the human IL-6 gene (Figure 1.3) is known to contain an AP-1 response element, which (as explained in Section 1.12) can be activated through JNK. The mechanism through which p38 activates IL-6 transcription in muscle is less clear: indeed more recent evidence from macrophages (Nyati et al., 2017) suggests that prolonged stimulation of p38 may decrease the abundance of IL-6 mRNA by stimulating degradation of the mRNA stabilising protein Arid5a.

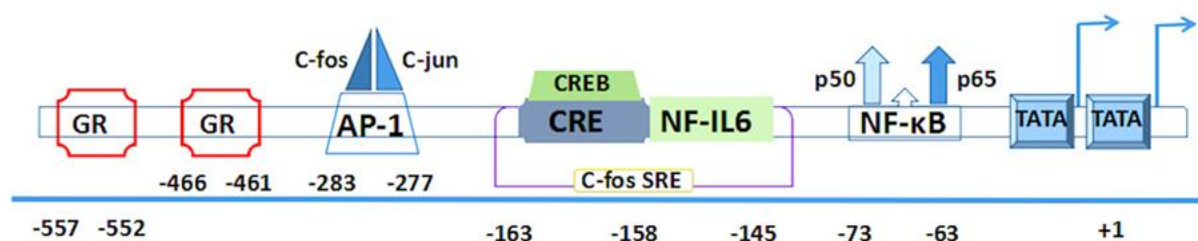


Figure 1.3. Schematic representation of the promoter region of the human interleukin-6 (IL-6) gene showing possible cis-regulatory elements.

GR: glucocorticoid receptor. AP-1: Activator protein 1. CRE: The cAMP response element. NF-IL6: nuclear factor–interleukin-6. NF-kB: Nuclear Factor Kappa Beta. TATA: three TATA like sequences (TATA boxes). CREB: CRE-binding protein. C-fos: cellular oncogene. Taken from (Luo and Zheng, 2016).

1.7.2 Protein synthesis

Protein synthesis by translation of mRNA requires numerous components, including: the mRNA to be translated; amino acids (see Section 1.9); amino acid specific aminoacyl-transfer RNAs (aminoacyl-tRNAs); functional ribosomes; regulatory protein factors; energy sources; and enzymes (Gingras et al., 1999). The translation process is separated into the following steps: initiation, elongation, and termination and these are described briefly below.

1.7.2.1 Initiation

Before peptide bond formation occurs, several components are required for the assembly of the translation system: the mRNA template; the two ribosomal subunits (40S and 60S); the aminoacyl-tRNA; and ATP, which serves as a source of energy (Proud, 2006). In order to facilitate the initiation complex, a series of regulatory proteins, the eukaryote initiation factors (eIFs) are required (Mitchell and Lorsch, 2008).

During this process, the ribosome recognizes the start codon (AUG), which then initiates translation (Proud, 2006). The scanning process involves the 40S ribosomal subunit binding at the mRNA 5'-end, where it scans through until it meets the AUG codon. This process consumes ATP. This process is facilitated by eukaryotic Initiation Factor 2 / Guanosine-5'-triphosphate complex (eIF-2-GTP) and additional eIFs. On the small ribosomal subunit, the tRNA initiator carrying methionine enters the P position, with the complex becoming functional when it binds to the large (60S) ribosomal subunit.

1.7.2.2 Elongation

The elongation step of the protein synthesis involves the addition of amino acid residues to the growing polypeptide chain (Proud, 2006). As the mRNA is translated, the ribosome moves from the 5'→3' end of the mRNA molecule. During elongation, EF-1 α -GTP and EF-1 $\beta\gamma$ elongation factors facilitate the delivery of the next aminoacyl-t-RNA that is encoded by the codon which appears next in the ribosomal A position (Rodwell et al., 2015). The peptide bond is then formed between the amino acids at the P and A positions under the catalysis of the peptidyltransferase enzyme (Proud, 2006). By the process of translocation, the ribosome then advances three nucleotides towards the mRNA 3'-end, which requires EF-2-GTP and GTP hydrolysis. Consequently, uncharged tRNA at the P position moves to the E position before release and the amino acyl t-RNA at the A position on the ribosome is moved to the P position. This process is repeated leading to elongation of the growing polypeptide chain until a stop codon is reached.

1.7.2.3 Termination

Termination occurs when a stop codon (UAA, UGA, or UAG) moves into the A position (Merrick, 1992, Proud, 2006). All three-stop codons are recognized by a single release factor, eRF. Once the eRF is bound, the completed polypeptide chain is released from the ribosome (Proud, 2006).

1.7.2.4 Post-translational Modifications of Human Interleukin-6

It has been reported that TNF- α and IL-6 induce IL-6 secretion from human fibroblasts (May et al., 1988a, 1988b; Santhanam et al., 1989). This IL-6 consisted of six or more differentially modified phosphoglycoproteins of molecular mass 23-30 kDa. These masses included three with mass from 23 to 25 kDa and three with mass from 28 to 30 kDa (May et al., 1988a, May et al., 1988b, Santhanam et al., 1989).

Using metabolic labelling, glycosidase digestion, and lectin chromatography experiments demonstrated that the mass of 23-25 kDa species are O-glycosylated and that the 28- to 30-kDa species are both O- and N-glycosylated (Santhanam et al., 1989).

Pulse-chase experiments were used to study newly synthesised IL-6 polypeptides, which were shown to quickly enter two separate protein modification pathways. One of these pathways led to O-glycosylation and the other led to both N- and O-glycosylation. Prior to the production of these polypeptides, further modifications (phosphorylation) occurred in the two pathways (Santhanam et al., 1989).

The treatment of human fibroblasts with the glycosylation inhibitor tunicamycin has been shown to lead to IL-6 production in the O-glycosylated form only (Santhanam et al., 1989). However, when human fibroblasts were treated with the translation inhibitor cycloheximide, IL-6 was produced in both forms of N- and O-glycosylation pathways. Interestingly, treating fibroblasts with the ionophore monensin (which is used to block the intracellular transport of cytokines, resulting in their accumulation in the Golgi region and endoplasmic reticulum (Jung et al., 1993) resulted in glycosylation inhibition, but did not inhibit IL-6 polypeptide production (Santhanam et al., 1989).

Other IL-6 species was revealed using immunoprecipitation, immunoblotting, and immunoaffinity chromatography techniques. These IL-6 species were found (from their mobility in dodecyl sulfate-polyacrylamide gel electrophoresis under reducing conditions to have apparent molecular masses of 17-19 kDa and 45 kDa, thereby indicating that IL-6 has

additional modifications (Santhanam et al., 1989). These studies of IL-6 illustrate the complexity of this cytokine. Interestingly, it has been suggested that the more immunosuppressive isoforms of the protein are those, which are less glycosylated forms (Bennett and Schmid, 1980; Santhanam et al., 1989).

1.8 Mammalian target of rapamycin (mTOR)

An important regulator of the process of translation (especially at the initiation step) is mammalian target of rapamycin (also known the mechanistic target of rapamycin). This is a serine/threonine kinase, which can play an important role in cells, including regulation of growth, proliferation, and survival, as well as protein synthesis (Lieberthal and Levine, 2009a). Its biological activity is selectively inhibited by rapamycin (also known as sirolimus), which was first identified in *Streptomyces hygroscopicus* in 1975 (Sehgal, 2003). Rapamycin can inhibit mTOR via the creation of a complex along with an intracellular protein called FK506-binding protein 12 (FKBP-12) (Lieberthal and Levine, 2009a). In cells there are two functionally active protein complexes containing mTOR, namely mTOR complex 1 (mTORC1) and mTOR complex 2 (mTORC2), each of which utilises a characteristic scaffolding protein. The scaffolding protein is called raptor for mTORC1 and rictor for mTORC2. The mTORC1 can be activated by growth factors and amino acids, allowing it to increase cell size and proliferation (Lieberthal and Levine, 2009a), and it is thought to play an important role in myocyte hypertrophy in skeletal muscle (Lieberthal and Levine, 2009b).

The activation of mTORC1 results in activation of phosphatidylinositol 3-kinase (PI3K - a lipid kinase), which phosphorylates the plasma membrane phospholipid phosphatidylinositol 4,5-bisphosphate (PIP2) to yield PIP3 (Lieberthal and Levine, 2009a). This then phosphorylates and activates the regulatory protein kinase Akt through 3-phosphoinositide-dependent kinase-1 (PDK1). PI3K activity is negatively regulated by PTEN, a phosphatase that dephosphorylates PIP3 back to PIP2. In addition, Akt phosphorylates and inhibits the tuberous sclerosis complex proteins (TSC), which inhibits the cytoplasmic GTPase, Rheb, a key activator of mTORC1. This process negatively regulates mTORC1 (Lieberthal and Levine, 2009a). If the ATP stores of the cell are reduced by stress (or by prolonged exercise in muscle), the AMP-ATP ratio increases, which activates AMPK. AMPK inhibits mTOR by phosphorylating and activating TSC2. After mTORC1 has been activated, it phosphorylates the protein kinase p70S6K and initiation factor 4E binding proteins 4EBPs. This promotes the translation of mRNAs (especially at the initiation step) resulting in an increase in global protein synthesis and cellular

hypertrophy, and the corresponding synthesis of proteins necessary for cell growth and cell-cycle progression. (Lieberthal and Levine, 2009a) (Figure 1.4).

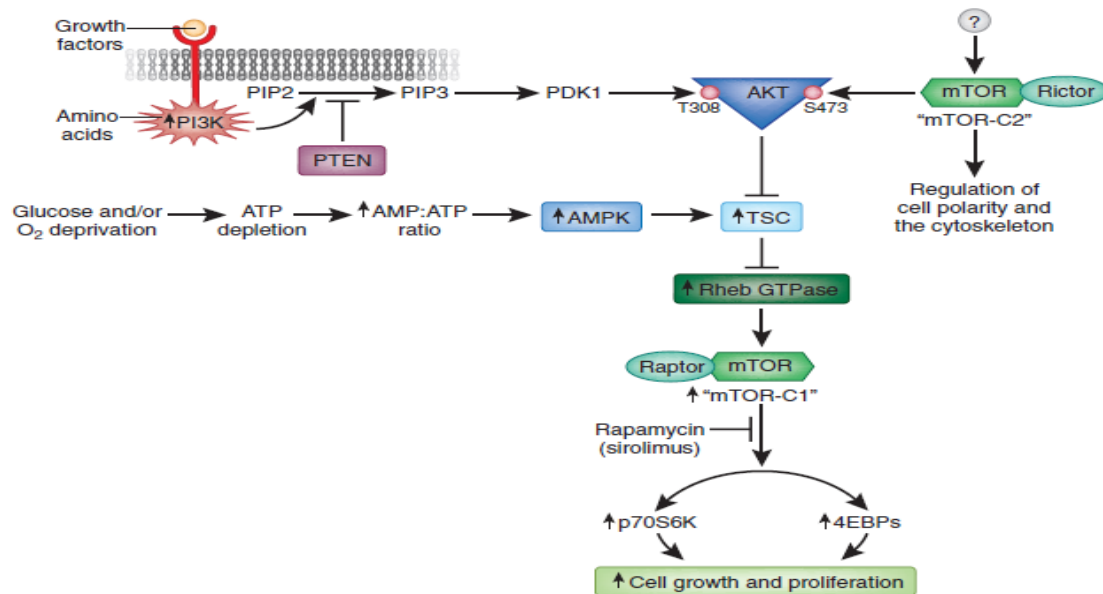


Figure 1.4. mTOR is a component of two major intracellular signalling complexes: mTORC1 and mTORC2.

These complexes fulfil different functional roles: stimulating cell growth and proliferation in the case of mTORC1 and the regulation of cell polarity and the cytoskeleton in the case of mTORC2. They are connected to different targets downstream by their individual scaffolding proteins, termed raptor (mTORC1) and rictor (mTORC2). Taken from (Lieberthal and Levine, 2009a).

A large fraction of total body protein in humans occurs in skeletal muscle and mTORC1 has been shown to be a major regulator of protein synthesis and total protein mass in the skeletal muscle (Watson and Baar, 2014b) (Figure 1.5).

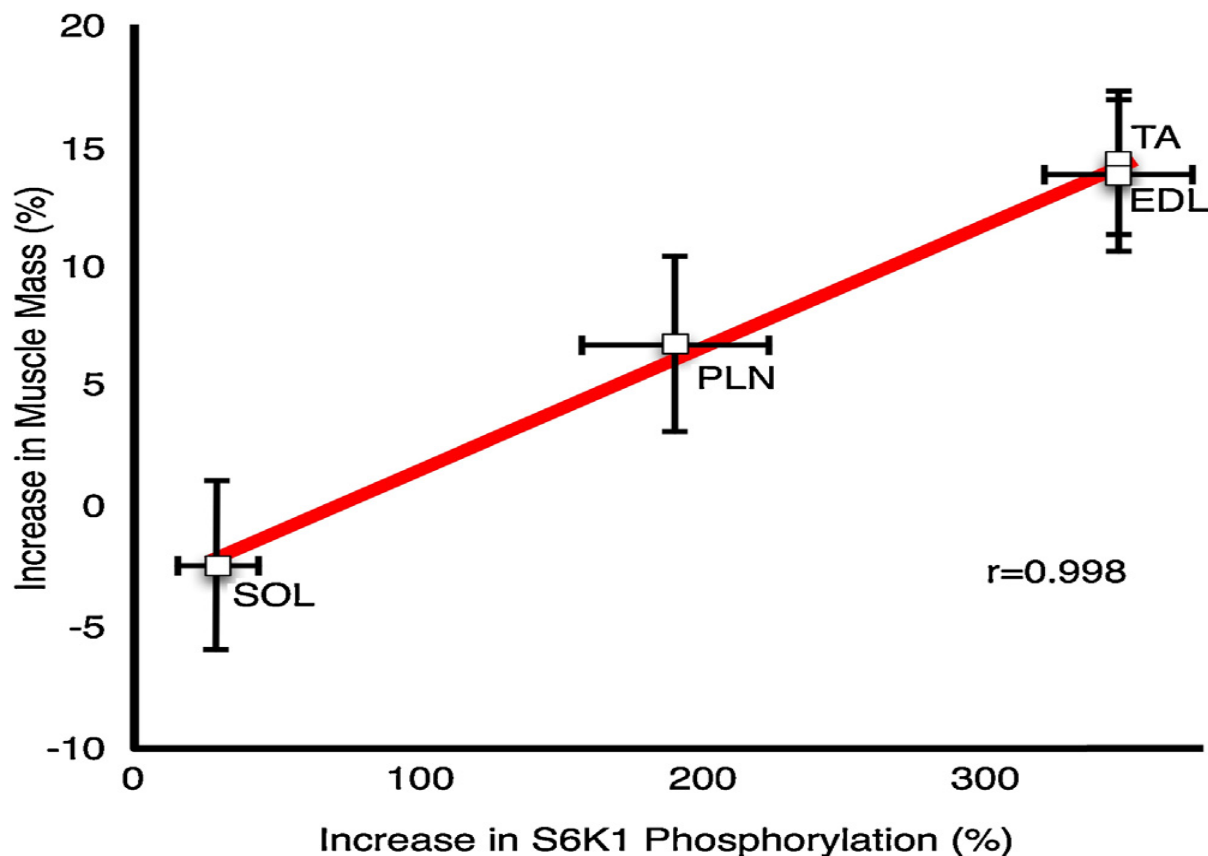


Figure 1.5. Relationship between mTORC1 activation and muscle hypertrophy.

In this graph, the growth in muscle mass resulting from 6 weeks of resistance training in rats is plotted against the post exercise (6 hours) phosphorylation of S6K1. A significant association is evident between increased muscle mass and mTORC1 activity. Taken from (Baar and Esser, 1999, Watson and Baar, 2014a)

Resistance exercise training can lead to hypertrophy of muscle, potentially because of the increased synthesis of protein due to the high activity of S6 protein kinase (p70S6k) through mTORC1 (Baar and Esser, 1999, Watson and Baar, 2014b).

An important influence on the activity of mTORC1 is the availability of free amino acids (Baar and Esser, 1999, Watson and Baar, 2014a) inside the cell which is partly dependent on the activity of plasma membrane amino acid transporters. Of particular importance is the SNAT2 transporter, which is described below.

1.9 The SNAT2 amino acid transporter

In order to build proteins (including IL-6), small neutral (zwitterionic) amino acids, including L-alanine, L-glutamine and L-serine, need to be transported into the cells (Pinilla et al., 2011) by active amino acid transporters of which the most important are sodium-coupled neutral amino acid transporters (SNATs) (Broer, 2014) (Figure 1.5). SNATs are encoded by genes of the SLC38 gene family. They perform secondary active transport (AT) i.e. pumping amino

acids into the cell against their electrochemical gradient) by coupling the transport to the electrochemical gradient of Na^+ across the plasma membrane which is maintained by the primary active transporter Na^+, K^+ -ATPase (the sodium pump) (Figure 1.6). In this mechanism, each amino acid is transported by an electrogenic mechanism involving co-transport with one Na^+ . This is called a symport mechanism (Broer, 2014).

So-called tertiary active transport of other amino acids such as L-leucine (Leu) can then be performed indirectly by coupling of (for example) the L-glutamine (Gln) gradient that is generated by the SNATs to transport of Leu through a System L amino acid exchanger (Figure 1.6). In this way SNAT transporters such as SNAT2 (SLC38A2) can indirectly control the intracellular Leu concentration which is an important regulator of mTORC1 (Evans et al., 2007b).

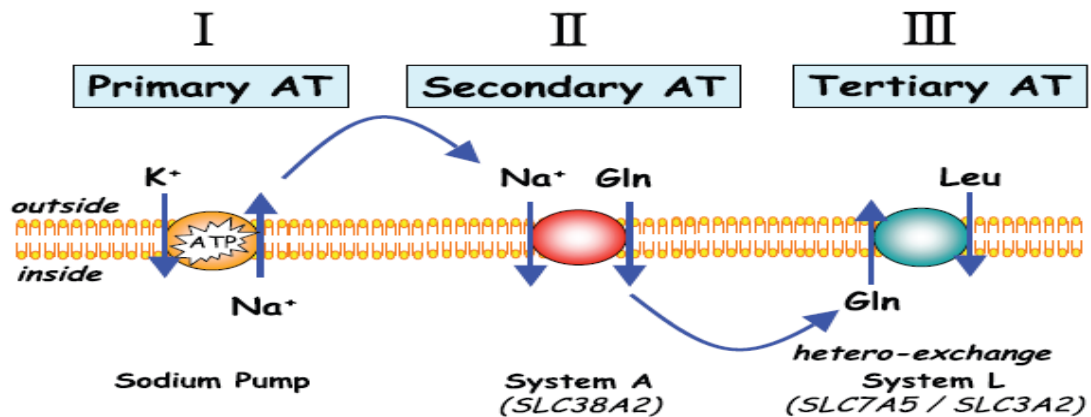


Figure 1.6. Integration of primary (I), secondary (II), and tertiary (III) active transport (AT) mechanisms may affect transmembrane distribution of particular amino acids (AAs).

The net movement of AAs to the intracellular pool from the extracellular pool is generated through the actions of secondary active transporters (e.g. System A/SNAT2 – also known as SLC38A2). Taken from (Hundal and Taylor, 2009).

There are 11 members of the solute carrier 38 (SLC38) family in the human genome, and this is true in other mammalian genomes. The best characterised transporters of this family are SNAT1 to SNAT5 inclusive (SLC38A1 to SLC38A5). Three of these (SNAT1, 2 and 4) are classed as so-called “System A” transporters i.e. Na^+ -linked transporters which efficiently transport L-alanine and are inhibited by low pH. The most prominent of these is SNAT2, in terms of its high level of expression in most human tissues including skeletal muscle (Pinilla et al., 2011). In the rat L6-G8C5 skeletal muscle cells that are used as a culture model in this thesis (Section 1.15) SNAT2 is the dominant isoform of System A transporter expressed in the cells and therefore accounts for nearly all of the System A transport activity in the cells (Evans

et al., 2007b). For this reason, in the remainder of this thesis, the terms System A and SNAT2 are used interchangeably and the transporter is referred to as System A / SNAT2.

The System A transporters are also characterised by their inhibition by the non-metabolisable competitive amino acid analogue 2-methylamino-isobutyric acid (MeAIB), which is a substrate for these transporters and its rate of transport into cells is used as an indicator of System A activity (Christensen et al., 1965, Franchi-Gazzola et al., 2006). One of the main physiological characteristics of these System A transporters is their sensitivity to pH i.e. the fact that their functionality is inhibited at physiologically attainable low extracellular pH (Mackenzie and Erickson, 2004, Broer, 2014).

In humans System A transporters can be found on chromosome 12: the number of amino acids is 486 for SNAT1 and 505 for SNAT2 (Pochini et al., 2014), and the N-terminal His residue is thought to confer most of the pH sensitivity on the SNAT2 transporter (Baird et al., 2006). In L6-G8C5 rat skeletal muscle cells SNAT2 can play an important role in the regulation of protein synthesis through mammalian target of rapamycin and ribosomal protein S6 kinase, and 4E-BP1 because it can control the intracellular free amino acid concentration which activates mTORC1 (Evans et al., 2007a). In addition to its effects on mTORC1 through transport of neutral amino acids into the cell, there is also evidence that SNAT2 can exert effects independent of its transport activity by acting as a so-called “transceptor” i.e. a transporter protein, which senses extracellular amino acids, pH and other extracellular stimuli and then sends a transport-independent signal into the cell. For example SNAT2 is thought to regulate its own gene expression and translation in the face of extracellular amino acid starvation by such a transceptor mechanism (Hyde et al., 2007). The transceptor signal is not fully understood but there is evidence that it occurs through the MAP kinase JNK (Hyde et al., 2007) and through cyclin dependent kinase 7 (CDK7) (Stretton et al., 2019). In L6-G8C5 cells, a pH-sensing transceptor signal is thought to be involved in the regulation of PI3K and Akt, thus explaining the stimulation of global protein degradation that occurs at low pH in these cells (Evans et al., 2008a). This is potentially important in the case of CKD patients with uraemic metabolic acidosis, who have a resistance to insulin signalling through PI3K and Akt, eventually leading to loss of protein synthesis and increased protein catabolism in their skeletal muscles and hence to muscle wasting.

1.10 Mechanotransduction

In view of the evidence (reviewed in Sections 1.3 to 1.6 above) that IL-6 secreted as a myokine during exercise exerts potent metabolic and anti-inflammatory effects on target cells, it is important to understand the biochemical mechanisms that link exercise (including muscle contraction and mechanical stress) to increased IL-6 expression in myocytes and its secretion into extracellular fluid. It is also important to understand how these mechanisms may change in response to the biochemical abnormalities that occur in CKD (such as uraemic metabolic acidosis - see Section 1.15 below). It is therefore important to understand the mechanisms involved in mechanotransduction by which mechanical stress on skeletal muscle is transduced into intracellular signals, which lead to muscle hypertrophy in response to resistance exercise, and which may play a role in the accompanying increase in biosynthesis and secretion of IL-6.

One of the key mechanisms driving skeletal muscle hypertrophy as an adaptation to resistance exercise is increased synthesis of muscle protein mediated by mammalian target of rapamycin complex 1 (mTORC1). However, the various factors involved in the hypertrophy cascade are imperfectly understood, including the initiating factors, the stimuli induced by exercise and the specific stimuli causing hypertrophy. A signal that is initiated, induced by exercise and which stimulates hypertrophy is known as a "hypertrophy stimulus", which is detected by a "hypertrophy sensor" (Wackerhage et al., 2018).

Resistance exercise triggering the synthesis of muscle protein and corresponding muscle hypertrophy is strongly dependent on a downstream hypertrophy signalling "hub" involving Akt and mTORC1 (Bodine et al., 2001, Marcotte et al., 2015, Pereira et al., 2017). Extensive research shows that muscle protein synthesis and post resistance exercise muscle growth can be reduced, or prevented entirely, by mTORC1 blockade with rapamycin in rodents (Kubica et al., 2004) and humans (Drummond et al., 2009). Overloading muscle through the synergist ablation model of muscle hypertrophy has been shown to have similar hypertrophic effects (Bodine et al., 2001, Goodman et al., 2011). Muscle size is also regulated by other signalling pathways and genes, but their contribution to muscle hypertrophy from resistance exercise is not fully understood (Verbrugge et al., 2018).

Even though the molecular mechanisms regulating muscle mass have been extensively studied, the initiating hypertrophy stimuli and the ultimate sensors of mechanical stress are still poorly understood (Wackerhage et al., 2018). The term "hypertrophy stimulus" denotes an initiating stimulus of sufficient magnitude and duration to trigger a skeletal muscle

hypertrophic response to resistance exercise. This stimulus is then detected by a “hypertrophy sensor” (Rindom et al., 2019). According to these definitions, hypertrophy regulators like IGF-1 or its MGF splice variant are not initiating hypertrophy stimuli, because there are not signalling events (i.e. hypertrophy stimuli) that change their expression after resistance exercise (Hameed et al., 2003). It has been suggested that true hypertrophy stimuli would involve a sophisticated signalling system that produces hypertrophy in response to resistance exercise, regardless of variations in load or sets (Wackerhage et al., 2018).

The most intuitive hypertrophy stimuli are mechanical signals (Wackerhage et al., 2018), as is shown by the atrophy of muscles that occurs in response to reduced mechanical load (Psatha et al., 2012, Appell, 1990). This suggests that maintaining baseline muscle mass requires a certain level of mechanical loading. Further evidence of the importance of mechanical signals is that hypertrophy of skeletal muscle can be achieved by mechanical overload, tested on rat muscles using cast-induced stretch or the ablation of plantar flexor synergists (Goldberg et al., 1975) (MacKenzie et al., 2009). However, it should be noted that these studies suffered from numerous confounding variables, such as damage or metabolic variation. The third line of indirect evidence is that exercise at low load (endurance) induces minimal hypertrophy, whereas exercise at high mechanical load (resistance) triggers significant growth of skeletal muscle (Wackerhage et al., 2018). However, near maximal muscle hypertrophy can occur in response to mechanical loads as low as $\approx 30\%$ of the 1RM (Medicine, 2009).

In skeletal muscle force transduction systems, there are several potential candidates for hypertrophy-triggering mechanosensors. Research into mechanical stimuli started in the 1950s, when researchers discovered the ability of cancer cells to grow on agar without being anchored, and continued in the 1970s with the discovery that cells anchor using focal adhesion complexes, which include proteins like vinculin, talin and integrins, and kinases, including focal adhesion kinase (FAK) or integrin-linked kinase (Ilk) (Iskratsch et al., 2014). In addition to anchoring cells on a substrate, focal adhesions can also mechanically connect the exterior to the cytoskeleton, as well as sense and trigger adaptations to mechanical stimuli (Iskratsch et al., 2014, Sun et al., 2016). In skeletal muscle, the equivalent of focal adhesions are costameres, which are Z-disc associated structures of muscle fibres that link the cytoskeleton to the extracellular matrix and transmit force laterally from the sarcomere to the extracellular matrix. The two costamere complexes are the vinculin-talin-integrin complex and the dystrophin-glycoprotein complex (Iskratsch et al., 2014). Costameres are essential for normal muscle

function, as shown by the fact that the mutation of costamere genes typically results in severe muscle diseases. For example, mutation of the dystrophin-encoding (DMD) gene causes Duchenne muscular dystrophy (Jaka et al., 2015).

In skeletal muscle, the focal adhesion kinase (FAK) (encoded by the gene PTK2) is a nonreceptor tyrosine kinase that moves to focal adhesions when the cell adheres to a substrate (Graham et al., 2015). In cultured C2C12 myotubes, IGF-1 can increase FAK Tyr397 autophosphorylation and FAK is required for IGF-1-induced hypertrophy and Tsc2, mTOR and S6K1 signalling (Crossland et al., 2013) and signals to other key downstream kinases including the MAPKs (see Sections 1.11 and 1.12). However, it is not clear whether a mechanical hypertrophy sensor can activate FAK and whether FAK is activated itself by mechanical load during resistance exercise. It seems unlikely that FAK is directly activated by mechanical load during resistance exercise, because it does not seem to have a mechano-activated protein domain, unlike filamin-C or titin (Glover et al., 2008). Laboratory testing showed that activity-related FAK Tyr576/577 phosphorylation was not affected by intense resistance exercise (4 sets of 10 repetitions) for both fed and fasted participants (Glover et al., 2008). However, 60-90 min post eccentric exercise, phosphorylated FAK Tyr397 was elevated (in comparison to what was observed following a concentric bout of exercise) exclusively at the distal site of the vastus lateralis muscle (Franchi et al., 2018). Therefore, while evidence suggests that FAK may have a role in the regulation of muscle size, it does not seem to be linked to a mechanosensor that directly senses mechanical load as a hypertrophy stimulus during resistance exercise (Wackerhage et al., 2018).

Focal adhesions are closely associated with phosphatidic acid-generating enzymes, such as phospholipases. Recent research has shown that mechanical stimuli, specifically the attachment to a soft or stiff substrate, promote the conversion of phosphatidylinositol 4,5-bisphosphate (PIP2) to phosphatidic acid. This synthesis was catalysed by phospholipase C γ 1 (PLC γ 1) and activated the Hippo pathway effectors Yap (Yes-associated protein 1, gene Yap1) and its paralogue Taz (gene Wwtr1) (Meng et al., 2018). Yap and Taz are mechanosensitive transcriptional co-factors that seem to regulate gene expression by co-activating Tead1-4 transcription factors (Dupont et al., 2011). In this way, they regulate muscle differentiation, satellite cell function (Wackerhage et al., 2014), and are affected by many exercise-associated stimuli (Gabriel et al., 2016) with increased Yap activity in muscle fibres causing hypertrophy (Goodman et al., 2015, Watt et al., 2018). No clear link has been suggested between Yap and

Taz and mTORC1, with studies even demonstrating that Yap with rapamycin treatment can cause hypertrophy (Goodman et al., 2015). However, some links are known to exist between Yap and mTORC1 (Wackerhage et al., 2018). For example, Yap suppresses the mTORC1 inhibitor PTEN (Tumaneng et al., 2012) and induces the expression of SLC7A5 and SLC3A2 that encode the LAT1 amino acid transporter (Hansen et al., 2015). (This is the L-leucine transporter shown in Figure 1.6, which increases the L-leucine supply to activate mTORC1). In contrast, even though PTEN expression did not decrease in the vastus lateralis 2.5 h and 5 h after human resistance exercise (Vissing and Schjerling, 2014) and in synergist-ablated, hypertrophying plantaris muscle (Chaillou et al., 2013), the expression of the LAT1-encoding genes SLC7A5 and SLC3A2, as well as other Yap targets such as Ankrd1, did increase in both situations. These data suggest that an unknown sensor may be triggered by mechanical load to increase phosphatidic acid and thereby activate Yap and Taz, which then increase LAT1 levels and sensitize the muscle under load to leucine stimulation of mTORC1 (Wackerhage et al., 2018). However, it is important to note that phosphatidic acid not only modulates Hippo signalling but can also activate mTORC1, the primary muscle protein synthesis regulator (Hornberger et al., 2006a). Hypertrophy-inducing eccentric contractions were found to elevate levels of phosphatidic acid in tibialis anterior muscles for up to 1 hour. Furthermore, use of butanol to inhibit phosphatidic acid synthesis has been shown to prevent the phosphorylation of mTORC1 activity markers, suggesting that phosphatidic acid mediates eccentric exercise-induced hypertrophic signalling (O’Neil et al., 2009). Although Z-disc-linked phospholipase D (Pld) was first identified as a phosphatidic acid-synthesizing enzyme and therefore not exclusively located in focal adhesions, it is now recognised that another source of phosphatidic acid in mechanically loaded muscle occurs in a reaction catalysed by diacylglycerol kinase- ζ (DGK ζ) (You et al., 2014). Together, these studies suggest that mechanical stimuli can activate phospholipases to synthesize phosphatidic acid, which in turn can activate mTORC1 and the Hippo effectors Yap and Taz (Wackerhage et al., 2014, Goodman et al., 2015). However, it is important to note that research has not identified the actual phosphatidic acid synthesis-stimulating mechanosensor governing hypertrophy, despite locating important signalling mechanisms in-between the mechanical stimulus and hypertrophy-mediating pathways.

As noted above, another important protein group that are part of costameres are integrins, with the $\alpha 7\beta 1$ -integrin isoform (partly encoded by the gene *Itga7*) having been linked to muscle size ($\alpha 7\beta 1$ -integrin overexpressing mice develop larger muscle fibres in response to exercise training than wild-type mice) (Wackerhage et al., 2018). In addition, it is possible that $\alpha 7\beta 1$ -

integrin might help to activate mTORC1 signalling post-exercise, as mTOR and its downstream target p70S6k are more phosphorylated at activity-related residues at rest and after eccentric exercise in $\alpha 7\beta 1$ -integrin overexpressing mice (Zou et al., 2011); (Wackerhage et al., 2018). However, it is currently not known how $\alpha 7\beta 1$ -integrin might be activated by mechanical hypertrophy stimuli during resistance exercise, or how $\alpha 7\beta 1$ -integrin would then activate mTORC1 and other signalling proteins that cause hypertrophy of the muscle fibre ((Wackerhage et al., 2018).

Costamere-based mechanosensors may also sense two additional types of mechanical stimuli that may be hypertrophic triggers, namely muscle fibre swelling, sometimes known as the “pump” (Schoenfeld and Contreras, 2014), and a resistance exercise induced stiffness of the extracellular matrix (Wackerhage et al., 2018). Although muscle swelling can also be caused by exercise-induced muscle damage (EIMD) (Peake et al., 2016), the “pump” is of much shorter duration (Wackerhage et al., 2018). Nevertheless, the entire muscle can swell after an intense exercise session (Farup et al., 2015). This swelling has been suggested to occur partly through the osmotic effect of lactic acid that accumulates following exercise (Usher-Smith et al., 2006), but also possibly through cation accumulation in the cells (Kemp, 2007). The reported stimulation of System A amino acid transporters by exercise (Henriksen et al., 1992, Henriksen et al., 1993, King, 1994) may also lead to accumulation of amino acid osmolytes e.g. L-glutamine in the cells (Figure 1.6). In primary rat myotubes, swelling in a hypoosmotic culture medium increases glutamine uptake by 71% more than isotonic culture medium (Wackerhage et al., 2018). However, integrin or cytoskeleton inhibitors prevent this uptake, indicating that the swelling is dependent on integrins and the cytoskeleton (Low and Taylor, 1998). Together these data suggest that differentiated muscle can respond to cell swelling with increased glutamine uptake and that this depends on integrin or cytoskeletal loading (Wackerhage et al., 2018). Intracellular L-glutamine is required for the uptake of protein synthesis-stimulating essential amino acids, such as L-leucine (Figure 1.6) (Nicklin et al., 2009), although it is unclear whether the swelling is enough to mechanically load the cytoskeleton, as well as whether cytoskeletal loading after resistance exercise is responsible for glutamine uptake and protein synthesis (Miller et al., 2005). After exercise-induced muscle damage, muscles can be swollen for several days (Yu et al., 2013), even when muscle protein synthesis should have returned to baseline (Miller et al., 2005). Given that costameres are the sites where the cytoskeleton connects to the extracellular matrix and where mechanical signals

can be sensed, it is probable that fibre swelling will strain costameres, thereby triggering a hypertrophic response (Wackerhage et al., 2018).

1.11 The effect of mechanical stress on MAP kinases and System A / SNAT2

Downstream from FAK in the signalling pathways described above there is activation of the mitogen-activated protein kinases (MAPKs) in muscle (Aronson et al., 1997). Mechanical loading, including mechanical stretch, can activate MAPK pathways, including p38 mitogen-activated protein kinase (Chambers et al., 2009a). A consequence of this may be activation of the anabolic System A sodium-coupled neutral amino acid transporter SNAT2 (slc38a2) which has been shown to be activated in mammalian cells by a range of different stimuli, mediated by MAPKs such as p38 (Aye et al., 2015, Bevington et al., 1998b, Lang, 2007). The activation of System A/SNAT2 also occurs in *ex vivo* preparations of skeletal muscle following muscular exertion *in vivo* (King, 1994, Henriksen et al., 1992, Henriksen et al., 1993). MAPK activation may therefore be a significant intermediate step between mechanotransduction/FAK/Yap activation and System A/SNAT2, mTORC1 activation and IL-6 protein synthesis (see Section 1.15 and Figure 1.7).

1.12 Mitogen-activated protein kinases (MAPKs)

The mammalian MAPKs consist of serine/threonine kinases which can respond to extracellular signals, including hormones, osmotic stress, mechanical stress (Section 1.10) and pro-inflammatory cytokines (Widmann et al., 1999). They can transfer these signals at an intracellular level, sending them into the nucleus and regulating different cell functions, such as proliferation, differentiation and gene expression (Cargnello and Roux, 2011a). There are several groups of MAPKs that can be expressed in mammals, for example extracellular signal-related kinases 1/2 (ERK 1/2), c- Jun amino (N)-terminal kinases 1/2/3 (JNK1/2/3), p38 isoforms $\alpha/\beta/\gamma/\delta$ (p38 $\alpha/\beta/\gamma/\delta$), and ERK5 (Cargnello and Roux, 2011a, Chang and Karin, 2001). There are also atypical MAPK groups, which comprise ERK 3/4, ERK 7 and Nemo-like kinase (NLK) (Cargnello and Roux, 2011a). Among MAPK groups, particular focus has been given to the study of ERK 1/2, JNKs and p38 isoforms. The signaling pathways for MAPKs consist of at least three steps: a MAP kinase kinase kinase (MAP3K), a MAP kinase kinase (MAP2K), and a MAPK (Roskoski, 2012). MAPK activation results in phosphorylation of certain transcription factors and proteins, which lie downstream and facilitate the cellular functions of these kinases. Of particular relevance here is the activation of IL-6 transcription by nuclear p38 and possibly JNK during Ca^{2+} - dependent muscle contraction ((Chan et al.,

2004b) and Section 1.7.1). In addition to the kinases themselves, there are a number of scaffolding proteins that interact with one another and with the kinases to transduce signals and promote the different cell functions (Roskoski, 2012). For example, the scaffolds involved in the signalling pathway for ERK 1/2 are kinase suppressors of Ras (KSR) and MP1, while the JNK-interacting protein group (JIP) are the scaffolds for the JNK pathway.

1.12.1 ERKs

The primary structure of ERK 1 and 2 proteins shows approximately 83% amino acid sequence homology, as well as sharing almost the same biochemical function (Roskoski, 2012). They are expressed in many tissues, such as skeletal muscle, the brain, and the heart (Cargnello and Roux, 2011a). ERK can be activated by several stimuli, including growth factors like platelet-derived growth factor (PDGF), epidermal growth factor (EGF), and insulin. While human ERK 1 is composed of 379 amino acids, rat and mouse ERK 1 enzyme is composed of 380 amino acid residues. ERK 2 consists of 360 amino acid residues in humans and 358 residues in rats and mice. The activation of ERK MAP kinase starts when an extracellular signal such as EGF activates a transmembrane receptor tyrosine kinase (RTK). This leads to the recruitment of growth factor receptor-bound protein 2 (Grb2), which will eventually be combined to the guanine nucleotide exchange factor son of sevenless (SOS) (Ramos, 2008). During the next stage, SOS binds to RAS which will then be converted to an active form by the removal of the guanosine diphosphate (GDP) from RAS, which is replaced by guanosine-5'-triphosphate (GTP). Downstream phosphorylation signals then lead to the activation of RAF, MEK and ERK (Ramos, 2008). Following this activation by phosphorylation, ERK is released from MEK and regulates a number of important functions in the nucleus, including transcriptional regulation of gene expression. ERK activation has been shown to occur in skeletal muscle following physical exercise. For instance, a study performed in humans found that ERK 1/2 was highly phosphorylated in the skeletal muscle of people who performed resistance exercise in comparison to those who did not (Williamson et al., 2003).

1.12.2 JNKs

JNK has been described as a prime example of a stress-activated protein kinase (SAPK) and is considered as a member of the cycloheximide activated-MAP-2 kinase family, which can be affinity purified by using *c-Jun* protein bound to beads (Hibi et al., 1993, Kyriakis and Avruch, 1990). Stress stimuli enhance the phosphorylation of JNK through Threonine and Tyrosine residues, as has also been found in ERKs (Kyriakis et al., 1991, Kyriakis and Avruch, 1996).

There are three isoforms of JNKs, JNK1, JNK2 and JNK3, which can also be called SAPK γ , SAPK α and SAPK β respectively (Cargnello and Roux, 2011a). There is more than 85% sequence similarity between the JNK isoforms, which are encoded by three genes encoding proteins with molecular weight that ranges from 46 to 55 kilo Dalton. JNK1 and JNK2 can be found in many tissues in the body, but JNK3 is limited to a small number of isolated locations, including neuronal tissue and cardiac myocytes (Cargnello and Roux, 2011a). Different stimuli can lead to the activation of JNKs such as cytokines, heat shock and UV irradiation. JNKs play an important role in the regulation of gene expression through phosphorylation of *c-Jun* due the fact that it is part of the activated protein 1 (AP-1) complex, which is responsible for controlling cytokine gene expression (Johnson and Lapadat, 2002) including the IL-6 gene in which AP-1 is one of the *cis*-acting factors which binds to a key 1.2kb fragment within the 5'-flanking region of the IL-6 gene (Figure 1.3). AP-1 is a heterodimer protein, which consists of proteins belong to Jun, Fos, Maf and ATF families (Johnson and Nakamura, 2007). AP-1 can be stimulated in response to a variety of different environmental stimuli, many of which are the same as those that lead to the activation of JNKs. The activation process of the JNK pathway begins when stimuli, such as cytokines, interact with their receptor in the cell surface. This is followed by MAP3K activation (Weston and Davis, 2007). After that MKK4 and MKK7, which are isoforms of MAP2K, are activated, followed by the activation and phosphorylation of JNK. Eccentric contraction in human skeletal muscle has also been demonstrated to lead to higher activity of JNK phosphorylation than occurs with concentric contraction (Boppart et al., 1999).

1.12.3 p38 isoforms

There are four isoforms of p38; p38 α , p38 β , p38 γ and p38 δ , the best known of which is p38 α , because of its existence in many cell types (Johnson and Lapadat, 2002). Many stimuli have been found to lead to the activation of p38, including osmotic shock, heat shock, mechanical stress and inflammatory cytokines (Johnson and Lapadat, 2002, Boppart et al., 2001). The activation of p38 begins when a stimulus such as IL-1 leads to the recruitment of TNF Receptor-Associated Factor-6 (TRAF6), which in turn causes the activation of MAPK kinase kinases (MAP3K) and the phosphorylation of Transforming growth factor beta-activated kinase 1 (TAK1) and then finally the activation and phosphorylation of p38 through MKK3 and MKK6 activation (Cuenda and Rousseau, 2007). In mouse myoblast cell line C2C12, p38 was found to be an important MAPK that can lead to the differentiation of myoblasts to myotubes (Cuenda and Cohen, 1999). Blocking p38 with a pharmacological inhibitor has been

shown to prevent myoblasts from transforming to myotubes. Inhibition of p38 has been suggested as a therapeutic target in RA, which is characterised by a dysregulation of pro-inflammatory cytokines such as TNF- α , IL-1 and IL-8 (Thalhamer et al., 2008). There was a detectable phospho-activation of p38 in rat skeletal muscle in response to resistance exercise, and in humans in response to cycling exercise (Chan et al., 2004b) suggesting that p38 is activated in response to the mechanical stress of muscle contraction (Boppart et al., 2001).

1.13 *In vitro* cell stretching

In their review of *in vitro* models of skeletal muscle stretching, Passey et al. (2011) state that “skeletal muscle tissue possesses a high degree of plasticity in that it has the ability to adapt specifically to the functional demands placed upon it or alterations in its environment”. It does this by reacting to variation in numerous factors, including the availability of specific amino acids, neuronal stimulation, the levels of cytokines or growth factors, or mechanical loading. This last variable represents the type of stress that can occur during resistance training or moderate exercise (Passey et al., 2011). In response to these stimuli, the muscle increases protein synthesis, which facilitates improved metabolism and muscle contraction capacity, which in turn results in eventual muscle hypertrophy. As it is widely believed that *in vitro* models (and some commonly used *in vivo* models) may be unable to accurately represent the normal physiological responses to exercise training, studies have tended to utilise human subjects and animal models to examine the molecular mechanisms that enable this kind of adaptive process (Spangenburg, 2009, Passey et al., 2011). However, in pursuit of experimental environments that allow for accurate control of study variables, it is desirable to develop *in vitro* model systems that are able to effectively model *in vivo* conditions (Passey et al., 2011). The most successful of these model systems have important similarities with muscle *in vivo*, as outlined below.

The most important tissue in glucose uptake and homeostasis *in vivo* is skeletal muscle (Abdul-Ghani and DeFronzo, 2010, Passey et al., 2011). Observations of muscle performance conducted *in vitro* and *in vivo* have noted that during exercise there is an increase in glucose uptake (Rose and Richter, 2005) and lactate efflux, and this has reproduced *in vitro* through application of the Vandeburgh system of stretch-relaxation protocols to muscle cultures. This was originally described in embryonic chicken myotube cultures mounted on a stretchable elastic membrane (Hatfaludy et al., 1989). *In vitro* stretch also enabled a calcium-dependent mechanism for glucose uptake to be demonstrated in skeletal muscle cells (Iwata et al., 2007),

which has been supported by *in vivo* studies of post-exercise calcium mediated glucose uptake (Santos et al., 2008).

In vitro and *in vivo* stretching of skeletal muscle can lead to the activation of many growth factors that eventually lead to the enhancement of protein synthesis and cell growth (Rauch and Loughna, 2005a). Stretching mouse C2C12 myocytes using passive static stretch tools (static Loughna cell stretching assemblies (Rauch and Loughna, 2005b, Rauch and Loughna, 2008b)) shows that p38 phosphorylation is increased in stretched cells when compared to the levels in non-stretched cells (Rauch and Loughna, 2005a). The previous findings of Boppart et al. (2001) in a study of rat skeletal muscle *in vivo* after resistance exercise showed that p38 also undergoes increased phosphorylation *in vivo* (Boppart et al., 2001) and this has also been observed following cycling exercise in humans (Chan et al., 2004b).

The development of skeletal muscle cells *in vitro* has many of the same patterns as *in vivo*, including increased levels of organizing muscle-specific proteins and the conversion of satellite cells to mature working multinucleated contractile myotubes (Stockdale and Miller, 1987, Vandeburgh et al., 1989). A study of skeletal muscle *in vitro* can be used in terms of measuring protein turnover regulation and cell proliferation (Vandeburgh et al., 1989). Mechanical stimulation through repetitive intermittent stretch-relaxing computerised tools was used *in vitro* in avian tissue culture, showing elevated protein synthesis and reduced protein degradation, which supports *in vivo* studies that show mechanical activity can increase protein synthesis (Vandeburgh et al., 1989, Hornberger et al., 2006b). The response of passive stretching on skeletal muscle *in vitro* has been shown to have the same response patterns as *in vivo* and organ-cultured skeletal muscle (Vandeburgh et al., 1989).

C2C12 skeletal myotube cultures have also been stretched using a commercial vacuum-driven Flexercell (FX-3000) device to investigate the way that glucose uptake is affected by the 5' adenosine monophosphate-activated protein kinase (AMPK), which is considered as a metabolic sensor in skeletal muscle (Chambers et al., 2009a). In this way, stretching was shown to stimulate glucose uptake depending on p38 activity: when p38 was blocked with the inhibitors SB203580 and A304000 the glucose uptake was reduced; whereas the glucose uptake was not affected when AMPK- α and PI3-K/Akt were inhibited.

Mechanical activity can lead to variation in protein synthesis, as there is a reduction during heavy muscular activity followed by an increase that depends on the availability of amino acids (Atherton et al., 2009b). In order to understand the mechanism behind this, Atherton et al.

(2009) used cyclic stretching to mimic eccentric contraction utilising myotubes that were differentiated from L6 skeletal myoblasts and plated in type I collagen coated Bio-flex six-well Flexcell plates (Atherton et al., 2009b). A computerised vacuum system then performed cyclic stretching using a Flexercell FX4000T (Flexcell International). Time was shown to play an important role in increasing protein synthesis in accordance with increases in mTOR, P70S6K, and 4E-BP1 post-exercise (Atherton et al., 2009a). Hornberger and Chien (2006) performed a study on skeletal muscles (*ex vivo*), which were stimulated by intermittent mechanical stretching, leading to increased protein synthesis in accordance with high activity of the phosphorylation of P70S6K. Since the bulk of this project will test different conditions using *in vitro* stretching, it should be noted that previous papers found that *in vivo* and *in vitro* stretching outcomes match in many parameters. For instance, Dreyer et al. (2006) observed that the level of protein synthesis was lower during resistance exercises in human subjects and was elevated post exercise (Dreyer et al., 2006). The same finding was also observed using *in vitro* stretching using cyclic cell stretching, as discussed above (Atherton et al., 2009b). Resistance exercise was also shown to increase mTOR activity (Dreyer et al., 2010), which supported the observation that passive stretching of skeletal muscle *ex vivo* can increase mTOR activity (Hornberger et al., 2004). Furthermore, there was an increase of glucose metabolism within human subjects who performed as mentioned earlier (Rose and Richter, 2005, Passey et al., 2011), which supported the observation by (Hatfaludy et al., 1989), which used an *in vitro* cell stretching model.

The commonly available commercial Flexercell system (see Chapter 2) for cell stretching uses a partial vacuum applied under a stretchable culture plate to stretch cell monolayers. An advantage of this system is that it is convenient, using commercially available multi-well plates rather than relatively fragile stretchable elastic membranes mounted in stretching frames (Hatfaludy et al., 1989) or myotubes stretched in a 3-dimensional collagen gel matrix (Powell et al., 2002, Cheema et al., 2003, Passey et al., 2011). While the latter provide an excellent physiological environment of extracellular matrix, they are difficult to use for experiments which require rapid physical access to the cells, for example in amino acid transport studies using radio-labelled amino acid and rapid rinsing of the cells.

A potential limitation of the Flexercell vacuum system however is that (by definition) applying a partial vacuum in a cell culture incubator reduces the oxygen and carbon dioxide concentration under the stretched cell monolayer, thus possibly affecting oxygenation and pH buffering; and vacuum could in principle also lead to vacuum cooling (Annaratone et al., 2013).

For this reason, the work described in this thesis compares three systems for stretching cells on Flexcell silicone plates (Chapter 2) i.e. (1) an *in vitro* model of continuous mechanical stretch in L6 skeletal muscle cells (using static Loughna cell stretching assemblies) (Rauch and Loughna, 2008b); (2) a vacuum-driven “Pull” system, generating a partial vacuum under the culture wells using a Flexercell system (FX-4000) and (3) using a purpose-built mechanical “Push” system which did not involve the potential confounding factor of a vacuum during stretching.

1.14 The choice of the *in vitro* model of skeletal muscle used in this project

For *in vitro* studies, a common approach is to utilise *ex vivo* muscle preparations, using refined myograph systems (e.g. Kent Scientific, Torrington, CT, U.S.A.) to mechanically stimulate isolated rodent skeletal muscle (Hornberger et al., 2004). A key issue with such *in vitro* preparations is that they lack a physiological blood supply and may therefore suffer from hypoxia, unless small bundles of isolated muscle fibres are used. However, the isolated fibre bundle preparation method requires micro-dissection, which is extremely time- and labour-intensive (Wendowski et al., 2017).

Human myotubes are also an excellent cell culture model for skeletal muscle studies and have been widely used in the literature, although variation between donors potentially increases the degree of variation in the system. These myotubes can be isolated from dormant satellite cells in adult skeletal muscles using either enzymatic digestion or cell migration from intact tissue (Aas et al., 2013), after which they can be differentiated *in vitro* into multinucleated myotubes. The capacity of human myotubes to grow, differentiate and undergo passaging is also more inconsistent, limited, and variable than in immortalised cell lines (Aas et al., 2013). These issues are exacerbated over time, with increasing passage numbers seeing a corresponding decline in their morphology, metabolic capacity and the ability to fuse to form myotubes (Aas et al., 2013). Previous studies have found that human skeletal muscle myotubes require stimulation by neuronal contacts in order to achieve spontaneous contraction (Aas et al., 2013). Similar observations have almost been made regarding the inability of rodent cell cultures to achieve spontaneous contraction (Guo et al., 2014).

Due to the aforementioned limitations, studies extensively rely upon myotubes grown from immortalised myoblast cell lines e.g. the L6 rat myoblast line and C2C12, a mouse myoblast line, (Philp et al., 2010, Philp et al., 2011). However, C2C12 myotubes are only of limited use in studies of acidosis-induced protein degradation, because they cause rapid acidification of the

culture medium. Lower acidification rates were found with the L6 sub-clone L6-G8C5 (Bevington et al., 1998a). It is possible to obtain highly differentiated L6-G8C5 myotubes by pre-treatment using retinoic acid and IGF-1 (Elsner et al., 1998). However, the present study did not utilise this approach as previous work from this laboratory (Pickering et al., 2003) suggested that they give a limited response to some catabolic stimuli for example glucocorticoid and acidosis (low pH). Pilot experiments in this laboratory (Dr E Watson – personal communication) indicate that cultured human myotubes may fail to show the protein catabolic response to acidosis that is observed in humans *in vivo* (Reaich et al., 1993). For this reason, the present study used spontaneously fused L6-G8C5 myotubes, which this laboratory has previously demonstrated shows a marked protein catabolic response and impaired protein synthesis in response to low pH, and expresses SNAT2 pH sensitive amino acid transporters as the predominant isoform of System A amino acid transporter (Evans, 2009, Blbas, 2018, Evans et al., 2007b, Evans et al., 2008b).

1.15 Hypothesis

The hypothesis to be tested in this project (using L6-G8C5 rat skeletal muscle cells as a pH-responsive *in vitro* model) is that the expression and biosynthesis of IL-6 in skeletal muscle cells is:

- a) stimulated by FAK and MAP kinases (p38 and JNK) and dependent on the System A/SNAT2 amino acid transporter, and
- b) inhibited by low extracellular pH acting through an inhibitory effect on MAP kinase activation and on System A/SNAT2 transporters

This hypothesis is summarised in the pictorial scheme shown in Figure 1.7.

This is of potential clinical and physiological importance because it provides a possible molecular explanation for the reported suppression of the release of IL-6 from exercising skeletal muscle following lactic acid accumulation that has been reported in patients who are prone to lactic acidosis owing to mitochondrial myopathy (Steensberg et al., 2001b). Whether the lactate anion itself contributes to this effect is unknown, but a possible explanation is that lactic acidosis (and its associated fall in muscle pH) may play a role. If this is true, an impaired IL-6 response to exercise may also occur in other acidotic patients (for example those with CKD) or in individuals who show marked lactic acidosis in response to exercise.

The model in Figure 1.7 is based on the following principal experimental observations that were reviewed above:

- The inverse correlation between the plasma concentrations of IL-6 and lactate following exercise in patients with mitochondrial myopathy (Steensberg et al., 2001b)
- The observation that p38 MAPK activation in L6 myotubes is a potent stimulator of IL-6 mRNA expression (Chan et al., 2004a).
- Studies of patients with CKD which showed depletion of free amino acids present in muscles *in vivo* following walking exercise, and the prevention of this effect by administering bicarbonate supplements to minimise acidosis (Watson et al., 2013).
- Evidence that inhibition of System A/SNAT2 transporters in L6-G8C5 cells by low extracellular pH depletes free amino acid pools in the cells, impairs mTORC1 signalling and global protein synthesis, and is mimicked by pharmacological inhibition or siRNA silencing of System A/SNAT2 (Evans et al., 2007b).
- Evidence that exercise *in vivo* activates p38 (Boppart et al., 2001).and JNK (Boppart et al., 1999) and System A transport activity(Henriksen et al., 1992, Henriksen et al., 1993, King, 1994).

The model in Figure1.7 was also supported by the following pilot data that was available in this laboratory at the start of this project:

- A preliminary observation of impaired phospho-activation of JNK in cultured L6-G8C5 myotubes following incubation at low extracellular pH (Evans K.F. - unpublished observations)
- An unpublished observation of inhibition of System A/SNAT2 transport activity in L6-G8C5 myotubes following pharmacological inhibition of JNK or p38 MAP kinase (Blbas, 2018).
- The observation using L6-G8C5 myoblasts, that siRNA silencing of SNAT2 can impair phosphoactivation of the MAP kinase JNK (Blbas, 2018).
- A trial of the effect of prolonged (17 or 48h)mechanical stretching of L6-G8C5 myotubes which showed an apparent stimulation of System A/SNAT2 transport activity (Clapp, 2010).

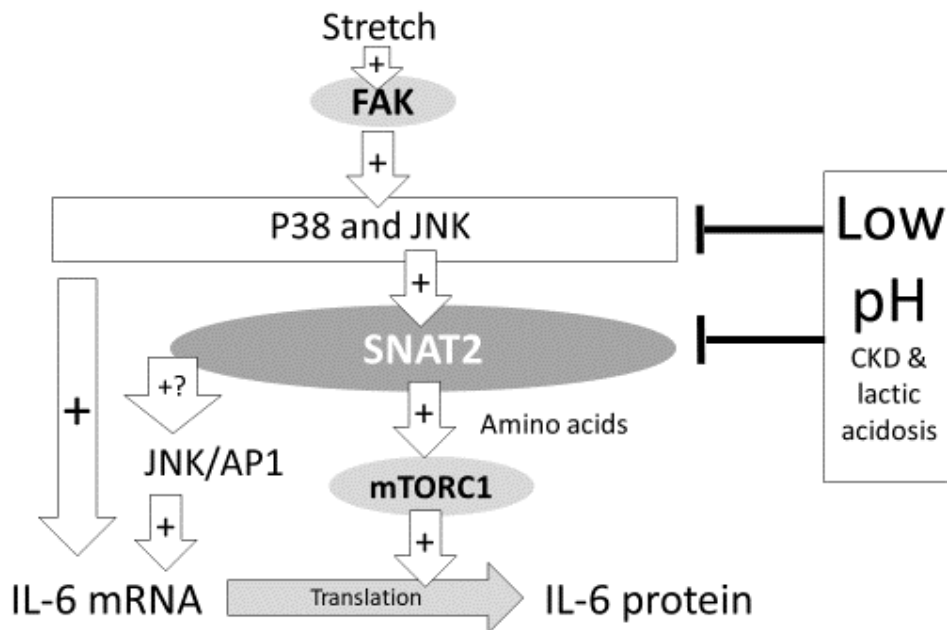


Figure 1.7. Schematic diagram showing how SNAT2, mechanical stretch and MAPK activation may be linked, and impaired by low pH, in L6-G8C5 cells.

The experimental aims of this study were to test the model in Figure 1.7 in L6-G8C5 cells in 3 phases as follows:

- 1) Chapter 3 to assess the effect of pharmacological inhibition of MAPKs on System A (SNAT2) amino acid transport activity in L6 skeletal muscle cells, to determine the effect of mechanical loading on MAPKs, and to observe the effect of low pH on these MAPKs.
- 2) Chapter 4 to set up 3 *in vitro* models of mechanical stretch and use these to reproduce and characterise further the apparent System A/SNAT2 activation by *in vitro* cell stretch that had been reported in pilot experiments (Clapp, 2010).
- 3) Chapter 5 to reproduce the previously reported p38 MAP kinase-dependent stimulation of IL-6 mRNA expression in L6 myotubes in response to ionomycin (Chan et al., 2004b), and to use this experimental system to investigate the effects of low pH predicted in Figure 1.7.

Chapter 2: Materials and Methods

2.1 General materials and reagents

All chemicals and reagents, including those of molecular grade, were purchased from Sigma unless explicitly stated otherwise. The following sources were utilised in the acquisition of sterile consumables for tissue culture: Petri dishes and 35 mm diameter 6-wells (Thermo Scientific); 96 well plates (Sarstedt); 22mm diameter 12-well plates (non-pyrogenic sterile polystyrene) (Corning Costar); and type I collagen coated Bio-flex 6-well plates (ref. BF-3001C, Flexcell International Corporation, NC, USA).

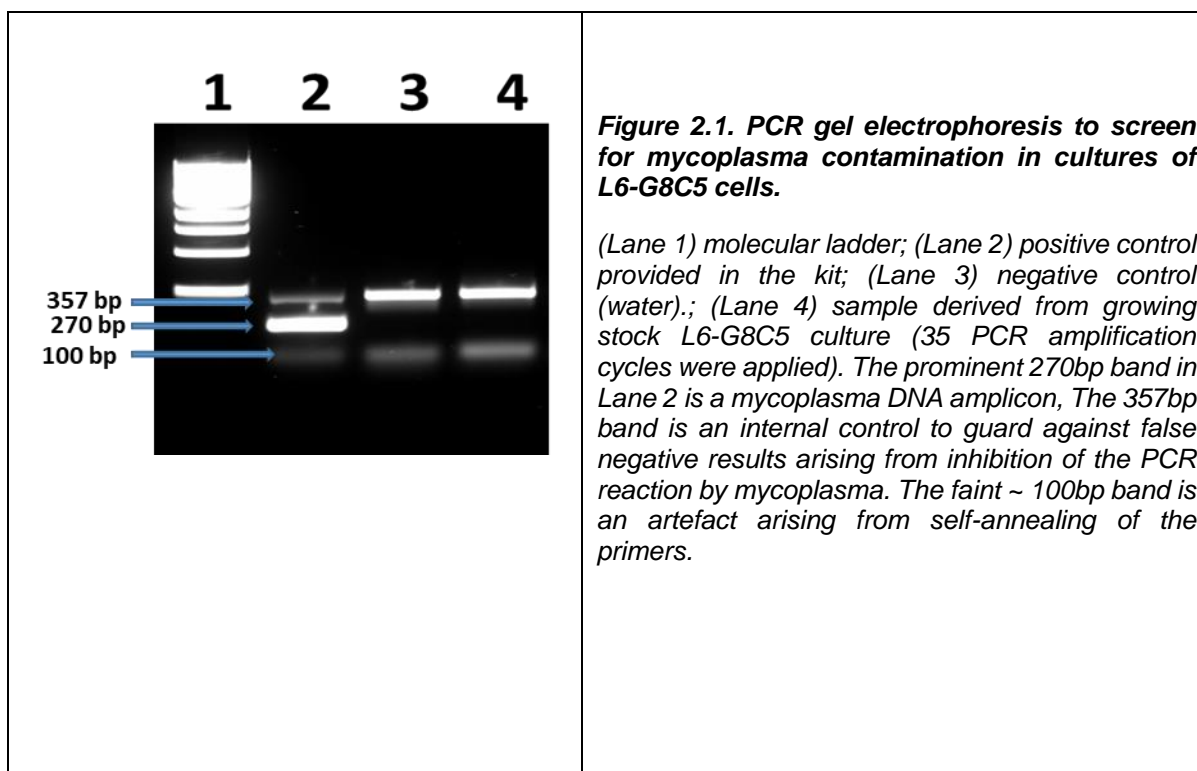
2.2 Cell culture models

2.2.1 L6 cells

L6-G8C5 is a sub-clone of the rat skeletal muscle cell line L6 (Yaffe, 1968). The justification of this choice of culture model is described in detail in Section 1.8, Chapter 1. When cultured in a low serum medium, L6-G8C5 fuses to form myotubes (Elsner et al., 1998). This skeletal muscle cell model has been used in the investigation of experimental manipulations, such as acidosis and their effects on global protein metabolism in muscle (Bevington et al., 1998b, Bevington et al., 2001, Bevington et al., 2002, Pickering et al., 2003, Evans et al., 2008a, Evans et al., 2007a, Clapp, 2010, Atherton et al., 2009a, Blbas, 2018), making it highly suitable for the current study. In addition, it is simple to culture L6-G8C5, and SNAT2 is strongly expressed in these cells (Evans, 2009). Stocks were acquired from ECACC (European Collection of Animal Cell Cultures) (ref. 9212111) and were used at passage number (10-20).

2.2.2 Screening cultures for mycoplasma contamination

Stock cultures were screened for mycoplasma contamination using the EZ-PCR Mycoplasma Test Kit (GENEFLOW; 20-700-10). The assay was done as described in the manufacturer's instructions. The assay relies on PCR amplification of a mycoplasma-specific region in the 16S rRNA gene, followed by agarose gel electrophoresis to detect amplified DNA fragments. The assay detects 96 mycoplasma species as well as acholeplasma and spiroplasma species according to the manufacturer's stated assay specificities.



2.2.3 L6-cells, maintenance and passaging

The cells were plated in 9cm Petri dishes at 10×10^4 cells per Petri in Growth Medium (GM), comprising Dulbecco's Modified Eagle Medium (DMEM-Life Technologies 11880-028) (Appendix A.1), which contains 5mM D-glucose and added pyruvate, supplemented with 10mg Phenol Red/l (Sigma-P5530), 100U/ml Penicillin G, 100µg/ml Streptomycin, 2mM L-glutamine and 10% v/v batch-tested foetal bovine serum (FBS) that had been heat inactivated at 56°C for 30 minutes before use. The plated cells were then grown in a culture incubator under humidified air at 37°C, 5% CO₂ until they reached ~80% confluence, after which they were passaged. (Care was taken to ensure that propagating stocks were not allowed to become confluent as this leads to formation of non-proliferating fused myotubes, thus eliminating the most myogenic cells from the population). For passaging, the GM was aspirated and each Petri dish was rinsed with 5ml of (1x) Hank's Balanced Salt Solution (HBSS, Life Technologies-1754651) (Appendix A.3), then incubated with 2ml of (1x) Trypsin-EDTA (T/E) (Invitrogen 25300) for 10 min at 37°C in the culture incubator to detach the cells from the Petri. The cells were re-suspended in 10ml of the GM described above and centrifuged at 500g for 5 minutes. After this, the supernatant was discarded, the cell pellet was re-suspended in 10ml of GM, and the suspension counted using a haemocytometer and re-plated at 10×10^4 cells/9cm Petri dish in 15ml of GM for the maintenance of stock cells.

2.2.4 Preparing L6 myoblasts for experiments

Certain experiments utilised unfused L6 myoblasts (i.e. those that had not formed myotubes from prior fusion of the cells) by seeding at a plating density of 43×10^4 per well on Bio-flex 6-well plates of the required size containing the GM (see Section 2.2.3). Cells were left in GM for three days before performed experiments.

2.2.5 L6-myotube formation

To obtain differentiated myotubes for experiments, the requisite L6 myoblasts were cultured in GM at the plating density noted above (see Section 2.2.4) (Figure 2.2A), then the serum content of the medium was reduced to 2% after 72 hours. The GM was aspirated and the ~70-80% confluent cultures were incubated in Minimum Essential Medium (MEM) (Invitrogen 21090-022), supplemented with 100U/ml Penicillin G, 100 μ g/ml Streptomycin, 2mM L-glutamine and 2% v/v heat inactivated foetal bovine serum (FBS) to induce fusion and formation of myotubes. The cultures were provided every two days with fresh medium (2% FBS in MEM, as described above), until day 8, when the myotubes were ready for experimental incubations (Figure 2.2.B).

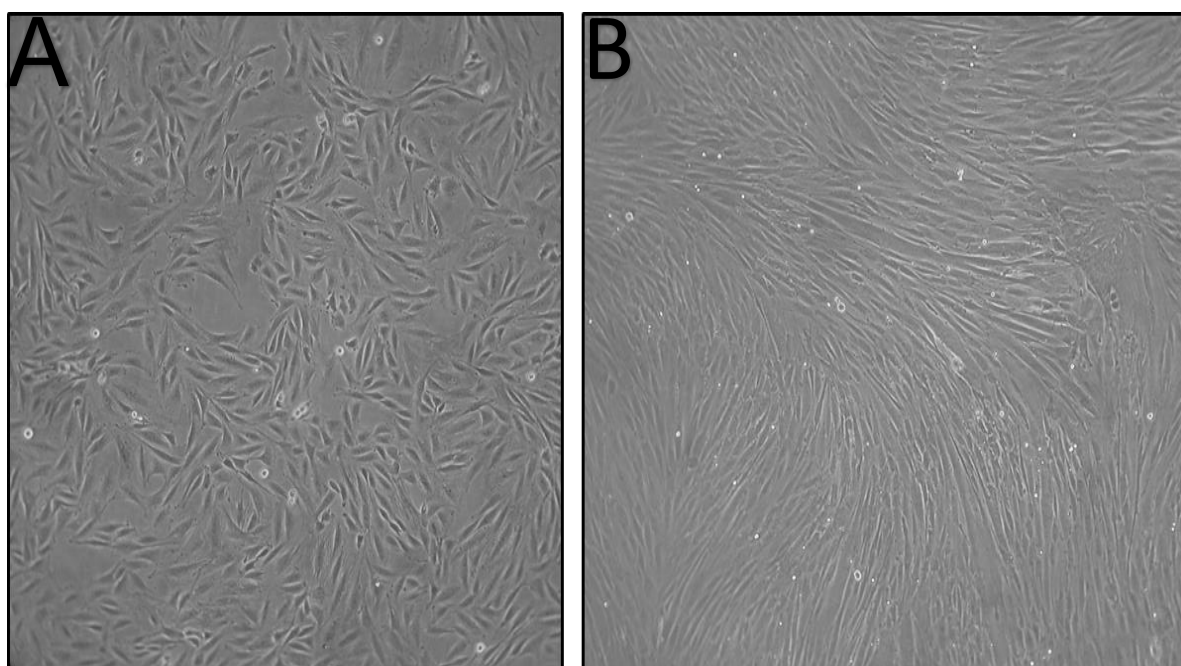


Figure 2.2. Photographs of L6-G8C5 cells.

(A) Sub-confluent L6-G8C5 myoblasts following 3 days of incubation in Growth Medium with 10% v/v foetal bovine serum (FBS). (B) L6-G8C5 myotubes after 3 additional days of incubating L6-myoblasts with 2% FBS in MEM, 100X magnification.

2.3 Passive continuous stretch technique

The process utilised in the current study was adapted from the approach described by Rauch and Loughna (Rauch and Loughna, 2008a) (Figure 2.3). This involved the seeding of L6-G8C5 cells on 35mm type I collagen coated Bio-flex 6-well plates (Flexcell International Corporation, NC, USA, BF-3001C). After they had fused to form myotubes, a series of 15mm diameter glass marbles embedded in a block of Perspex (one marble per well) was placed underneath each of the wells (as shown in Fig 2.3A). Then, a 3kg weight was placed on top of the culture plate, creating an approximately 18% linear stretch of the culture surface. The linear stretch was calculated as described in (Rauch and Loughna, 2008a) by measuring the vertical movement of the culture plate (using a mm rule) and the known radius of the culture well (and then applying Pythagoras' Theorem). The relationship between vertical movement, % stretch and the weight applied in Kg is shown in Fig 2.4B (Clapp, 2010).

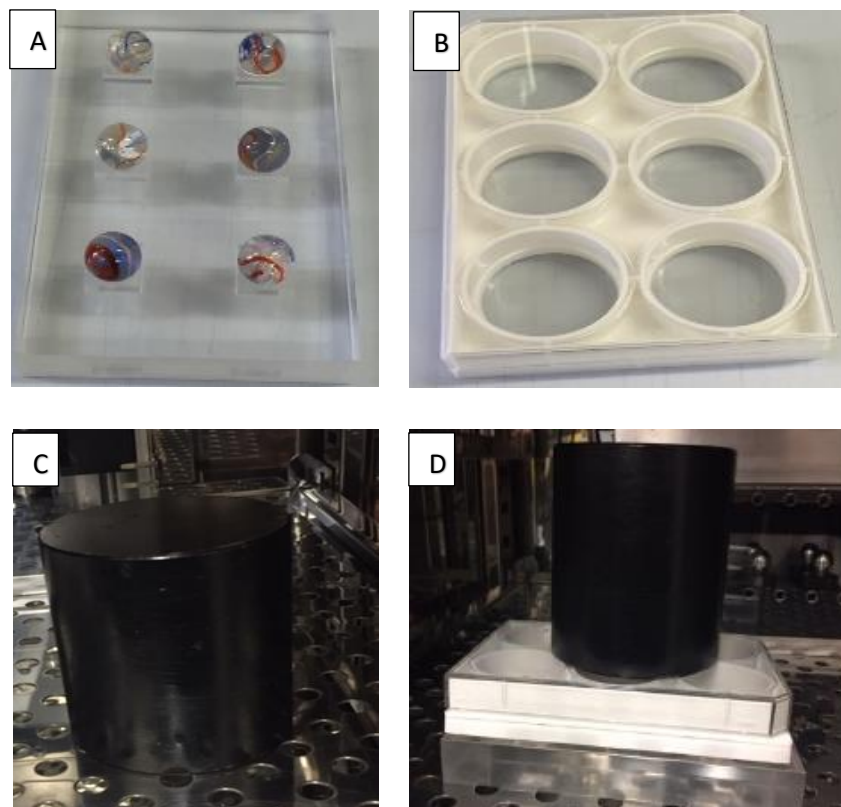


Figure 2.3. The *in vitro* model of continuous mechanical stretch comprising.

A) Marbles embedded in a block of Perspex, B) A 35mm type I collagen coated Bio-flex well plate,. C) a 3kg weight. D) the complete assembly with all components in place.

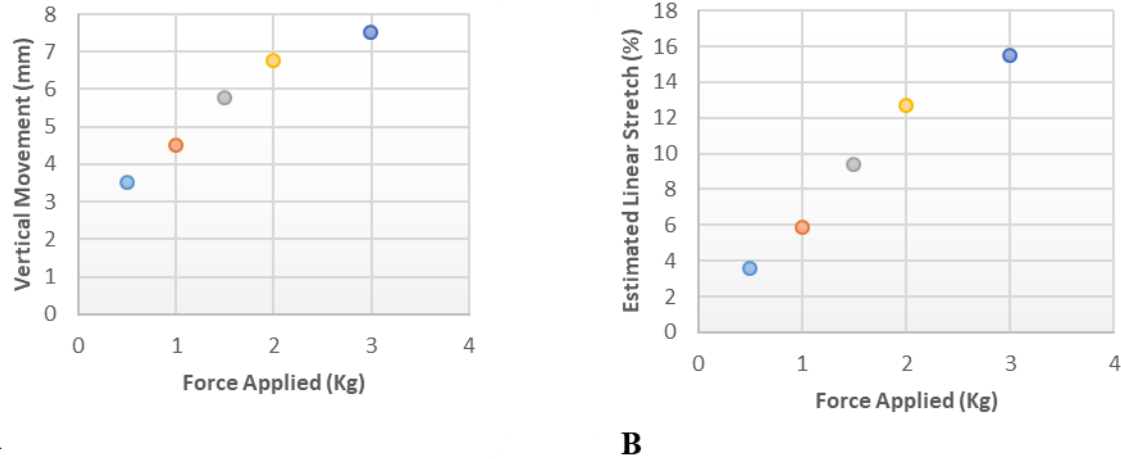


Figure 2.4. Estimation of linear stretch of the cultures in the previous figure. (A) the proportional relationship between the measured vertical movement of the highest point on the culture surface and the loads applied to the top of the culture plate. (B) the estimated linear stretch of the L6-G8C5 myotubes. (Redrawn from (Clapp, 2010)).

2.4 Cyclic stretch by vacuum suction – the “pull” technique

L6-G8C5 cells were seeded on type I collagen coated Bio-flex 6-well Flexcell plates and stretched using a computer-controlled vacuum suction Flexercell Strain Unit FX-4000 (Flexcell International Corporation, NC, USA) (Figure 2.5). Cells were cyclically stretched using the protocol originally described in (Goto et al., 2003) comprising a 2 second sine wave stretch with a 4 second release that resulting in an 18% maximum stretch as shown in Figure 2.6. In each experiment, a second Flexcell plate of cells was simultaneously incubated on the same vacuum manifold under exactly the same conditions, but the orifice in the manifold through which the vacuum was drawn was blocked (as shown in Figure 2.5D) thus preventing stretching, in order to act as a negative control. This was done to control for any non-specific effects arising from mounting the Flexcell plate in the vacuum manifold e.g. local variation in temperature, humidity or pCO₂.

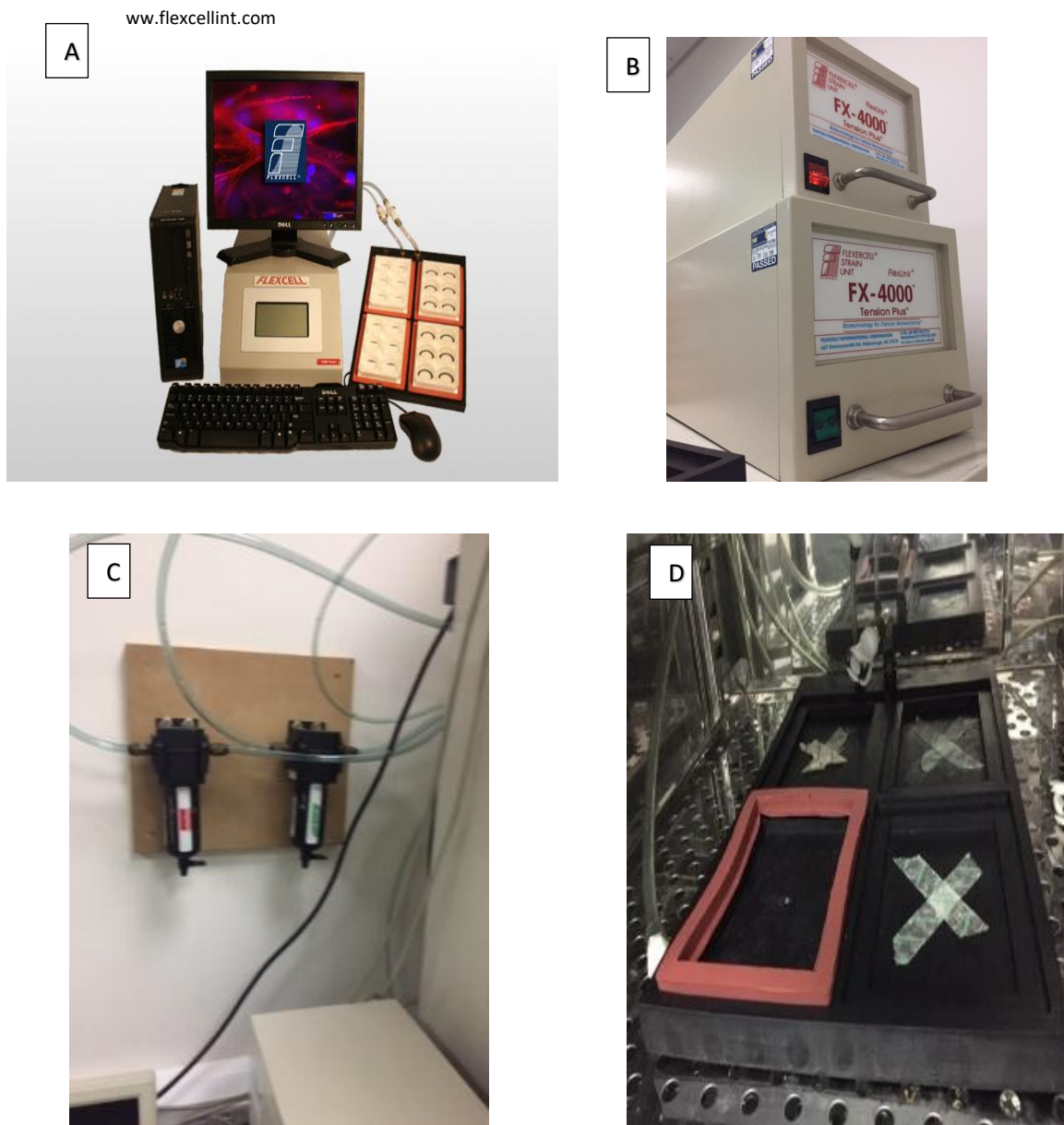


Figure 2.5. An illustration of the FX-4000 cell stretching system.

A) Overview of the system from the manufacturer's website (www.flexcellint.com); B) The strain control units coupled to a PC; C) The vacuum airflow regulators mounted between the vacuum pump and the vacuum manifold; D) The vacuum manifold mounted in the culture incubator, showing one of the red rubber seals in which the stretchable culture plate is mounted, and the adjacent mountings in which the vacuum orifice has been blocked with masking tape.

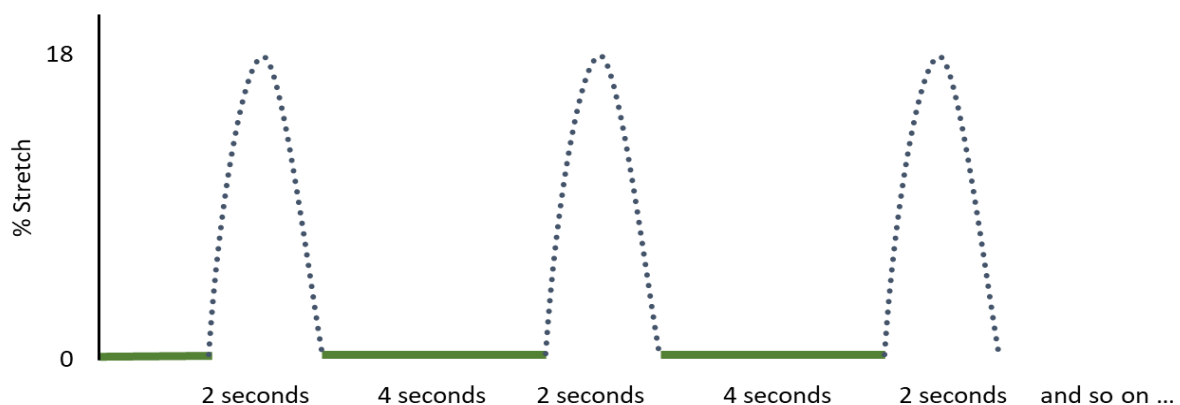


Figure 2.6. This figure shows the time course of the stretch applied to L6-G8C5 myotubes during cyclic stretch, comprising a 2 second sine wave stretch with a 4 second release resulting in a maximum 18% linear stretch (Goto et al., 2003).

2.5 Cyclic stretch by motor-driven pistons – the “push” technique

To allow mechanical stretch to be applied to Flexcell plates without the need for a vacuum-driven computer-controlled stretching system, a motor-driven system of pistons was designed to apply force to the stretchable culture surface by pushing from below. This was designed and manufactured in collaboration with Mr Praful Chauhan (Biomedical Joint Workshops Manager, Core Biotechnology Services, University of Leicester). Rather than pulling the cells attached to the membrane using negative pressure, as in the FX-4000, it instead pushes them upwards intermittently. This was done by mounting the Flexcell plate in a stationary black steel frame (Figure 2.7). Stretching was achieved (as in the static Rauch and Loughna method – Section 2.3) by vertical motion of pistons (capped with silver-coloured steel hemispheres) (Figure 2.7) and mounted on a cradle which was driven up and down by a direct-current (DC) motor. The amount of vertical travel of the steel hemispheres was adjusted to give the same amount of vertical displacement of the floor of the culture well as on the Rauch and Loughna assembly (Figure 2.4A). This vertical travel was adjustable by means of a screw thread under each steel hemisphere. The “up-delay” or “down-delay” in the motion of the cradle at its limits of travel was also adjustable by means of controls on the front of the instrument (Figure 2.7).

This allowed the time course of the stretch pattern to be adjusted to approximate to that of the vacuum system shown in Figure 2.6.



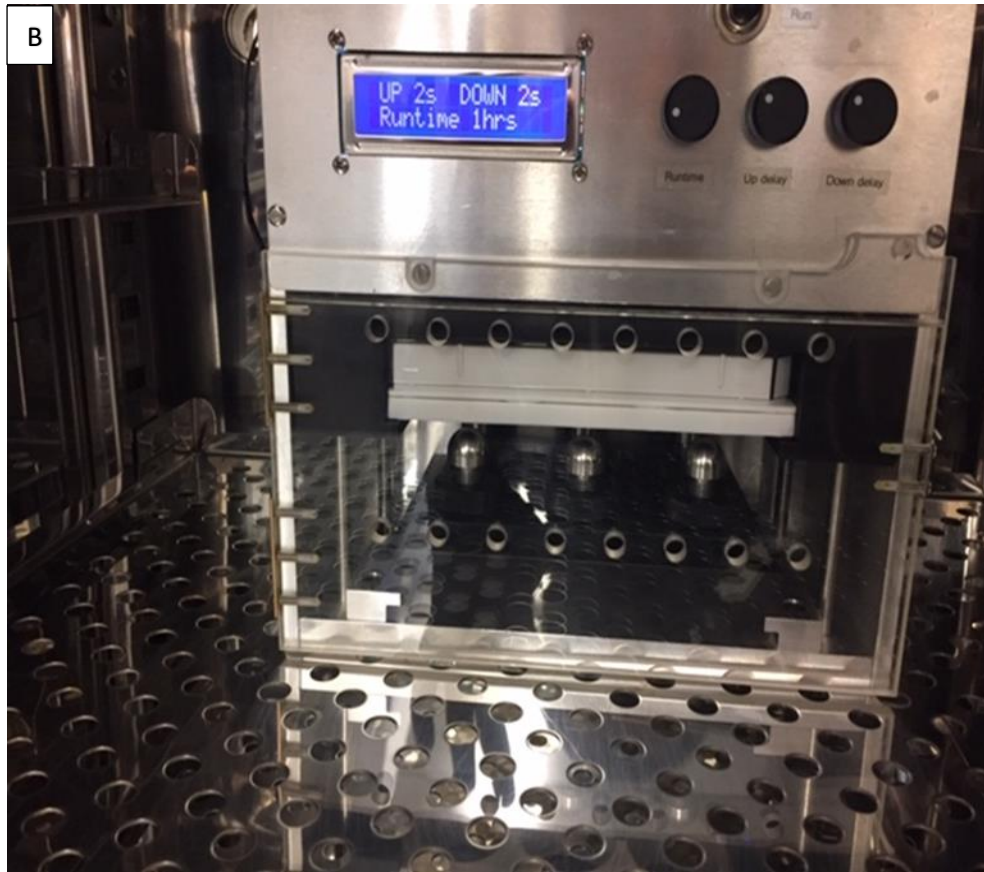


Figure 2.7. Images showing the push-based system for cell stretching driven by a direct-current (DC) motor .A) the push system mounted in the culture incubator with the culture plate removed to show the silver-coloured steel hemispheres on top of the pistons. The pistons are lowered in this image. The control unit which controls time and stretch regimens can be seen in the top half of the image. B) Showing the white Bio-flex culture plate mounted in its black steel frame, with the pistons partly raised underneath it.

2.6 Medium for experimental incubations

The basal medium utilised in creating the experimental test media was Minimum Essential Medium (MEM) (Invitrogen 21090-022) (Appendix A.2), which was supplemented with 100U/ml Penicillin G, 100µg/ml Streptomycin, and 2mM L-glutamine. When the test media required serum, the selected source was 2% v/v heat-inactivated Dialysed Foetal Bovine Serum (DFBS, Invitrogen ref 26400).

As MEM has an approximate pH of 7.33 in a 5% CO₂ atmosphere, and is further acidified to 7.26 when cultured for 24 hours with confluent L6-G8C5 myotubes (Table 1 in (Bevington et al., 1998b)) all experimental incubations at the physiological pH of 7.4 were conducted through the addition of an additional 8mM NaHCO₃ to the medium. To achieve pH values of 7.1 or 7.7, the pH was adjusted by addition of HCl or further NaHCO₃ respectively. As adding NaHCO₃ involves adding a Na⁺ load, the Na⁺ concentration was kept constant in such pH

variation experiments by addition of the required amount of NaCl. Other variations in the experimental test media are specifically noted in the figure legends in the results chapters.

2.7 Protein assays

Measurement of the total protein concentration of the cell cultures was carried out through the use of a Folin (Lowry) protein assay (Lowry et al., 1951). Protein in lysates intended for Western blotting was analysed using the BioRad Detergent Compatible (DC) assay (BioRad, UK, 500-0116).

2.7.1 Lowry Protein Assay

The total protein content of cell lysates in transport activity experiments was measured using the Lowry protein assay (Folin assay) (Lowry et al., 1951). The protein content in the samples was calibrated using BSA protein standards (Appendix B.4) made up at 0 to 500µg / ml in 0.5M NaOH. Each assay was conducted as follows: fresh Reagent C was prepared by combining Reagent A and Reagent B (see Appendix B.2 and B.3 respectively) in a ratio of 50:1 (A:B v/v); and Ciocalteu's Folin phenol reagent (Sigma F-9252) was 3-fold diluted with ultra-pure water in a ratio of 1:2 v/v. Then 600µl of Reagent C was added to 50µl of BSA standards or cell protein samples in 0.5M NaOH, and immediately vortexed. After exactly 10 min, 60µl of the diluted Ciocalteu reagent was added and vortexed again. Finally, the mixture was incubated at room temperature for 30 min. The OD was read at 650nm using a Titertek Multiskan Plus MKII spectrophotometer and the protein concentration of the samples was calculated by linear interpolation using the optical density of the protein standards.

2.7.2 Bio-Rad detergent-compatible (DC) protein assay

The Lysis Buffer (Appendix B.5.1) utilised in the preparation of cells for Western blotting (Section 2.9) contained detergent. As this interferes with the Lowry protein assay, a Bio-Rad detergent-compatible (DC) protein assay kit (Bio-Rad 500-0113) was utilised in measuring the protein content of the cell lysates for Western blotting. In this kit, Reagent A comprises an alkaline copper tartrate solution (with 20µl of supplementary reagent S added to each ml of reagent) and Reagent B, which is a diluted Folin-like reagent. The following process was used for the assay: 5µl of cell lysate or standards (0-2000µg/ml BSA in 1% IGEPAL detergent) was added to 96 well plates in triplicate, then 25µl of kit Reagent A and 200 µl of Reagent B was added to each well, and incubated at room temperature for 15 min. The absorbance was read at 750nm and the protein concentration in the samples was calculated using the optical density of the protein standards.

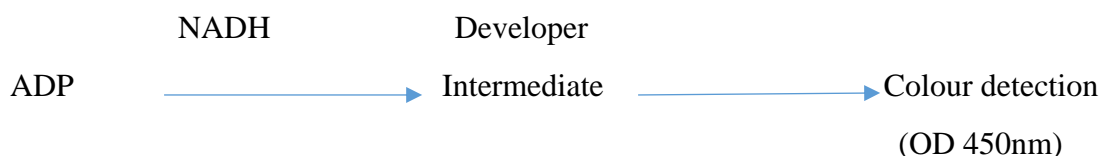
2.8 Enzyme-linked Immunosorbent assay (ELISA) for IL-6

Enzyme-linked Immunosorbent assay (ELISA) was performed for supernatants collected from L6 cell supernatants. An ELISA kit from R&D (R&D, R6000B) was used to measure IL-6 secretions under different experimental conditions. Standards were set up at 8 concentrations from 0 to 4000 pg/ml to create a calibration curve. Standards, samples and a recombinant IL-6 positive control were added to wells of 96-well plates which had been pre-coated with capture antibody (provided with kit R6000B), and incubated for two hours at room temperature. The solutions were then discarded and an ELISA washing buffer which was provided with the kit was used to wash the plates five times, following which a 100µl aliquot of an HRP conjugated anti-Rat IL6 antibody was added to each well and then incubated again for two hours at room temperature. The solutions were then discarded and the ELISA washing buffer was used to wash the plates another five times. After this 100µl of Substrate Solution was added to each well and then incubated for 30 min at room temperature and was protected from light. Finally, plates were read on a 96 well microplate reader (Varioskan Flash, ThermoFisher) at an assay wavelength of 450 nm and at a control wavelength of 540 nm to correct for turbidity in the wells. This 540nm turbidity measurement was subtracted from all of the 450nm values. The quantity of IL-6 produced in each well was calculated by interpolation from the standard curve. All samples were assayed in duplicate.

2.9 Creatine phosphokinase activity

A creatine phosphokinase (CPK) assay kit (abcam, ab155901) was utilised to investigate whether any of the tested conditions might lead to cell injury in L6 cells. This kinase can convert creatine to phosphocreatine and ADP. The assay is based on an NADH-linked enzyme reaction coupled to the rate of formation of ADP with generation of an intermediate which, in the presence of a developer, can then create a colour that is detectable at an OD of 450 nm. The stages of this reaction are as follows:

CPK



This assay was performed as follows. The supernatant was collected from each well. Standard solutions of NADH were set up using a 10mM NADH stock solution, to create a six point calibration curve. Standards, samples or a CPK positive control were added to each well of a 96-well microplate. Then, the reaction mix (CK assay buffer, CK Enzyme Mix, CK Developer, ATP and CK Substrate) was added and mixed in each well of the microplate. The wells were then incubated at 37°C for 40 min and read at an OD of 450 nm.

2.10 Transport activity assay (^{14}C MeAIB uptake measurement)

In order to assess the activity of System A amino acid transporters in intact cells, measurements were taken of the quantity of selective System A substrate α -[1- ^{14}C]-methylaminoisobutyric acid (^{14}C MeAIB) (NEN-Du Pont NEC 671) absorbed by the cells at room temperature in 5 min. After incubating the cells in 22mm culture wells using experimental test media modified for the purpose of each experiment, the cells were rinsed twice using 1ml of Hepes-buffered saline (HBS) (Appendix A.4), after which 500 μl of HBS was added to each well. The transport experiment was started by the addition of an aliquot of ^{14}C MeAIB, sufficient to create a final concentration of 10 μM ^{14}C MeAIB (21 kBq/ml) in the culture well. In some culture wells, 10mM unlabelled MeAIB (Sigma M-2383) was also present in the medium as a negative control to assess non-specific binding of ^{14}C MeAIB in the well. In order to mix the ^{14}C MeAIB with the medium, the plate was swirled immediately after the addition of the aliquot of ^{14}C MeAIB and incubated at room temperature (25°C) for exactly 5 min. Then the transport was immediately halted by placing the plate on a tray of ice. The medium was aspirated and the wells washed three times with 1ml of ice-cold 0.9% w/v NaCl. The cells were then rapidly checked under a phase contrast microscope to ensure that they were still attached to the wells, after which the plates were stored at -20°C until processed as described below.

2.10.1 Preparation of cell lysates for counting the radio-activity

After the transport activity incubation, cell lysates were prepared by scraping each well in 200 μ l 0.05M NaOH. The scrapings were then transferred into 1.5ml microcentrifuge tubes and incubated in a water bath at 70°C for 30 min to digest the cells. From the digested cells, 110 μ l was added to 4ml of Ecoscint A scintillant (National diagnostics LS-273), then incubated at room temperature for 2 hours in the dark to allow chemiluminescence to decay. Samples were counted with quench correction to determine the number of disintegrations per min (dpm) on an LKB 1219 liquid scintillation counter. The ^{14}C -MeAIB dpm count in the non-specific binding control cultures was subtracted from the count in the other cultures to determine level of net ^{14}C -MeAIB transport into the cells. The number of pmol transported was calculated from the ^{14}C -MeAIB specific radio-activity of 50pCi/pmol or 110dpm/pmol as was indicated by the manufacturer.

2.11 Measuring ^{14}C -urea as an intracellular water space marker

^{14}C -urea has previously been validated as a method for estimating cell water space in adherent cultures of mammalian cells (Burns and Rozengurt, 1983). To correct for trapped extracellular water in the rinsed monolayer cultures, more recent authors have also included a radio-labelled extracellular water space marker such as inulin in the assay (Chien et al., 2016). However, some cell lines yield negative apparent cellular water space if corrected with this extracellular marker, possibly indicating that it binds to extracellular matrix (A Bevington unpublished observations).

Cells were plated at 43×10^4 cells per well on 35mm diameter 6-well culture plates, in 2ml of Growth Medium (DMEM, Life Technologies 11880-028, which contains 5mM glucose and added pyruvate, supplemented with 10mg Phenol Red/L, 100 U/ml Penicillin G, 100ug/ml Streptomycin, 2mM glutamine and 10% v/v heat inactivated foetal bovine serum (HIA-FBS)). Cells were cultured for 3 days before commencing fusion to form myotubes.

Following the incubation of the cells in 35 mm culture wells in the required experimental test media the volume experiment was started by the direct addition of a aliquot of ^{14}C -urea (as for ^{14}C MeAIB in Section 2.10). In order to mix the ^{14}C -urea with the medium, the plate was swirled immediately after the addition of the aliquot of ^{14}C -urea and incubated at room temperature (25°C) for exactly 5 min. Then the transport was immediately halted by placing the plate on a tray of ice. The medium was aspirated and the wells washed three times with 1ml of ice-cold 0.9% w/v NaCl. The cells were then rapidly checked under a phase contrast

microscope to ensure that they were still attached to the wells, after which the plates were stored at -20°C until processed as described in 2.10.1.

2.12 Sodium Dodecyl Sulphate Polyacrylamide Gel Electrophoresis (SDS-PAGE)

2.12.1 Preparing the samples for SDS-PAGE

After completion of the required experimental incubation (described in the data Figure legends), the culture plates were immediately put on ice. Each 35mm well was then scraped in 200µl of pre-chilled Lysis buffer (Appendix B.5.1), then each lysate was transferred to a 1.5ml micro centrifuge tube on ice and centrifuged on a refrigerated micro centrifuge at 13,000 rpm for 10 min at 4°C to remove insoluble debris. This stage was followed by a Bio-Rad DC protein assay (Section 2.6.2) which sought to determine the quantity of cell lysate required to deliver 30µg of protein. The calculated amount of lysate was mixed with the same volume of SDS-reducing sample buffer (Appendix B.5.2), then the mixture was placed on a heating block (Grant QBT2) at 100°C for 5 min to denature the proteins and remove disulphide bridges.

2.12.2 Running the gel

Discontinuous Laemmli gels (Laemmli, 1970) (1.5mm thick with 12% polyacrylamide in the resolving gel) were arranged in an electrophoresis tank with a running buffer (Appendix B.5.5). The samples (Section 2.10.1) were loaded into the sample wells in the stacking gel, with molecular weight standards (Full-Range Rainbow MW Markers 10-250kDa, Fisher Ref 11580684) in one lane. The electrophoresis was then run on a Bio-Rad Mini-Protean® system at 200 volts until the bromophenol blue dye front neared the end of the gel.

2.12.3 Immunoblotting

After separation by SDS-PAGE, the proteins were blotted onto 0.45µm nitrocellulose membranes (Fisher Ref 10773485) in a wet transfer cell in a transfer buffer (Appendix B.5.4) at 80 volts for 2 hours. This was carried out in the presence of an ice block, with continuous stirring to ensure that the transfer remained cool throughout. The membranes were washed three times with x1 Tris-buffered Saline with 0.5% Tween 20 (TTBS) (Appendix B.5.6) and blocked with 5% w/v milk powder in x1 TTBS for one hour, after which they were washed three more times with x1 TTBS and incubated overnight at 4°C on a rocker with one of the primary antibodies shown in Table 2.1. After incubation with the primary antibody, three further washes were conducted using x1 TTBS. The membranes were then incubated with the relevant secondary antibody presented in Table 2.1 for a further two hours at room temperature

in order to label the bound primary antibody. The membranes were then washed three times with x1 TTBS, for a period of 10 min per wash, and chemiluminescence was generated on the membranes using an ECL kit (Thermo Scientific-34080). Detection of the chemiluminescence was carried out using Kodak BioMax Light film or a ChemiDoc™ Touch Imaging System. The positions of the bands were compared against the molecular weight standards in order to confirm the size of the detected proteins.

2.12.4 Quantification and data analysis

The bands were quantified by using digital images of the membrane taken, as described above. Densitometry was conducted using Image Lab™ software.

Table 2.1 Details of antibodies

Antibody Against:	Source	Ref No.	Dilution	Diluted in	Blocking agent	Secondary Antibody
p^{Thr202}-ERK1/ p^{Tyr204}-ERK2	Cell Signaling	9101	1:1000	5% w/v BSA in TTBS	5% Milk powder	R
Total-ERK2	Cell Signaling	9108	1:2000	5% w/v Milk powder in TTBS	5% Milk powder	R
p^{Thr183/Tyr185} JNK	Promega	V7931/7	1:4000	5% w/v BSA in TTBS	5% BSA	R
Total JNK2	Cell Signaling	9258	1:4000	5% w/v Milk powder in TTBS	5% Milk powder	R
p^{Thr180/Tyr182} p38	Promega	V121A/7	1:1000	5% w/v BSA in TTBS	5% BSA	R
Total p38	Cell Signaling	9217S	1:1000	5% w/v Milk powder in TTBS	5% Milk powder	M
p^{Tyr576/577} FAK	Cell Signaling	3281S	1:1000	5% w/v BSA in TTBS	5% BSA	M
Total FAK	Cell Signaling	3285S	1:1000	5% w/v BSA in TTBS	5% BSA	M

R: HRP conjugated Goat anti Rabbit IgG (1:1000) (Dako P0448)

M: HRP conjugated Goat anti Mouse IgG (1:1000) (Dako P0260)

2.13 RNA techniques

2.13.1 RNA extraction

The TRIzol technique (based on guanidinium thiocyanate-phenol-chloroform extraction) was used to extract the RNA from L6-G8C5 cells (Chomczynski and Sacchi, 1987).

After the experimental incubation period, the test medium was aspirated and 0.6ml TRIzol per 35mm well was then added and the cells were incubated in Trizol at room temperature for 5 min and the resulting cell digest was transferred into autoclaved screw capped 2ml polypropylene tubes, then frozen at -80°C until ready for RNA extraction. After thawing, the tubes were microcentrifuged at 13,000rpm for 15 min at 4°C in order to remove any insoluble material. The TRIzol solution was then transferred to a fresh tube, to which chloroform (200µl/ml of TRIzol) was added. The tubes were thoroughly vortexed and incubated for a further 10 min at room temperature, after which they were microcentrifuged at 13,000rpm for 15 min at 4°C. This process resulted in the formation of three phases. The RNA was contained in the aqueous phase, so this was removed and transferred to a new tube. The addition of isopropanol (500µl/ml of original TRIzol extract) enabled the RNA to be precipitated, and then the tubes were vortexed and incubated at room temperature for 10-15 min. They were then microcentrifuged at 13,000rpm for 15 min at 4°C to create an RNA pellet, which was washed in 75% ethanol, then dissolved in RNAase-free diethyl pyrocarbonate-treated DEPC water (20µl). The RNA concentration was quantified from the optical density at 260nm using a Nanodrop (ND 1000) Spectrophotometer (Thermo Scientific, Northumberland, UK) and an example of how RNA concentration was quantified is presented in Appendix D.1. Finally, the RNA extracts were stored at -80°C.

2.13.2 Reverse transcription

RNA was reverse transcribed to cDNA using the Promega Reverse Transcription System (Promega, Hampshire, UK A3500). RNA samples (0.5µg/µl of DEPC water) were heated to remove any secondary structure (at 70°C for 10 min) and a 1µl aliquot was taken for reverse transcription. The composition of the reaction buffer is provided in Table 2.2. The tubes were placed on a PCR thermal cycler (Techne Genius, TC-3000X) at 42°C for 1 hour, then raised to 95°C for 5 min, and then lowered to 4°C for 5 min. The resulting cDNA was stored at -20°C.

Table 2.2 RT- Reaction

<i>For a single 20µl reaction</i>	<i>Volume (µl)</i>
<i>MgCl₂</i>	<i>4</i>
<i>10X Reverse Transcription Buffer</i>	<i>2</i>
<i>10mM dNTP Mix</i>	<i>2</i>
<i>Rnasin Ribonuclease Inhibitor</i>	<i>0.5</i>
<i>AMV Reverse Transcriptase</i>	<i>15 Units</i>
Primers¹	1µl
RNA	1µl
Water	to 20µl

¹A mixture comprising a 1:1 ratio of random and oligo dT primers was used. Preliminary experiments demonstrated that this approach produced higher yield than using each primer

2.13.3 Real time qPCR for detailed studies of IL6 and SNAT2 mRNA expression using Taqman assays

The results presented in Chapter 5 for the expression of rat IL-6 and SNAT2 mRNA were obtained through real-time qPCR utilising an Applied Biosystems Fast 7500 Real-Time PCR system and software package, with optimised gene specific amplification primers and probes (TaqMan gene expression assays, Applied Biosystems, Warrington, UK) as follows:

Rat IL-6 - assay ID number Rn01410330_m1

Rat SNAT2 - assay ID number Rn00710421_m1

Rat TBP (TATA-box binding protein) (assay ID number Rn01455646_m1) was used as a house-keeping gene (Kelleher et al., 2014) and the coefficient of variation between experiments was 4.29 %.

PCR reactions were set up in 20µl volumes that comprised the following: 10µl TaqMan Gene Expression Master Mix (Applied Biosystems, Warrington, UK,), 1µl TaqMan gene expression assay (including primers and probes), and 8µl nuclease-free water. This created 19µl of master mix, which was applied to the plate and then supplemented with 1µl of cDNA. For negative controls, the 19µl of master mix was instead supplemented with 1µl of DEPC water. PCR was performed for all genes using the 7500 Fast Real-Time PCR System profile shown in Table 2.3. The samples were analysed in pairs on the same plate (both the target and housekeeping genes) to enable direct comparisons, with contamination being monitored using ‘blank’ reactions.

Table 2.3 Real time qPCR thermal cycle

Thermal cycle						
Stage 1	Stage 2	Stage 3		Stage 4		
Repeats 1	Repeats1	Repeats 40		Repeats 1		
50°C	95°C	95°C	60°C	95°C	60°C	95°C
2 min	10 min	15 sec	1 min	15 sec	1 min	15 sec

The expression of IL-6 and SNAT2 related to TBP expression was calculated using the 2- $\Delta\Delta C_T$ method (Pfaffl, 2001).

2.13.4 SNAT2 silencing in L6 myoblasts with small interfering RNAs (siRNAs)

A SNAT2 silencing procedure was conducted using a validated siRNA with custom-synthesised siRNA oligonucleotides supplied by Eurogentec, as previously outlined (Evans et al., 2007a, Evans et al., 2008a). The oligonucleotides were supplied in solution as ds siRNA in 50mM TRIS-HCl, 100mM NaCl, and pH 7.6 at a concentration of 100 μ M. The SNAT2 silencing siRNA (SIL) had a forward sequence of 5'-CUGACAUUCUCCUCCUCGUdTdT which was directed against base position 1095 onward in the SNAT2 gene sequence (Evans et al., 2007a, Evans et al., 2008a). In order to control for possible non-specific functional effects of siRNA transfection, the procedure utilised in parallel transfections a previously validated scrambled siRNA control (Scr) (forward sequence 5'-CGCUCAACUCUACUUGUCCdTdT) that shared the same overall base composition as SNAT2 SIL (Evans et al., 2007a, Evans et al., 2008a).

L6 myoblasts were plated in DMEM Growth Medium at 10×10^4 per 35 mm well. After overnight incubation, the DMEM Growth Medium was discarded and 1ml of fresh GM was added to the wells and the cells were transfected with SNAT2 siRNA using a Profection Promega Calcium Phosphate Transfection Kit (Promega Cat. #E1200). The precise composition of the transfection mixture is presented below (Table 2.6). Prior to use, the stock of pre-annealed siRNA oligonucleotide supplied by the manufacturer was diluted to 20 μ M by the addition of nuclease-free water. The contents of Tube 1 and Tube 2 (Table 2.4) were then mixed by pipetting and 150 μ l was added drop-wise to the culture well. The culture plate was then gently agitated to ensure that the transfection mixture was distributed evenly over the cells. The final concentration of siRNA in the culture medium was 30nM: the cells were incubated in a culture incubator at 37°C for 16 hours, after which the medium was changed, doubling the standard volume of Growth Medium (4 ml to each well) for a further 24 hours. The medium was aspirated on day 4, after which experimental incubations and measurements were performed.

Table 2.4. siRNA transfection mixture for L6 transfection.

Tube 1		Tube 2			
Transfection Mixture Label	2xHBS* (μl)	20μM Scr. SNAT2 siRNA (μl)	20μM SIL SNAT2 siRNA (μl)	Nuclease-Free Water (μl)	2M CaCl₂ (μl)
Scr	310	7	----	264	39
SIL	310	----	7	264	39

*Hepes-buffered saline (Promega-E110A).

2.14 Measurement of intracellular Ca²⁺ using Fluo-4 fluorescence

Free intracellular Ca²⁺ in L6 myoblasts was assayed fluorometrically by binding of Ca²⁺ to the calcium chelator dye Fluo-4 (Heding et al., 2002). The change of Ca²⁺ dependent fluorescence was measured on a NOVOstar fluorescence plate-reader (BMG LABTECH, Offenburg, Germany). Cells were plated on Poly-D-lysine hydrobromide treated plastic 6mm wells on ELISA strips or 96-well plates at 5 x 10⁴ cells per well in 60 μl per well of the Growth Medium (GM) described in Section 2.2.3. Cells were cultured for 18 hours before commencing dye-loading experiments. After that, the Growth Medium was gently aspirated from each well which was then rinsed with 200μl of Physiological Salt Solution (PSS) (Appendix A.5). Then, the cells were loaded with fluo-4-AM ester (Fisher-11504786) for 45 min at 37°C under a 5% CO₂ atmosphere. The concentration of fluo-4-AM was 2μM and the loading buffer was PSS supplemented with BSA (0.1% w/v) (PSS-BSA) (Liu et al., 2010). After that, the wells were rinsed three times with 200μl of PSS-BSA, and then 200μl of fresh PSS- BSA was added to each well and cells were incubated again in a humidified incubator at 37°C to allow time for the Fluo-4 AM to be de-esterified by the cells to generate the free Fluo-4 dye. Then the fluorescence intensity was read on the NOVOstar plate-reader at an excitation wavelength of 488nm, and detecting at >500nm at 37°C. The calibration of the fluo-4 signal was performed by adding a final concentration of 0.5nM ionomycin Ca²⁺ ionophore in the presence of a total concentration of 4mM CaCl₂ to the PSS-BSA medium, in order to equilibrate the concentration of intracellular and extracellular Ca²⁺. The fluorescence signal was allowed to stabilise for 10 min and this signal was called F_{max}. Then, (in the presence of ionomycin as above) the cells were rinsed with PSS-BSA + 2mM EGTA to chelate Ca²⁺ and again the fluorescence signal was allowed to stabilise for 10 min and this signal was called F_{min}.

The intracellular Ca²⁺ concentration was calculated using the formula:

$$[\text{Ca}^{2+}]_i = K_d * (F - F_{\min}) / (F_{\max} - F),$$

where the dissociation constant K_d of the fluo-4-AM - Ca^{2+} complex was taken to be 350nM (Yamasaki-Mann et al., 2009).

2.15 Statistical analysis

The data presented have been derived from a minimum of three independent experiments, unless stated otherwise, and were analysed with GraphPad Prism 7.0. Normally distributed data are presented as the mean \pm SEM, and were analysed using Student's t-test or (for data sets involving multiple comparisons) repeated measures ANOVA followed by *post hoc* testing with Tukey's multiple comparisons test. Non-normally distributed data are presented as linked data curves for the individual experiments. These were analysed using Friedman's nonparametric repeated measures ANOVA, followed by *post hoc* testing with Dunn's multiple comparisons test.

Chapter 3 Regulation of MAPK activation in L6 cells

3.1 Introduction

It has been known for more than 20 years that the MAP kinase signal transduction pathways play an important role in exercise signalling (Sakamoto and Goodyear, 2002, Cargnello and Roux, 2011b, Tsuzuki et al., 2018). The MAP kinase family of intracellular signalling cascades is expressed in all eukaryotic cells and includes the extracellular signal regulated kinase 1 and 2 (ERK1/2), the c-Jun NH₂- terminal kinase (JNK), p38, and the extracellular signal- regulated kinase 5 (ERK5 or big MAP kinase, BMK1) (Cargnello and Roux, 2011b, Wang et al., 2019). These pathways are stimulated by a wide variety of environmental stressors and growth factors (Tsuzuki et al., 2018, Nakayama et al., 2019) and have been implicated in a large number of physiological processes, including cell proliferation, differentiation, hypertrophy, inflammation, apoptosis, carbohydrate metabolism, and gene transcription (Shrestha, 2017, Di Meo et al., 2019). Thus MAP kinase proteins exert a profound effect on cellular function (Cargnello and Roux, 2011b).

Preliminary experiments from this laboratory (Blbas, 2018) suggested that System A (SNAT2) transporter activity in L6-G8C5 myotubes is significantly dependent on MAP kinase signalling through the JNK and p38 pathways.

As outlined in the hypothesis in Section 1.15, the importance of these pathways is that they may be involved in the activation of System A / SNAT2 in response to cell stress, which might occur through actions that include mechanical stretch or the application of a change in osmolarity.

This aim of the chapter was to extend the preliminary observations (Blbas, 2018) , to examine the effect of mechanical loading on MAPKs, and to observe the effect of low pH on these MAPKs.

- In (Figures 3.1 and 3.2), myotubes were treated with MAPK inhibitors and then SNAT2 activity was measured as described in Section 2.10.
- In (Figures 3.3-3.5), myotubes were incubated under different pH conditions and then the phosphorylation of MAPKs was measured as described in Section 2.12.
- In (Figures 3.7-3.9) myotubes were cyclically stretched by an FX-4000 cell stretcher as described in section 2.4 and then phosphorylation of MAPKs was measured as described in Section 2.12.

3.2 Results

3.2.1 Dependence of System A / SNAT2 transporter activity in L6-G8C5 cells on MAP kinase activity

As described in Section 1.8, it is possible to assay the activity of System A amino acid transporters (including SNAT2 which is the most strongly expressed System A transporter in L6-G8C5 cells (Evans et al., 2007a)), through the measurement of the uptake of the ^{14}C -labelled amino acid analogue MeAIB into intact cells.

It was shown that incubation with pharmacological inhibitors of JNK or p38 significantly inhibited System A / SNAT2 transporter activity in L6-G8C5 cells, even in the resting unstressed state, but that inhibition of signalling through the MEK/ERK pathways had no significant effect under these conditions even when employing a high concentration of MEK inhibitor PD98059 (50 μM) (Figure 3.1). The effect required 4h of pre-incubation with the MAPK pathway inhibitors (presumably to allow them time to enter the cells) and the effect persisted even though the inhibitors were not present during the subsequent transport assay. In 3 further experiments, incubation with these inhibitors only during the ^{14}C -MeAIB transport assay (i.e. without pre-incubation) had no detectable effect (Figure 3.2) suggesting that the inhibitors were acting on the intended intracellular kinases rather than exerting an off-target direct inhibitory effect on the transporters on the cell surface.

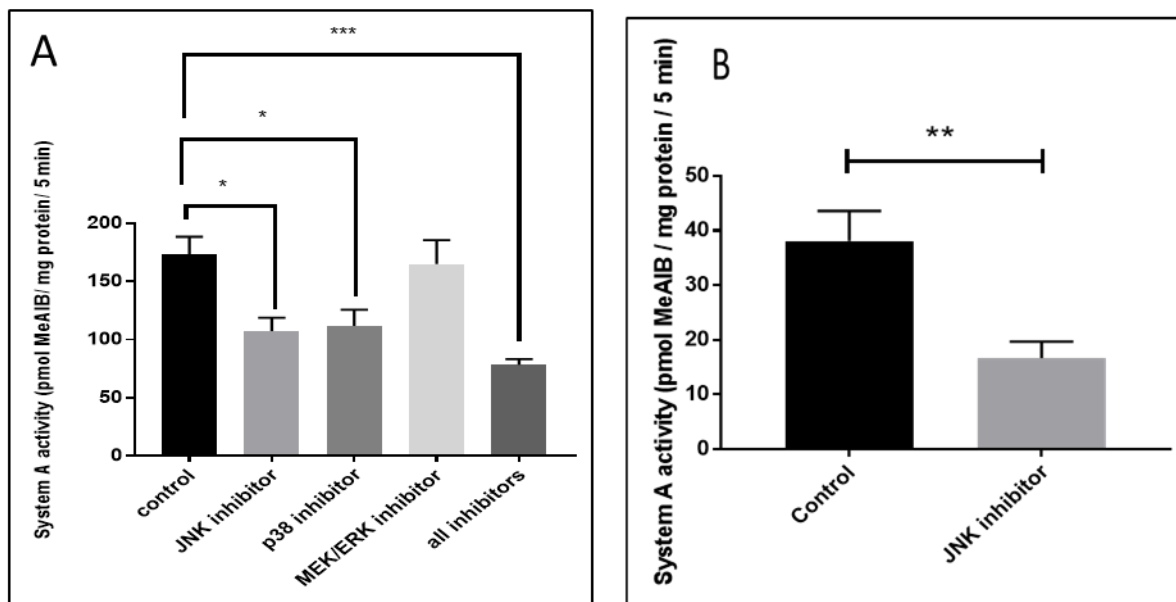


Figure 3.1. The effect of pre-incubation with MAPK inhibitors on the activity of System A transporters in L6-G8C5 myotubes.

A) Cells were pre-incubated for 4h at pH 7.4 in MEM/2% DFBS with MAPK inhibitors (JNK inhibitor SP600125 (10 μ M), p38 inhibitor SB202190 (5 μ M), MEK/ERK inhibitor PD98059 (50 μ M) and all inhibitors together. The 14 C-MeAIB transport was then immediately assayed in 5 min incubations in HBS medium at pH 7.4 in the absence of the inhibitors. The control was run with no inhibitors, Pooled data are shown from $n = 3$ independent experiments, with 5 replicate culture wells in each experiment. . *Denotes significant difference from Control $P < 0.05$. *** Denotes significant difference from Control $P < 0.001$. B) (Inset) Effect of incubation as in (A) but for 6h with JNK inhibitor SP600125 at higher dose (30 μ M). Data from 2 experiments with 5 replicate culture wells in each (** $P = 0.003$).

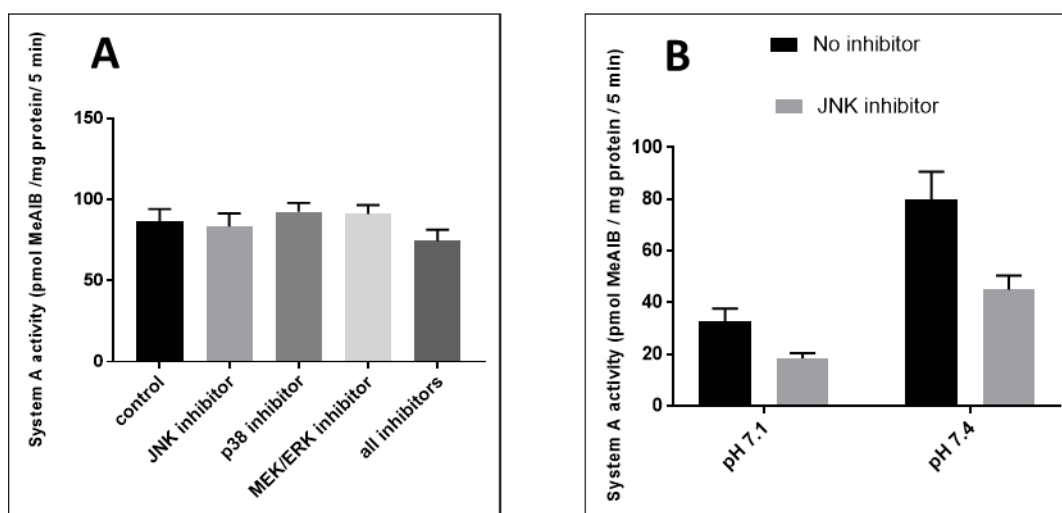


Figure 3.2. The acute effect of MAPK inhibitors on the activity of System A transporters in L6-G8C5 myotubes.

A) Incubation with these inhibitors was performed as in the previous figure but only during the ^{14}C -MeAIB transport assay (i.e. without pre-incubation). The ^{14}C -MeAIB transport was rapidly assayed by incubating for 5 min at room temperature in HBS medium with no inhibitors, JNK inhibitor ($10\mu\text{M}$ SP600125), p38 inhibitor ($5\mu\text{M}$ SB202190), MEK/ERK inhibitor ($50\mu\text{M}$ PD98059) or all inhibitors together. Pooled data are shown from $n = 3$ independent experiments, with 5 replicate culture wells in each experiment. B) Acute effect of high dose JNK inhibitor. Incubation was performed as in (a) but with $30\mu\text{M}$ JNK inhibitor SP600125 applied only during the 5 min ^{14}C -MeAIB transport incubation in HBS medium at the pH shown. Pooled data are shown from two independent experiments, with 5 replicate culture wells in each experiment. (2-way ANOVA showed a significant effect of pH ($P < 0.0001$) and of JNK inhibitor ($P = 0.0005$) but no significant interaction between pH and JNK inhibitor ($P = 0.1207$)).

At the doses of inhibitors that were used in Section 3.2.1, (even when the 3 inhibitors were used in combination) the cells still showed a significant residual System A / SNAT2 transport activity (Figure 3.1A). A 3-fold higher concentration of the JNK inhibitor SP600152 ($30\mu\text{M}$), accompanied by a longer pre-incubation (6h), was therefore tested (Figure 3.1B), but still failed to abolish System A / SNAT2 transport activity. However, unlike the negative result in Figure 3.2a, it was found that incubation with this high dose of SP600125 ($30\mu\text{M}$) for only 5 min (during the 5 min ^{14}C -MeAIB transport assay) also inhibited the transporters (Figure 3.2B). This may mean that an effective dose is achieved inside the cells more rapidly at high dose, but an off-target cell surface effect of the drug on the transporters themselves cannot be ruled out.

3.2.2 The effect of low pH on MAPKs in L6 Myotubes

In view of the well-documented pH sensitivity of System A amino acid transporters and the possible mutual interaction between System A and MAPKs (outlined in the schematic diagram in Section 1.15 Figure 1.7) it is important to assess the effect of the pH of extracellular fluid on MAPK activation. Here, JNK, p38, and ERK1/2 activation were assessed by immunoblotting for the phospho-activated forms of the proteins after 1-hour of incubation of the cells in test media at different pH values. Compared to the control (pH=7.4) (Figure 3.3), treatment of cells with acidic medium (pH 7.1) resulted in a decrease in p-JNK, implying inhibition of the kinase. This study also found that p-p38 was similarly decreased at pH 7.1 (Figure 3.4), again indicating pH sensitivity. Interestingly, like p-JNK; p-p38 was upregulated in the alkaline condition of pH 7.7 (see Figures 3.3 and 3.4) although this effect was more variable and did not achieve statistical significance. However, this was not the case with p-ERK1/2 (Figure 3.5), which showed no changes in response to different pH environments.

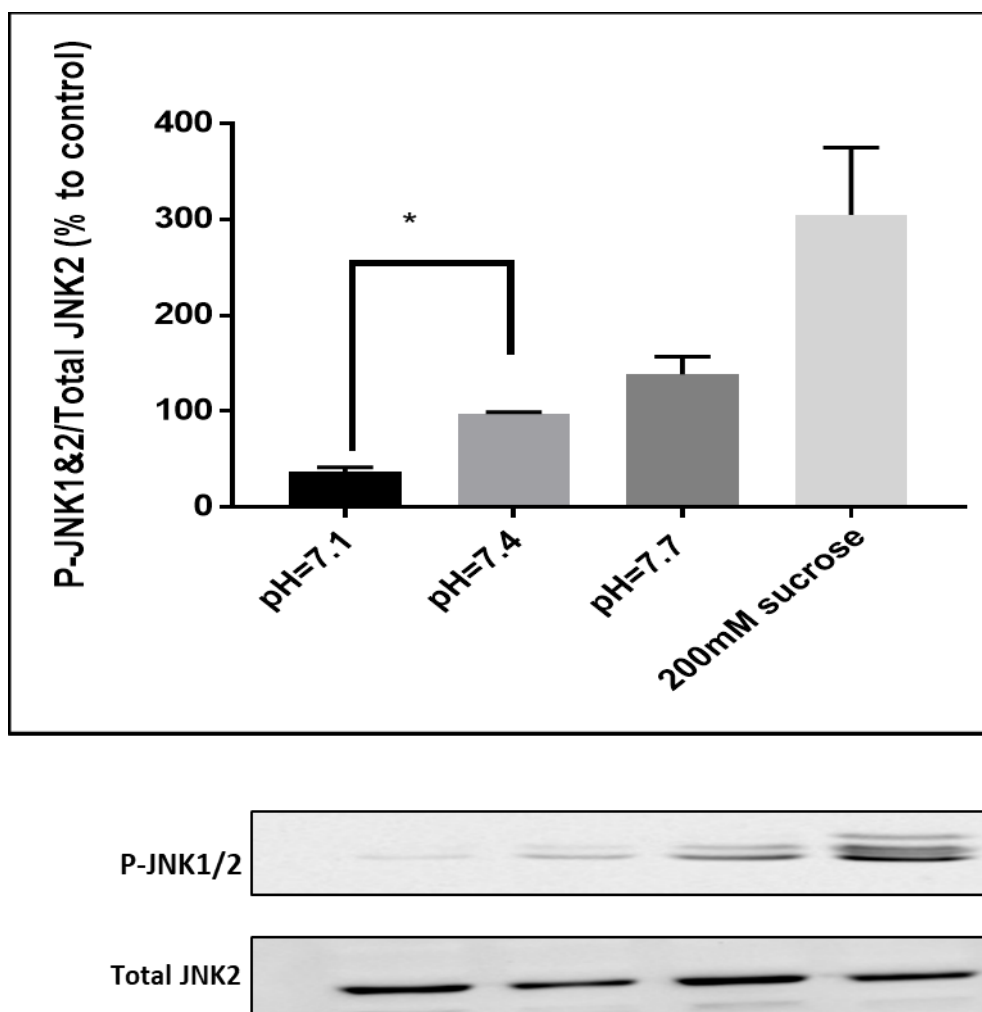


Figure 3.3. The effect of different pH media on p-JNK in L6-G8C5 myotubes.

Cells were incubated in MEM adjusted to give the required pH under a 5% CO₂ atmosphere, at different pH (pH=7.1, pH=7.4, pH=7.7, and with 200mM sucrose as a hyper-osmotic positive control) in MEM/2% DFBS for one hour in the incubator. After 1 hour incubation in the test media, the plates were immediately placed on a tray of crushed ice. The media were then rapidly aspirated and each well immediately scraped in 200μl of Lysis Buffer. Immunoblots of proteins were prepared; probing with anti-p-JNK1/2 antibody and the bands (46/54 kDa) were quantified by densitometry using the ChemiDoc Touch Imaging System. Pooled data are shown from n=3 independent experiments, with 4 replicate culture wells in each experiment. * Denotes significant difference from Control (pH= 7.4) ($P < 0.05$).

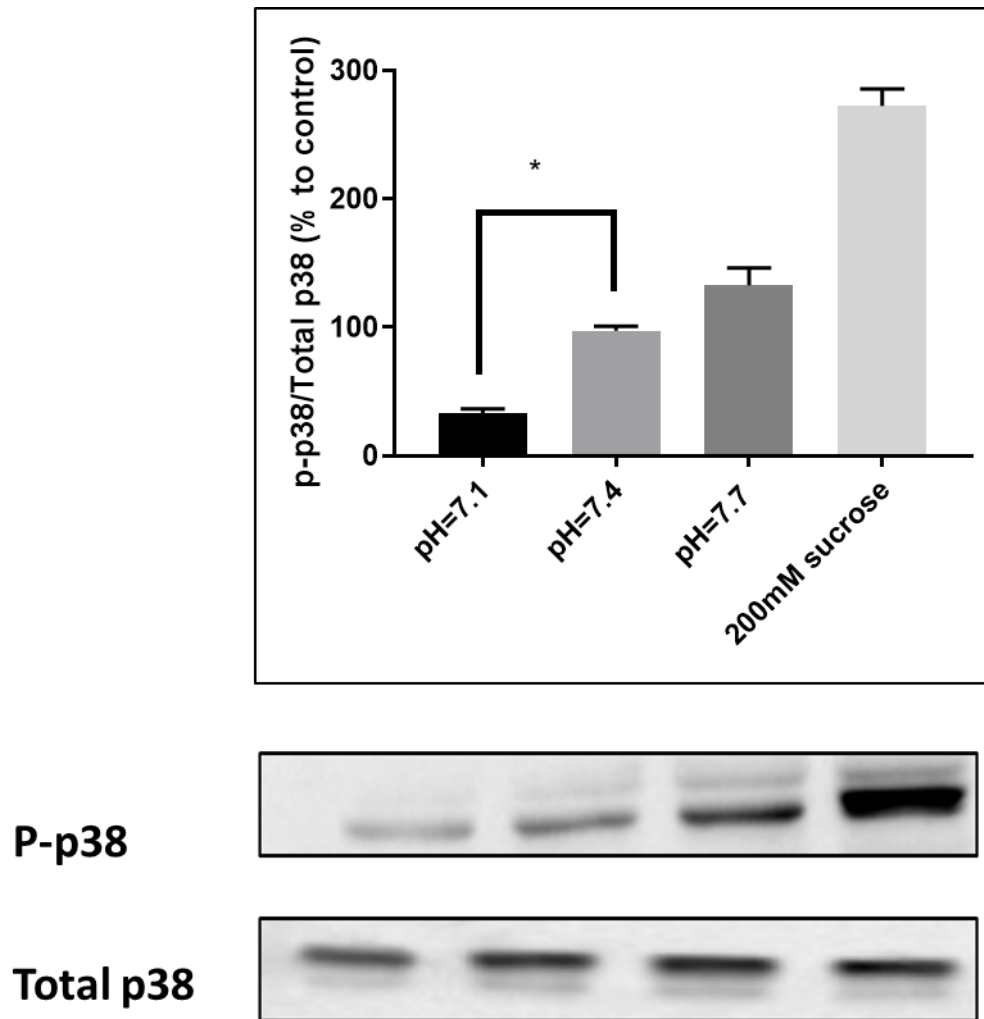


Figure 3.4. The effect of different pH media on p-p38 in L6-G8C5 myotubes.

Cells were pre-incubated at different pH (pH=7.1, pH=7.4, pH=7.7, and with 200mM sucrose as a hyper-osmotic positive control) in MEM/2% DFBS for one hour in the incubator. After 1 hour incubation in the test media, the plates were immediately placed on a tray of crushed ice. The media were then rapidly aspirated and each well immediately scraped in 200 μ l of Lysis Buffer. Immunoblots of proteins were separated by SDS-PAGE; probing with anti-p-p38 MAPK antibody and the bands (43 kDa) were quantified by densitometry using the ChemiDoc Touch Imaging System. Pooled data are shown from n=3 independent experiments, with at least 4 replicate culture wells in each experiment. * Denotes significant difference from Control (pH= 7.4) ($P<0.05$).

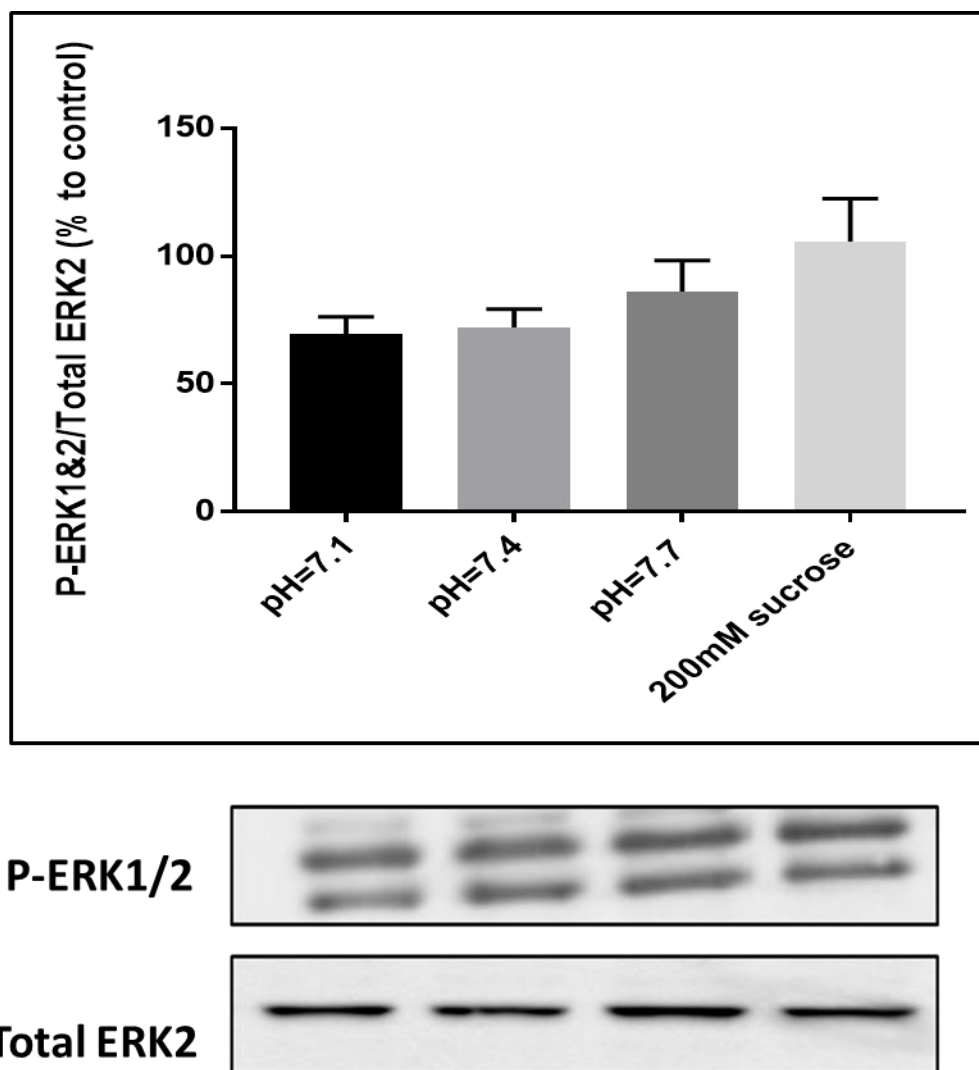


Figure 3.5. The effect of different pH media on p-ERK-1 in L6-G8C5 myotubes.

Cells were pre-incubated at different pH (pH=7.1, pH=7.4, pH=7.7 and with 200mM sucrose as a hyper-osmotic stress) in MEM/2% DFBS for one hour in the incubator. After 1 hour incubation in the test media, the plates were immediately placed on a tray of crushed ice. The media were then rapidly aspirated and each well immediately scraped in 200 μ l of Lysis Buffer. Immunoblots of proteins were separated by SDS-PAGE; probing with anti- Phospho-p44/42 MAPK (ERK1/2) and the bands (44/42 kDa) were quantified by densitometry using the ChemiDoc Touch Imaging System. Pooled data are shown from n=4 independent experiments, with at least 4 replicate culture wells in each experiment.

3.2.3 The role of JNK in the inhibition of System A by low pH

As with all System A transporters, acutely lowering the extracellular pH from 7.4 to 7.1 during the 5 min System A transport assay acutely inhibits the System A transporter activity in L6-G8C5 cells (Evans et al., 2007a). This rapid effect of low pH is thought to arise from direct protonation of the extracellular C-terminal histidine residue of the SNAT2 transporter (Baird

et al., 2006). However, the observation that inhibiting JNK or p38 partly inhibits System A activity (Figure 3.1A), and that pH 7.1 inhibits phospho-activation of JNK (Figure 3.3) and p38 (Figure 3.4) suggests an alternative explanation i.e. that the effect of low pH on System A is mediated by the pH effect on JNK or p38. This was tested by measuring the acute effect of high dose JNK inhibitor applied acutely during the transport assay (Figure 3.2B). Even at this high dose, the percentage decline in System A/ SNAT2 activity by applying pH 7.1 versus pH 7.4 was unaltered, and 2-way analysis of variance (2-way ANOVA) detected no significant interaction between JNK inhibitor and pH. There is therefore no detectable role for JNK in the pH sensitivity of System A / SNAT2 transport activity in these cells.

3.2.4 The role of cell swelling

Cell shrinkage by hyper-osmotic stress (sucrose loading) is a potent stimulator of phospho-activation of JNK and of p38 in L6-G8C5 myotubes (as seen in the sucrose positive controls in Figures 3.4 and 3.5). It has also been known for many years that activation of sodium-hydrogen exchange (NHE) transporters in the plasma membrane (for example NHE1 (Lang, 2007)) can lead to cell swelling and this plays a significant role in physiological cell volume regulation (Lang, 2007). In L6-G8C5 cells the cytosolic pH is tightly regulated and shows no detectable fall when extracellular pH is lowered to 7.1 (Table 5 in (Bevington et al., 1998a). The apparent decrease in JNK and p38 activation observed at pH 7.1 (Figures 3.3 and 3.4) might therefore occur because of cell swelling caused by the NHE activation that is necessary to regulate cytosolic pH. To test this explanation, changes in cell volume were screened by equilibration of ^{14}C -urea (Burns and Rozengurt, 1983) between extracellular and intracellular water spaces (Figure 3.6). As a positive control, cells were incubated in medium that had been made hypo-osmotic (approximately 240 mOsM) by omitting NaCl. Even though this positive control showed an apparent increase in cell volume after 2h of incubation, the cell swelling expected because of Na^+/H^+ exchange at low pH (7.1) was not observed at any time point. On the contrary, after 7 hours a slight decrease in volume may have occurred with declining pH (Figure 3.6), especially when the transport of amino acid osmolytes into cells through System A . SNAT2 transporters was inhibited by adding synthetic System A substrate MeAIB as a competitive inhibitor (Evans et al., 2007a). This apparent shrinkage is probably an underestimate because it has also been shown that a significant concentration of MeAIB can be accumulated by these cells within 7 hours (Bevington et al., 2002) which could potentially lead to osmotic swelling.

As cell shrinkage with sucrose-loaded medium strongly *activates* JNK and p38 in these cells (Figures 3.3 and 3.4), it is therefore very unlikely that stress arising from the small apparent cell shrinkage observed at pH 7.1 in Figure 3.6 could cause the *decrease* in P-JNK and P-p38 observed in Figures 3.3 and 3.4.

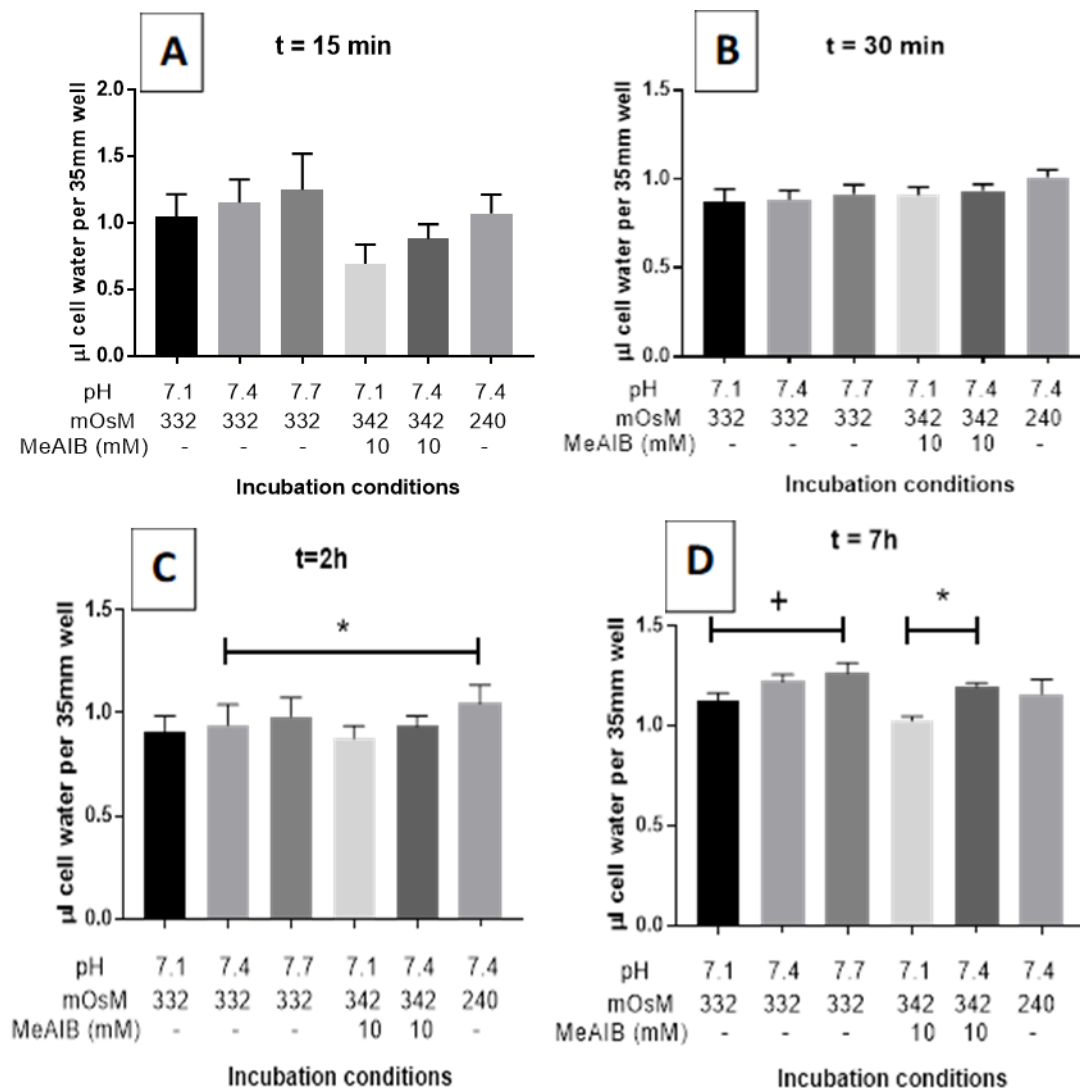


Figure 3.6. Screening for cell volume changes assessed by equilibration of L6-G8C5 myotubes with ^{14}C -urea in MEM/2% DFBS which had been modified as shown on the x-axis. Pooled data are shown from 2 independent experiments with 3 replicate culture wells in each. (* $P < 0.05$; + borderline significant, $P = 0.0539$). Cell water per culture well was calculated by dividing the total ^{14}C measured in each well by the concentration of ^{14}C per μl in the culture medium.

3.2.5 The acute effect of cyclic stretching on the phosphorylation of MAPKs in L6-G8C5 myotubes

As MAP kinase activation is thought to play a role in mechanotransduction signalling in skeletal muscle (as reviewed in Section 1.14) the effect of cyclic stretching on phospho-activation of MAP kinases was assessed in L6-G8C5 myotubes. Even a short period (1, 5 or 10 min) of stretching significantly increased P-p38 phospho-activation (Figure 3.7). Moreover, the phospho-activation of P-JNK was also increased significantly after a similar duration of stretching compared to the control (as in Figure 3.8). However, stretching the cells had no detectable effect on the phosphorylation of p-ERK1/2 (Figure 3.9).

As rising pH was associated with increased phospho-activation of JNK and p38 in Figures 3.3 and 3.4, care was taken in these stretching experiments to minimise disturbance to the pH. As placing the culture plates on the stretching equipment requires opening the culture incubator door, the resulting loss of atmospheric CO₂ could in principle raise the pH of bicarbonate-buffered medium. This effect was minimised by working as rapidly as possible. In some initial experiments an additional 20mM supplementary Hepes buffer (Gibco Ref 15630) was added to the medium, but this was found to be unnecessary. Negligible change was observed in the colour of the Phenol Red pH indicator (see Figure 4.2 in the next chapter) and, to assess the effect of any small changes not detected by Phenol Red, a parallel stretchable Flexcell culture plate of cells was run alongside the stretched plate in the incubator. A blot from such a parallel unstretched control plate is shown in Figure 3.7B and shows no significant increase in phospho-activation signal at the time points at which stretched plates showed a response.

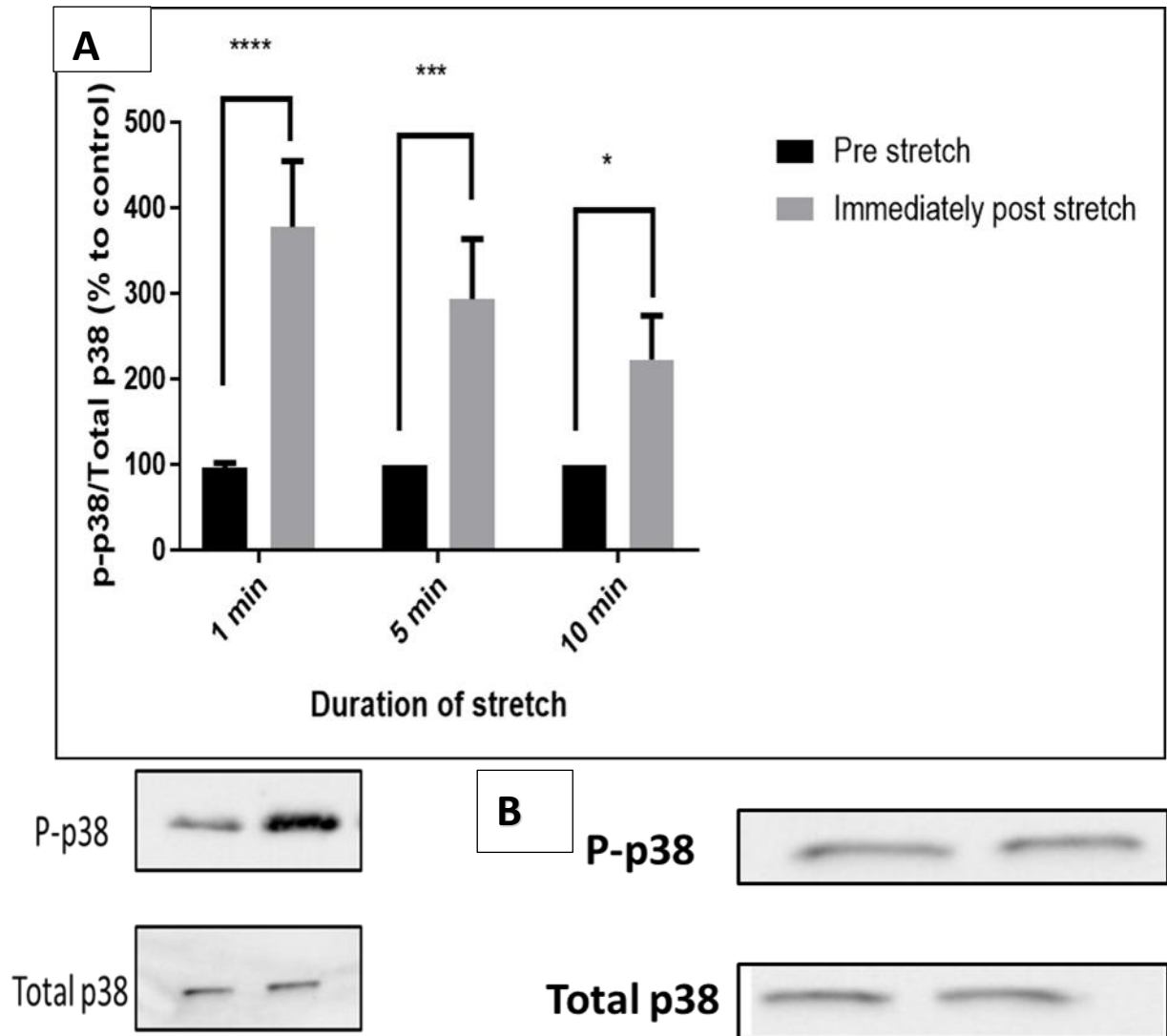


Figure 3.7. Effect of 1 min or 5 min or 10 min of cyclic stretch on P-p38 activity.

A) L6-G8C5 myotubes were cultured on collagen-coated Flexcell silicone-based culture wells. The medium used was based on MEM at pH 7.4 and contained 2mM L-Gln with 2% dialysed foetal bovine serum. Myotubes were stretched using a Flexcell FX-4000 system as described in Section 2.4 (Goto *et al.*, 2003). After stretching, the media were then rapidly aspirated and each well immediately scraped in 200 μ l of Lysis Buffer. Immunoblots of proteins were separated by SDS-PAGE; probing with anti-Phospho-p38 MAPK and the bands (43 kDa) were quantified by densitometry using the ChemiDoc Touch Imaging System. 2-Way ANOVA. Data compiled from 3 experiments are presented. B) An example of a control blot that was run in parallel with (A) on an unstretched plate. **** Denotes significant difference from Pre-stretch Control ($P < 0.0001$). *** Denotes significant difference from Pre-stretch Control ($P < 0.001$). * Denotes significant difference from Pre-stretch Control ($p < 0.05$).

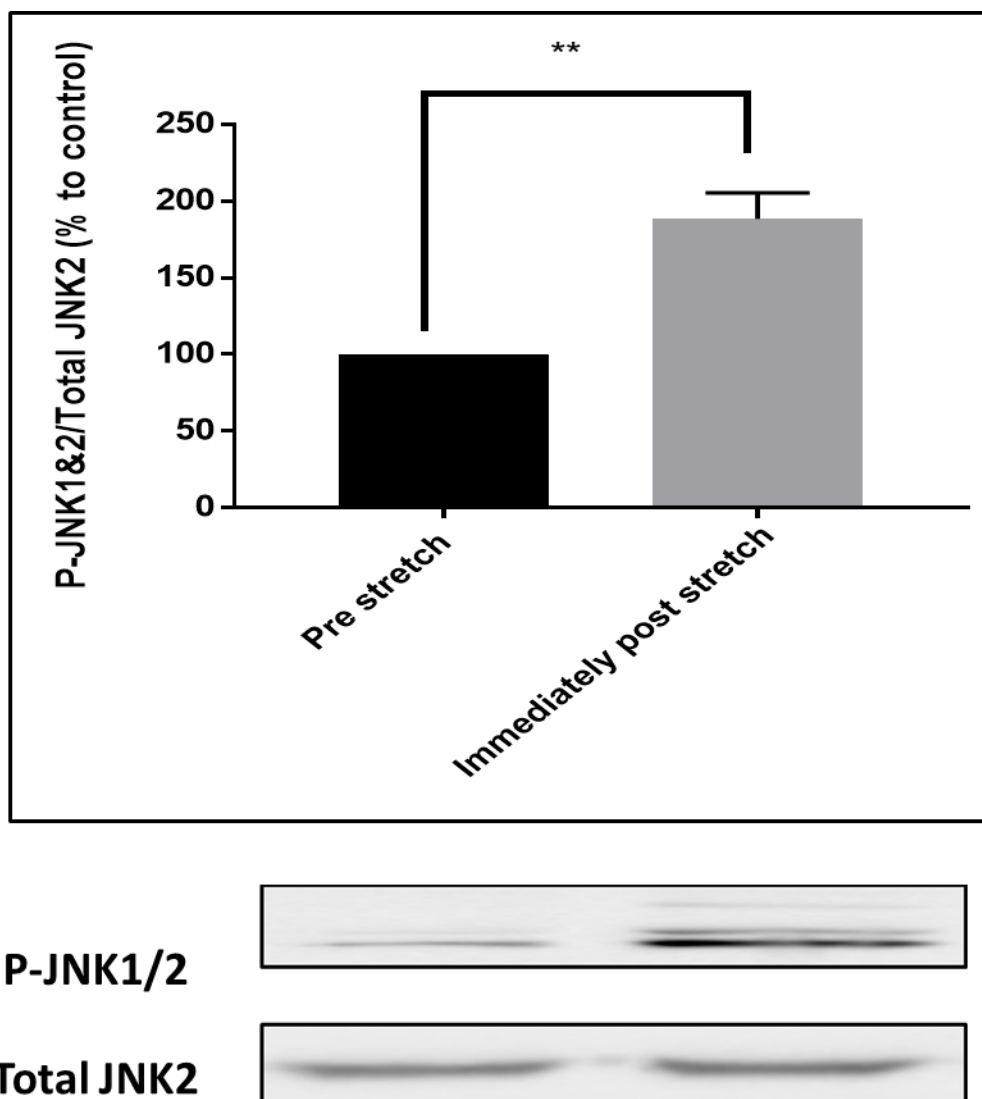


Figure 3.8. Effect of 10 min of cyclic stretch on P-JNK activity.

*L6-G8C5 myotubes were cultured on collagen-coated Flexcell silicone-based culture wells. The medium used was based on MEM at pH 7.4 and contained 2mM L-Gln with 2% dialysed foetal bovine serum. Myotubes were stretched using a Flexcell FX-4000 system as described in Section 2.4 (Goto et al., 2003). After stretching, the media were then rapidly aspirated and each well immediately scraped in 200µl of Lysis Buffer. Immunoblots of proteins were separated by SDS-PAGE; probing with anti-Phospho-JNK MAPK and the bands (46/54 kDa) were quantified by densitometry using the ChemiDoc Touch Imaging System. Pooled data are shown from n=4 independent experiments. ** Denotes significant difference from Pre-stretch Control ($P < 0.01$).*

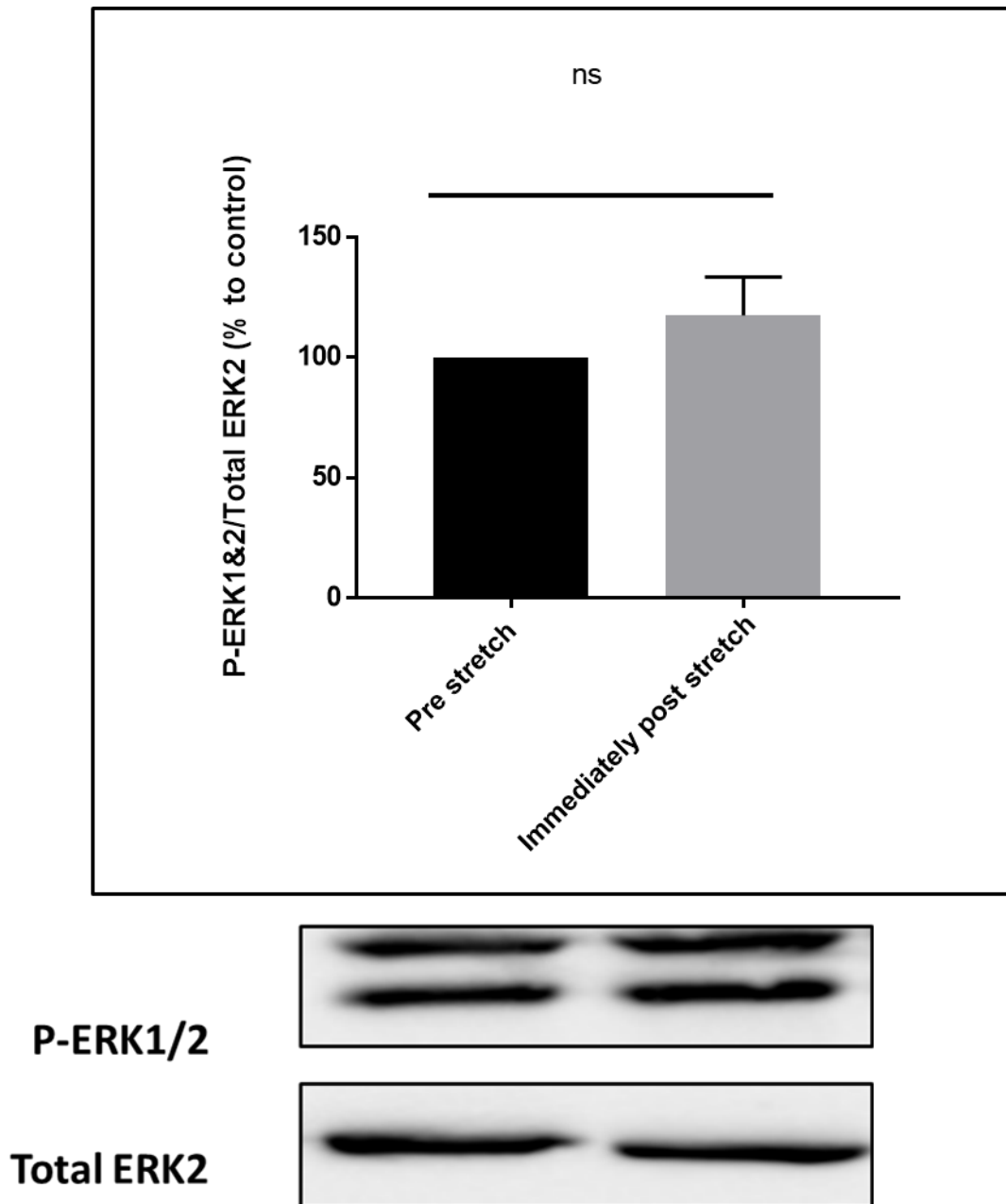


Figure 3.9. Effect of 10 min of cyclic stretch on p-ERK-1/2 activity.

L6-G8C5 myotubes were cultured on collagen-coated Flexcell silicone-based culture wells. The medium used was based on MEM at pH 7.4 and contained 2mM L-Gln with 2% dialysed foetal bovine serum. Myotubes were stretched using a Flexcell FX-4000 system as described in Section 2.4 (Goto et al., 2003). After stretching, the media were then rapidly aspirated and each well immediately scraped in 20 μ l of Lysis Buffer. Immunoblots of proteins were separated by SDS-PAGE; probing with anti-Phospho-p44/42 MAPK (ERK1/2) and the bands (44/42 kDa) were quantified by densitometry using the ChemiDoc Touch Imaging System. Pooled data are shown from n=3 independent experiments.

3.3 Discussion

3.3.1 Inhibition of MAP kinases inhibits System A / SNAT2 activity in L6-G8C5 myotubes

It was hypothesized in this chapter that MAP kinases affect the System A / SNAT2 transporter, which has implications for the control of SNAT2 and hence protein synthesis. Using doses of JNK inhibitor SP600125 (Nieminen et al., 2006), p38 inhibitor SB202190 (Cheng et al., 2006) and MEK inhibitor PD98059 (Hotokezaka et al., 2002) that are regarded as selective for these kinases, the data presented in this chapter suggest that the System A / SNAT2 transport activity in L6-G8C5 myotubes shows a detectable dependence on JNK and p38, even in unstressed cells. The inhibitory effect of these selective doses of the inhibitors was seen when the cells were pre-incubated with the inhibitors for 4 hours followed by rapid removal of the inhibitors and assay of transport in medium without these drugs (Figure 3.1) suggesting that transport into the cells to gain access to the intended kinases was required. In contrast, acute exposure of cells to the inhibitors only during the 5 min transport assay (Figure 3.2) failed to inhibit the transporters, suggesting that the inhibitory effect was not a direct cell surface action on the transporters themselves.

The observed apparent insensitivity of System A / SNAT2 transport to MEK inhibition with PD98059 should not be taken as evidence that the Ras-Raf-MEK-ERK pathway has no role in System A / SNAT2 regulation in these cells. Other experiments in this laboratory have shown that, at the dose used here, PD98059 fails to block phospho-ERK activation in these cells (Nicole Simms, Department of Infection, Immunity & Inflammation, unpublished observation). The reason for the failure of this widely used inhibitor is unknown, but it is possible that L6-G8C5 myotubes show a pathway of MEK-independent ERK activation similar to that which has been reported in human neutrophils (Simard et al., 2015).

3.3.2 pH sensitivity of MAP kinases

In view of this apparent coupling of the acid-inhibitable transporter System A / SNAT2 to JNK and p38, the effect of physiological pH changes on the phosphoactivation of these kinases was determined. Interestingly, at low pH 7.1; p38 and JNK phospho-activation were significantly inhibited, indicating that they follow a similar pattern to SNAT2 in terms of sensitivity to low pH (Evans et al., 2007b, Evans et al., 2008b, Blbas, 2018). This was accompanied by an apparent (but variable) phospho-activation on raising the pH to 7.7 (Figures 3.3 and 3.4). The reason for the variability in the pH 7.7 result is unknown, but might be linked to possible damaging effects of pH 7.7 on cell viability that are noted later (in Figure 5.11, in Chapter 5).

Inhibition of JNK by low pH, leading to an impaired JNK signal to System A / SNAT2 is potentially a mechanism by which low pH could inhibit these transporters, but no evidence for blunting of the pH sensitivity of System A transporters by the JNK inhibitor SP600125 was found in this chapter (Figure 3.2B). However, in view of the possible role of MAP kinases in mechanotransduction in skeletal muscle (Section 1.14) and the significant generation of lactic acid through glycolysis during exercise (Cairns, 2006) this acid-dependence of JNK and p38 may be of physiological significance following exercise, potentially blocking some of the mechanotransduction signals.

It is also interesting to note that the strong pH dependence of JNK observed here is not a universal feature of all muscle cell types. In contrast to L6-G8C5, *activation* of JNK has been reported in the smooth muscle-derived BC3H1 cell line by incubation at pH 7.1 (Price and Mitch, 1995).

3.3.3 Sensing of pH by MAP kinases

The effect of extracellular pH on the intracellular protein kinases JNK and p38 observed here cannot be a direct effect of pH on the kinase proteins themselves, because the extracellular pH range used here has no effect on cytosolic pH in L6-G8C5 myotubes (Table 5 in (Bevington et al., 1998a)). In a number of cell types osmotic stress, resulting in changes in cell volume, is a potent activator of MAP kinases. Whereas JNK and p38 are strongly activated in L6-G8C5 cells by osmotic shrinkage (Figures 3.3 and 3.4), hypo-osmotic cell swelling activates p38 in other cells (Tilly et al., 1996). Cell swelling in myocytes has been suggested to be functionally important in skeletal muscle during contraction (possibly leading to muscle fatigue) (Usher-Smith et al., 2006). This swelling has been suggested to occur partly because of the osmotic effect of lactic acid generated by glycolysis and accumulating in the cells (Usher-Smith et al., 2006), but also possibly as a result of transport of cations such as Na^+ across the sarcolemma (Kemp, 2007) for example during extrusion of H^+ from the cells by Na^+/H^+ exchangers. Therefore a possible explanation for the inhibitory effect of low pH on JNK and p38 phospho-activation (Figures 3.3 and 3.4) is that the regulation of cytosolic pH in these cells by Na^+/H^+ antiport exchangers is driving osmotically active Na^+ ions into the cells leading to cell swelling which might inhibit p38 and JNK activation. At least with the ^{14}C -urea-based method for assessing cell volume that was used here, no acid-induced cell swelling was detected in these cells (Figure 3.6). On the contrary, a small cell shrinkage may have occurred under acidic conditions (Figure 3.6). This may have occurred because acid-inhibited System A amino acid

transporters, especially SNAT2, are an important controller of the intracellular concentration of amino acid osmolytes such as L-glutamine (Evans et al., 2007a) and therefore potentially affect cell volume. In contrast, low pH (7.0) has been reported elsewhere to induce swelling of L6 cells in about 30 min (Sen et al., 1995). The reason for the discrepancy between this and the present study is unknown.

The mechanism of pH sensing by JNK and p38 remains unclear. However, as it has previously been shown in this laboratory, using L6-G8C5 myoblasts, that siRNA silencing of SNAT2 can impair phosphoactivation of JNK (Blbas, 2018), it is possible that the pH sensing mechanism of SNAT2 (Evans et al., 2007b, Evans et al., 2008b, Blbas, 2018) may be partly responsible for the pH sensitivity of JNK.

As the total protein content of the cultures in Figure 3.6 was approximately 0.5mg per 35mm well, the cell water space detected by this ¹⁴C-urea distribution assay was about 2 μ l per mg protein, similar to the value reported in other adherent monolayer cultures using an alternative water space marker 3-O-methyl-D-glucose (Kletzien et al., 1975). Ideally the experiments here should be confirmed using flow cytometry forward angle light scatter (Tzur et al., 2011) which is the current method of choice for detecting changes in cell volume. However this requires cell detachment and is therefore unsuitable for myotubes, especially as this would break integrin-extracellular matrix interactions which may be an important influence on System A transporters and on Focal Adhesion Kinase (Figure 1.7, Section 1.15) (McCormick and Johnstone, 1995).

3.4 Conclusion

The data presented in this chapter suggest that, as in the hypothesis outlined in Chapter 1 (Section 1.15), JNK and p38 kinase activation is coupled to System A (SNAT2) amino acid transporters, and that JNK and p38 (like System A / SNAT2) are inhibited by low pH (Evans et al., 2007b, Evans et al., 2008b, Blbas, 2018).

Previous studies have established that the activation of MAP kinases (JNK and p38) is possible in skeletal muscle through the use of static stretch, and is accompanied by a smaller effect on ERK (Boppart et al., 2001). The observation in this chapter that mechanical stretch activates JNK and p38 in L6-G8C5 cells seems consistent with this, although no effect was detected on ERK. This and the data in Section 3.2.1 suggest that stretch should also activate System A / SNAT2 and (from the data on the effect of low pH on MAPKs above) this effect of stretch

should be blunted by low pH. Testing these predicted effects of stretch on System A / SNAT2 is the subject of the next chapter.

Chapter 4 Characterisation of experimental systems for studying mechanical stretch effects on System A in L6 cells

4.1 Introduction

The hypothesis to be tested in this chapter is that the anabolic System A sodium-coupled neutral amino acid transporter (SNAT2) (slc38a2) can be activated in L6-G8C5 rat skeletal muscle cells by mechanical stretch *in vitro*. At the start of these experiments, it seemed likely that this effect would be observed for the following reasons:

- Data from the previous chapter had shown that the activity of these transporters is dependent on the MAP kinases JNK and p38, and that mechanical stretch leads to phospho-activation of these kinases
- In skeletal muscle there is evidence that these transporters are activated by muscular exertion (King, 1994, Henriksen et al., 1992, Henriksen et al., 1993). For example an *ex vivo* study showed that System A can be activated in muscle of rats that had been running on a treadmill for a duration of up to 1 hour (King, 1994).
- Such an effect on System A (SNAT2) transport activity seems plausible in view of an earlier report (Chambers et al., 2009b) that 15% stretch applied to mouse C2C12 myotubes or to mouse extensor digitorum longus muscle activates glucose transport by a p38-dependent mechanism. Electrical stimulation of L6 myotube contraction has also been reported to stimulate glucose transport (Yano et al., 2011).
- An earlier small series of pilot experiments which were done in this laboratory had suggested that mechanical loading by *in vitro* cell stretch can lead to an apparent System A (SNAT2) activation (Clapp, 2010) either by 48 hours of continuous passive stretch or by 17 hours or 48 hours of cyclic intermittent stretch (*ibid*).

Therefore, the aims of experiments in this chapter were to reproduce the apparent effect of SNAT2 activation by *in vitro* cell stretch that had been reported in pilot experiments (Clapp 2010), and to optimise the effect by comparing it in different models of mechanical stretch in L6-G8C5 skeletal muscle cells using:

- Continuous stretch of L6 myotubes as in (Figure 4.3) with static Loughna cell stretching assemblies (Rauch and Loughna, 2008b) as described in (Section 2.3).
- Two models of cyclic stretch:

1. A vacuum-driven “Pull” system, generating a partial vacuum under the culture wells as described in (Section 2.4). L6 myotubes were stretched by this machine (FX-4000) as in (Figures 4.1 and 4.5) and myoblasts were used as in (Figures 4.7 and 4.8).
2. A purpose-built mechanical “Push” system, which did not involve the potential confounding factor of a vacuum, as described in (Section 2.5). L6 myotubes were stretched by this machine as in (Figure 4.6).

4.2 Results

4.2.1 Positive control for MAPK response in stretched cells

To confirm that MAP kinases in the cells were retaining their responsiveness to mechanical stretch that was observed in Chapter 3, replicates of the immunoblotting experiments to detect phospho-activation of p38 were run alongside the series of stretch experiments described in this chapter. p38 activation was chosen as the positive control in view of the earlier report of stretch-induced activation of glucose transport by this kinase (Chambers et al., 2009b). A clear p38 response to stretch was observed (Figure 4.1).

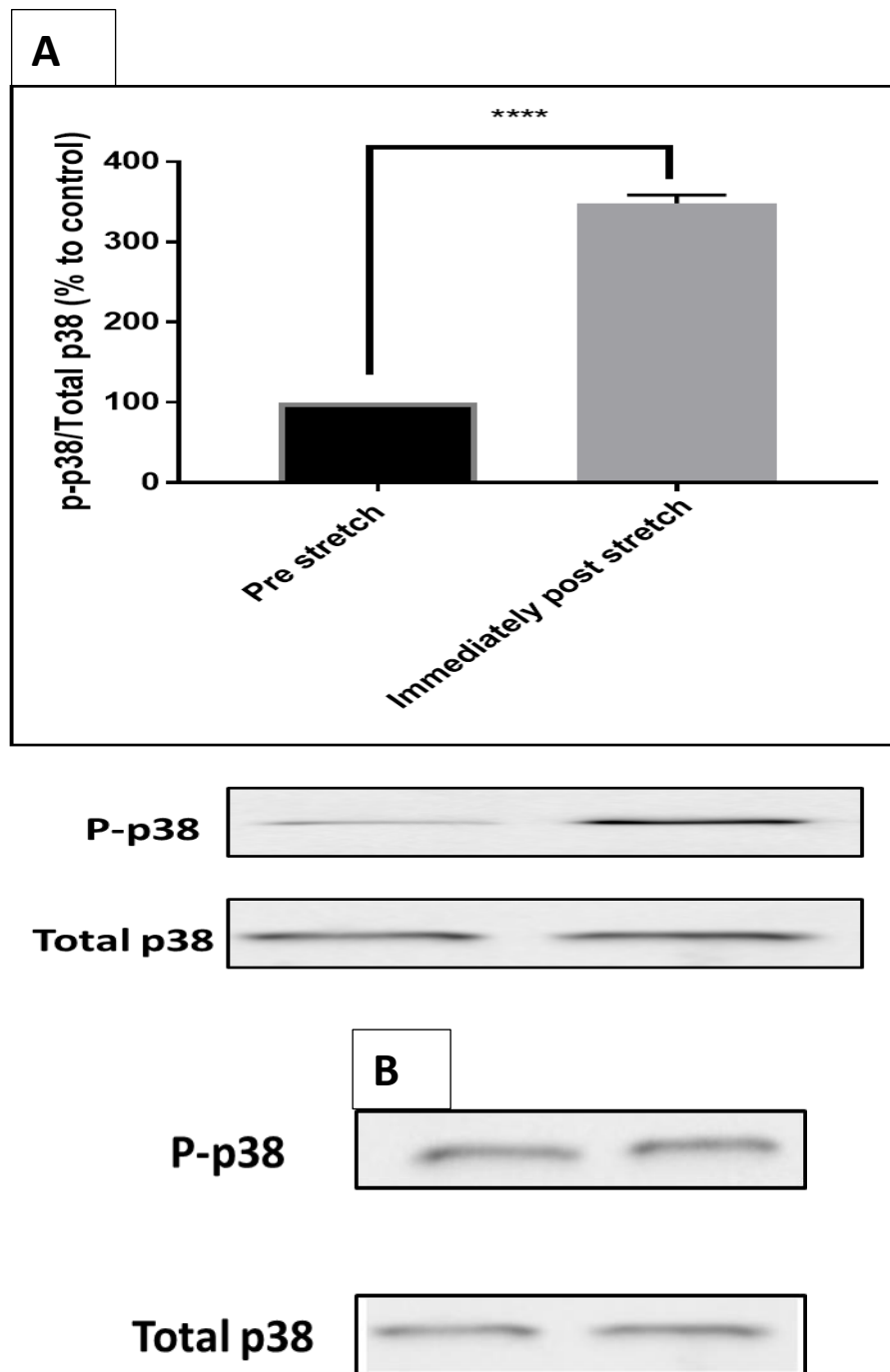


Figure 4.1. Effect of 5 minutes of cyclic stretch on p-p38 activity.

A) L6-G8C5 myotubes were cultured on collagen-coated Flexcell silicone-based culture wells. The medium used was based on MEM at pH 7.4 and contained 2mM L-Gln with 2% dialysed foetal bovine serum. Myotubes were stretched using a Flexcell FX-4000 system as described in section 2.4 (Goto *et al.*, 2003). After stretching, the media were then rapidly aspirated and each well immediately scraped in 200µl of Lysis Buffer. Immunoblots of proteins were separated by SDS-PAGE; probing with anti-Phospho-p38 MAPK and the bands (43 kDa) were quantified by densitometry using the ChemiDoc Touch Imaging System. Pooled data are shown from n=3 independent experiments. B) An example of control blot that was run in parallel with (a) on an unstretched plate. **** Denotes significant difference from Pre-stretch Control ($P = <0.0001$).

4.2.2 Monitoring of pH drift

As disturbance to the 5% CO₂ atmosphere in a culture incubator can be a problem during cell stretching experiments, potentially leading to inadequate gassing of the culture medium and pH drift (especially in short incubations), the colour of the phenol red in the stretched and control plates was monitored and shown to remain stable (Figure 4.2).

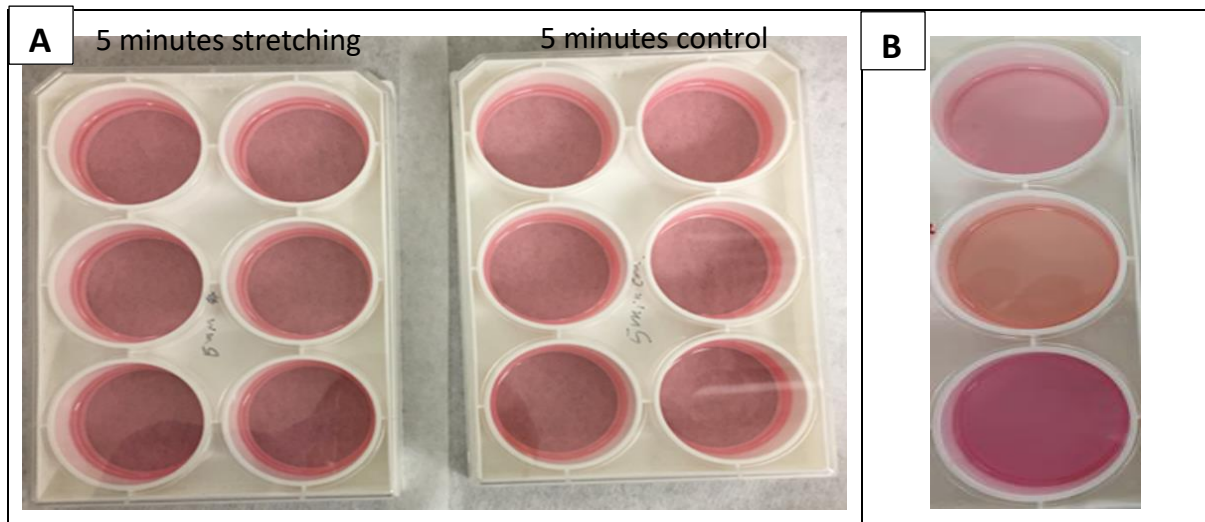


Figure 4.2. Images showing stable phenol red colour following 5 minutes of cyclic stretching in the culture incubator.

A) (Left) cultures which had been subjected to 5 minutes of stretching on a Flexcell FX-4000 system. (Right) control cultures which had been incubated on the same system without applying vacuum stretching. B) Visual calibration of the phenol red colour showing MEM with 2mM L-Gln with 2% dialysed foetal bovine serum adjusted to pH 7.4 (top), pH 7.1 (middle) and pH 7.7 (bottom) after equilibration in a 5% CO₂ culture incubator.

4.2.3 Effect of continuous stretching of L6-G8C5 myotubes on System A (SNAT2) amino acid transport activity

As previous pilot experiments (Clapp, 2010) had detected an apparent stimulation of transport activity and a possible (but statistically insignificant) increase in SNAT2 mRNA expression after 48 hours of continuous stretch, initial experiments in this project sought to reproduce these effects (Figure 4.3). Analysis of the whole time course by 2-way ANOVA detected no significant stimulatory effect of stretch on System A (SNAT2) activity. Indeed, when the 48 hours data alone were analysed, a marginally significant *decrease* in activity in response to stretch was detected (Figure 4.3).

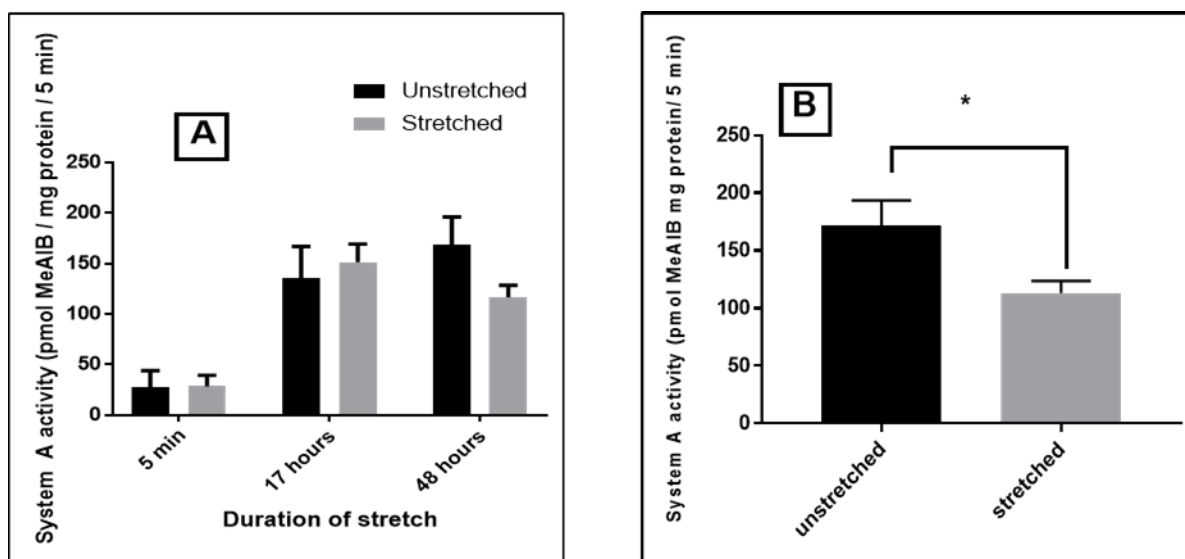


Figure 4.3. Time course of the effect of passive continuous stretch on System A (SNAT2) transporter activity in L6-G8C5 myotubes.

L6-G8C5 myotubes cultured on collagen-coated Flexcell silicone-based culture wells were placed on glass spheres and stretched for the times indicated by applying a 3kg weight on the top of the culture plate, as described in Section 2.3 (Rauch and Loughna, 2008b). The medium used was MEM at pH 7.4 with 2mM L-Gln and 2% dialysed foetal bovine serum. A) Analysis of the whole data set by 2-way ANOVA, taking stretch and time as the experimental variables, detected no significant effect of stretch ($P = 0.3334$), but a significant effect of time ($P < 0.0001$). B) Analysis of the 48h data in isolation by unpaired *t*-test detected a marginally significant inhibitory effect of stretch ($*P = 0.0213$)- Data compiled from 5 independent experiments are presented, with 4 replicate culture wells in each experiment.

4.2.4 The effect of cyclic stretch on the activity of System A (SNAT2) on L6-G8C5 myotubes

In view of the negative results above, the effect of stretch was also examined by cyclic stretch, which may be a more physiologically relevant model for effects of exercise on skeletal muscle. However, as prolonged cyclic stretch has been reported to induce apoptosis in L6 myoblasts (Liu et al., 2009), further experiments were restricted to shorter duration than in Section 4.2.3.

As can be seen in Figure 4.4A, when L6-G8C5 myotubes were stretched by a vacuum-driven FX-4000 system for up to 1 hour using cyclic intermittent stretch, no obvious effect on System A (SNAT2) transport was observed, with the possible exception of a transient increase in transport rate after only 1 minute of stretch (Figure 4.4B). Moreover, to assess whether the method of stretching was affecting the outcome of the experiment, stretching was also

performed without applying a vacuum by using a mechanical device (the “Push” system described in Section 2.5) for myotube stretching over a similar time course. This again showed no significant effect of stretch on System A activity (Figure 4.5).

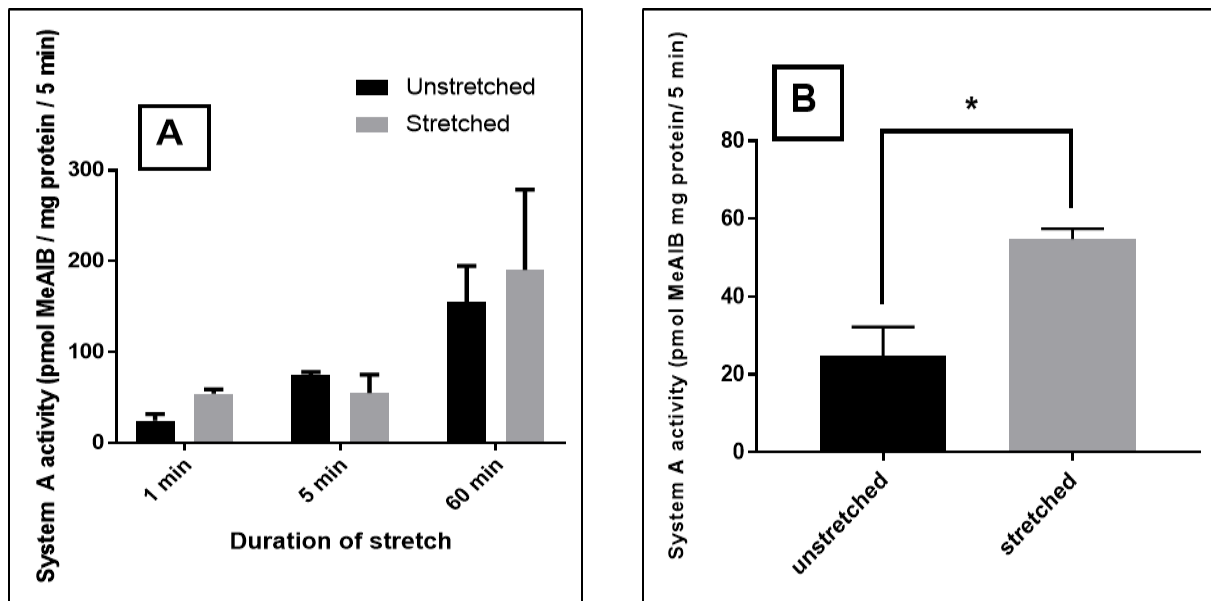


Figure 4.4. Time course of the effect of vacuum-induced cyclic stretch on System A (SNAT2) transport activity in L6-G8C5 myotubes.

L6-G8C5 myotubes cultured on collagen-coated Flexcell silicone-based culture wells were subjected to cyclic stretching using a Flexcell FX-4000 system as described in Section 2.4 (Goto et al., 2003) and stretched for the times indicated.. The medium used was MEM at pH 7.4 and contained 2mM L-Gln with 2% dialysed foetal bovine serum. A) Analysis of the whole data set by 2-way ANOVA, taking stretch and time as the experimental variables detected no significant effect of stretch ($P = 0.5022$), but a significant effect of time ($P = 0.0008$). B) Analysis of the 1 minute data in isolation by paired t-test detected a marginally significant stimulatory effect of stretch ($*P = 0.0248$)- Data compiled from 3 experiments are presented, with 6 replicate culture wells in each experiment.

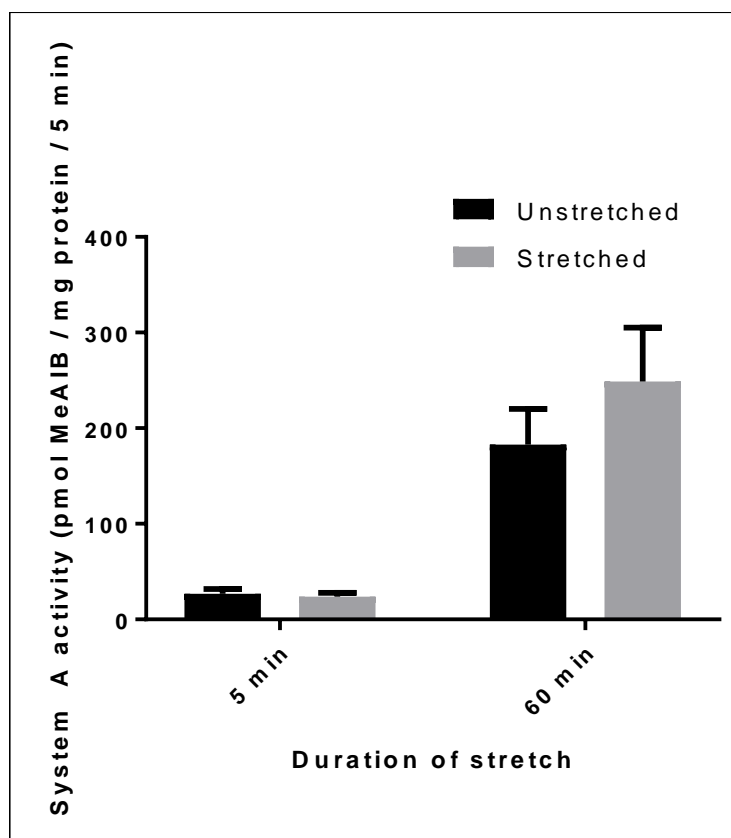


Figure 4.5. Time course of the effect of cyclic stretch induced by mechanical pushing on System A (SNAT2) transport activity in L6-G8C5 myotubes.

L6-G8C5 myotubes cultured on collagen-coated Flexcell silicone-based culture wells were subjected to cyclic stretching using a Push system as described in Section 2.5 and stretched for the times indicated. The medium used was MEM with 2mM L-Gln and 2% dialysed foetal bovine serum. Analysis of the whole data set by 2-way ANOVA, taking stretch and time as the experimental variables detected no significant effect of stretch ($P = 0.2397$), but a significant effect of time ($P < 0.0001$). Data compiled from 3 experiments are presented, with 6 replicate culture wells in each experiment.

4.2.5 The effect of cyclic stretch on the activity of System A (SNAT2) in L6 myoblasts

It has previously been observed that the physiological catabolic response of L6-G8C5 cultures to low pH is unexpectedly lost when very highly fused myotube cultures are used (Pickering et al., 2003). For that reason, the effect of stretch was also studied here using unfused myoblasts, to determine whether the cultures were becoming refractory to stress in the fused state. However, again no significant effect was recorded on System A (SNAT2) transport after *in vitro* stretch of these myoblasts (Figures 4.6 and 4.7).

It has also been proposed that cultures of L6 myotubes may show a delayed response to cyclic stretch. (Atherton et al., 2009a) found that there was an increase of the phosphorylation of

mTOR at Ser2448 when a delay was imposed after a bout of L6 myotube cyclic stretching. However, there was not an effect on mTOR during stretching (*ibid*). In the transport experiments that are shown in (Figures 4.4, 4.5 and 4.6) the 5 minutes ^{14}C -MeAIB transport assay was performed by working as rapidly as possible after stretching had stopped. In practice, this meant that the transport measurement started approximately 1 minute to 2 minutes after the end of stretch. In Figures 4.4 to 4.6, this led to detection of an apparent (but statistically insignificant) increase in transport of about 20% after 1 hour of stretching. Therefore, L6 myoblasts were subjected here to cyclic stretch for 1 hour and System A (SNAT2) transport activity was measured immediately post-stretch (as in Figure 4.6) and also post-stretch after leaving the stretched cultures in the incubator for a further 1 hour to see if there was an effect of further delay on transport. As shown in Figure 4.7, there was no effect of stretch at all in the cultures that had been subjected to the extra 1 hour delay.

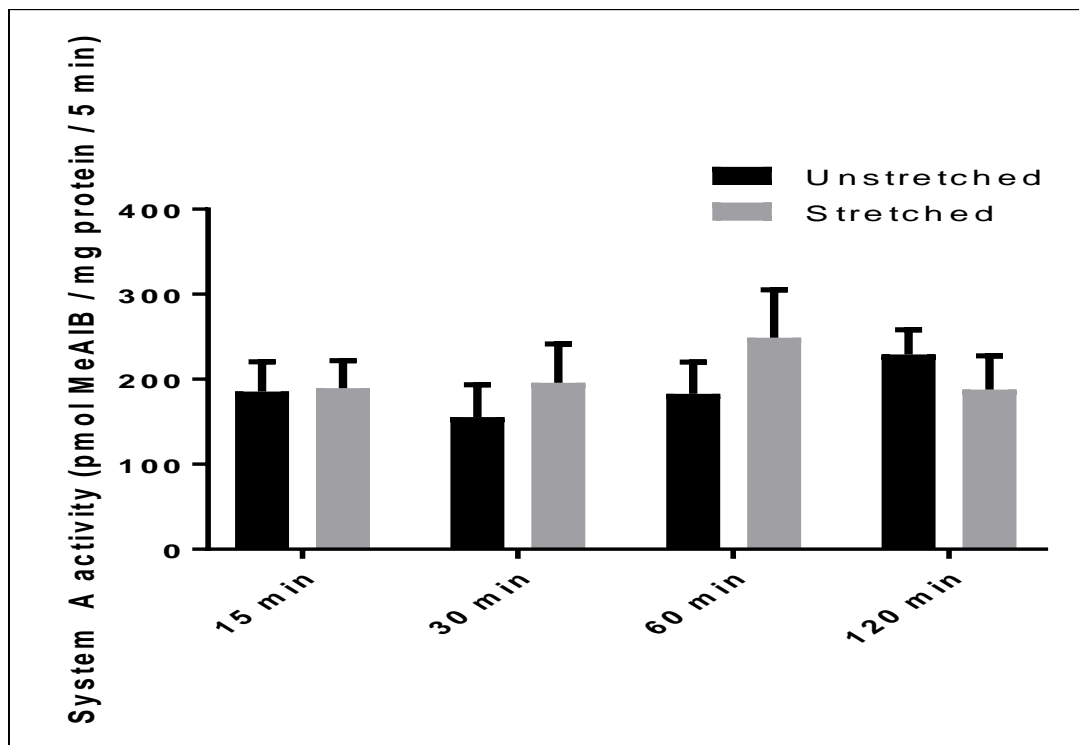


Figure 4.6. Time course of the effect of vacuum-induced cyclic stretch on System A (SNAT2) transport activity in L6-G8C5 myoblasts.

L6-G8C5 myoblasts cultured on collagen-coated Flexcell silicone-based culture wells were subjected to cyclic stretching using a Flexcell FX-4000 system as described in Section 2.4 (Goto et al., 2003) and stretched for the times indicated.. The medium used was MEM at pH 7.4 and contained 2mM L-Gln with 2% dialysed foetal bovine serum. Analysis of the whole data set by 2-way ANOVA, taking stretch and time as the experimental variables detected no significant effect of stretch ($P = 0.4359$), Data compiled from 3 experiments are presented, with 6 replicate culture wells in each experiment.

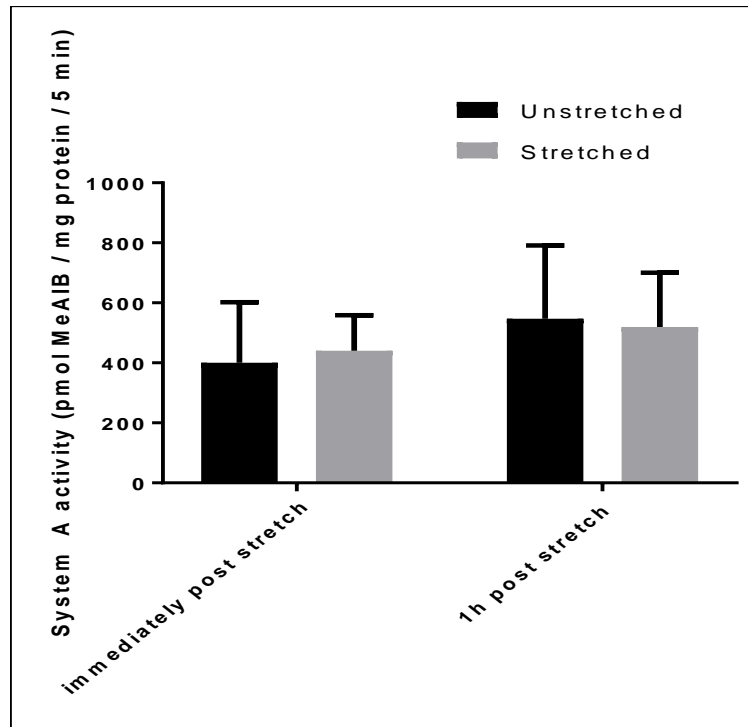


Figure 4.7. Effect of 1 hour of cyclic vacuum-induced stretch and 1 hour of post-stretch incubation on System A (SNAT2) transport activity in L6-G8C5 myoblasts.

L6-G8C5 myoblasts cultured on collagen-coated Flexcell silicone-based culture wells were subjected to 1 hour of cyclic stretching using a Flexcell FX-4000 system as described in Section 2.4 (Goto et al., 2003), followed by a 1 hour post-stretch incubation. The medium used was MEM at pH 7.4 and contained 2mM L-Gln with 2% dialysed foetal bovine serum. Analysis of the whole data set by 2-way ANOVA, taking stretch and post-stretch incubation as the experimental variables detected no significant effect of stretch ($P = 0.9642$). Data compiled from 4 experiments are presented, with 6 replicate culture wells in each experiment.

4.3 Discussion

4.3.1. The effect of stretch on System A (SNAT2) transporters

In testing the hypothesis that System A (SNAT2) transporters can be activated in stretched L6-G8C5 cells *in vitro*, this chapter sought to investigate the effect of mechanical loading on these cells and to optimise the stretch methods to examine the effect on the transporters. It was hoped that this optimisation would also provide insights into the role of different proteins involved in the hypothesis being tested in this project, especially MAPKs. In practice, no significant effect was observed.

There is abundant evidence, from the data in Chapter 3 of this thesis, from previous work in this laboratory (Blbas, 2018), and from a range of cell types stressed with hypertonic medium or by amino acid deprivation (López-Fontanals et al., 2003, Franchi - Gazzola et al., 2006, Hyde et al., 2007), that MAP kinases exert a major activating influence on SNAT2 transporters. There is also strong evidence, both from the data in Chapter 3 and from other laboratories (Hornberger and Chien, 2006, Kook et al., 2008, Chambers et al., 2009b, Fu et al., 2018) that mechanical stretch, both in stretched myotubes and in passively stretched skeletal muscle, acutely activates MAP kinases. Furthermore, in rat skeletal muscle studied *ex vivo* System A transport is activated by exercise (King, 1994, Henriksen et al., 1992, Henriksen et al., 1993). It is therefore surprising that when L6-G8C5 myoblasts and myotubes were stretched for different periods, using the range of techniques applied here, no significant stimulation of transport was observed, with the possible exception of a transient increase following very short duration stretching of L6-G8C5 myotubes (1 minute, in Figure 4.4B). Indeed continuous stretch for 48h showed a tendency to decrease transport (Figure 4.3B).

4.3.2. Technical artifacts

Very prolonged *in vitro* cell stretching may lead to cell death, as demonstrated by Liu *et al.* (2009), who used a Flexcell 4000 system to conduct cyclic stretching of rat myoblasts (L6) for up to 24 hours and found that apoptosis occurred through caspase activation as a result (Liu et al., 2009). For this reason, such prolonged cyclic stretching was not applied in the present experiments. The cyclic stretching protocol that was applied here is derived from the work of Goto *et al* (Goto et al., 2003). Applying an 18% linear stretch in this way has been criticised on the grounds that it is too severe and may lead to rupture of myotubes (Schultz and

McCormick, 1994, Zhan et al., 2007, Kook et al., 2008). For this reason, the cultures in the present project were routinely checked for signs of myotube rupture or detachment in three ways: by phase contrast microscopy, by monitoring the total protein content of the cultures at the end of the experiment, and by assay of the myotube lysis marker CPK in the medium (see Chapter 5). Spontaneous rapid fusion of L6-G8C5 myotubes leading to fragile highly fused cultures may occasionally make them vulnerable to spontaneous detachment, especially when they are then subjected to stretch. This was only observed in one short series of experiments in this project (Appendix C.1). This did not suppress System A transport activity. On the contrary, this caused a marked artifactual increase in transport activity in the remaining adherent cells, especially in the stretched cultures (Appendix C.1).

A significant time-dependent increase in System A transport activity is routinely observed during short incubations with the L6-G8C5 cell line (Figures 4.2, 4.4, 4.5), possibly caused by rapid conditioning of the medium with autocrine insulin-like factors which are produced by myotubes (Perrone et al., 1995). Insulin potently stimulates System A activity in L6 myotubes (Hyde et al., 2002). For this reason, the apparent transient stretch-induced rise in transport observed here in 1 minute stretching experiments should be treated with caution: because relatively small errors in timing the experiment could lead to a large error in the System A activity measured.

Cyclic vacuum-induced “pull” stretch and continuous or cyclic “push” stretch all yielded similar negative results in these experiments, suggesting that the failure to observe stretch-induced transport activation was not simply a technical artefact arising from vacuum or temperature effects on the cell monolayer.

4.3.4. Rapid inactivation of the effect of stretch on System A (SNAT2) transport

Even though the responsiveness of p38 activation to stretch was shown to be retained in the cultures used here (Figure 4.1), it is possible that the transport activity was not assayed sufficiently rapidly at the end of the stretching experiments to detect the stimulation of transport by the JNK and p38 kinases predicted from the effects of stretch in Chapter 3. The failure to observe the predicted effect might arise because phosphorylation events activated by stretch are rapidly inactivated by phospho-protein phosphatases (PPases) when stretching ceases. PPase up-regulation by prolonged stretch might also explain the apparent decrease in transport activity after 48 hours of stretching (Figure 4.3B).

In contrast clear activation of System A transporters by exercise has been detected in *ex vivo* preparations of rat muscle in spite of prolonged *post mortem* processing of the tissue (King, 1994, Henriksen et al., 1992, Henriksen et al., 1993) suggesting that rapid inactivation was not a problem there. However, in exercising muscle the lifetime of phosphorylation events may be radically different from that in stretched myotubes. Myosin ATPase and CPK activity in exercising muscle generates high intracellular concentrations of inorganic phosphate (Pi) by degradation of phosphocreatine (Arnold et al., 1985) and Pi is known to be a potent inhibitor of PPases in intact cells (Abbasian et al., 2015). Such effects would be absent in the present study.

4.3.5. Implications of this negative result

The failure here to observe the predicted rise in System A (SNAT2) transport activity following mechanical stretch suggests that an important part of the hypothesis outlined in Section 1.15 is not supported by the experimental evidence. The hypothesis predicted that such a MAPK-mediated stretch effect on System A transport, and its inhibition by the action of low pH on MAPK activation and on the System A transporters themselves, would lead to a downstream decline in IL-6 gene expression (via p38) and a decline in synthesis of the IL-6 protein (via SNAT2 activity and mTORC1). Testing these downstream predictions is the subject of the next chapter.

Chapter 5 Regulation of expression of Interleukin-6 (IL-6) in L6 cells

5.1 Introduction

The contraction of human skeletal muscle causes the expression and release of IL-6, which then has numerous metabolic effects, such as the activation of AMPK, which influences fatty acid oxidation and insulin-stimulated glucose disposal *in vivo* (Section 1.12). IL-6 may exert beneficial effects in serious inflammatory states, like chronic kidney disease (Stockdale and Miller), especially when secreted without other pro-inflammatory cytokines, such as TNF- α . However, the presence of acidosis resulting in System A/SNAT2 inhibition in CKD patients could theoretically result in expression of IL-6 being particularly weak, for the reasons explained in the hypothesis section of this thesis (Section 1.15). The resulting depletion of important amino acids is in principle problematic because the protein kinase complex mTORC1, which plays a crucial role in protein synthesis (including possibly synthesis of the IL-6 protein itself), is sensitive to amino acids. In addition exercise-induced lactic acidosis could in principle worsen this problem when CKD patients exercise (Watson et al., 2013a), which might have further adverse effects on mTORC1 and the production of IL-6 and, and result in a corresponding drop in global protein synthesis.

The experiments described in this chapter aim to test these possibilities to better understand the effect of low pH in stretched skeletal muscle cells (L6 cells) (*in vitro*), in an attempt to mimic some aspects of what happens in exercising skeletal muscle in CKD patients. This model (using the FX-4000 system as described in 2.4) involving lengthening of the cells could mimic eccentric contraction of skeletal muscles, but cannot mimic concentric muscle contraction.

This study proposes to test the following hypothesis:

- 1) In mechanically stressed skeletal muscle cells, *in vitro* mechanical stretching can lead to MAPK activation, resulting in increased expression of IL-6 mRNA and (at least *in vivo* (King, 1994, Henriksen et al., 1992, Henriksen et al., 1993)) to System A/SNAT2 up-regulation, followed by mTORC1 activation and ultimately the up-regulation of translation and global protein synthesis and synthesis of the IL-6 protein.
- 2) The above pathway is inhibited (and IL-6 myokine expression and output lessened) as a result of the associated inhibition by acidosis of MAP kinases and SNAT2 (Evans et al., 2007b, Evans et al., 2008b, Blbas, 2018).

3) Similar effects should be obtained by experimental MAPK inhibition or SNAT2 gene silencing by siRNA.

However, before this hypothesis can be tested, it is important to note that a key feature of muscle contraction which cannot be simulated *in vitro* by mechanical stretch alone is the rise in intracellular Ca^{2+} concentration (Iwata et al., 2007) which has been shown previously to be an important factor regulating IL-6 gene expression in L6 myotubes (Chan et al., 2004b). In earlier studies with those cells this requirement was satisfied by treating the cells with the Ca^{2+} ionophore ionomycin (Chan et al., 2004b) and, for this reason, ionomycin was also used in the experiments described in this chapter.

In (Figures 5.1A, 5.2, 5.4 and 5.5) myotubes were incubated with ionomycin for 6 hours and IL-6 expression was measured as described in Section 2.13.3. However, myoblasts were used in (Figure 5.1B).

In (Figures 5.7 and 5.8) SNAT2 was silenced in myoblasts as described in Section 3.13.5 and IL-6 expression was measured as described in Section 2.13.3.

In (Figure 5.9) myotubes were cyclically stretched as described in Section 2.4, under different pH conditions and then IL-6 expression was measured as described in Section 2.13.3.

5.2 Results

5.2.1 The effect of stimulation with ionomycin and p38 MAP kinase inhibition on IL-6 gene expression in L6-G8C5 myotubes

In L6 myotubes, it has been shown previously that ionomycin induces p38 MAPK activation in the nucleus, which increases the expression of IL-6 mRNA (Chan et al., 2004b) and a p38 inhibitor drug (SB203580) blocked the effect on IL6 expression (Chan et al., 2004b). The previous results in Chapter 3 (Figure 3.7) demonstrate p38 activation by mechanical stretch (and inhibition of p38 by low pH as in Figure 3.4). It is therefore possible that mechanical stretch or low pH will also affect IL-6 expression. The initial aim of this investigation was to reproduce the effect of ionomycin on IL-6 mRNA expression reported by Chan *et al.* (Chan et al., 2004b), and to attempt to block this expression using a different p38 inhibitor SB202190. This inhibitor differs from the one used by Chan *et al.* but showed significant effects on System A/SNAT2 activity in L6-G8C5 cells (see Figure 3.1A). In agreement with Chan *et al.* a very marked 50-fold increase in IL-6 mRNA was observed in response to ionomycin and

interestingly, this expression of IL-6 mRNA was significantly inhibited by pharmacological p38 inhibition, despite the use of a different p38 inhibitor (Figure 5.1A).

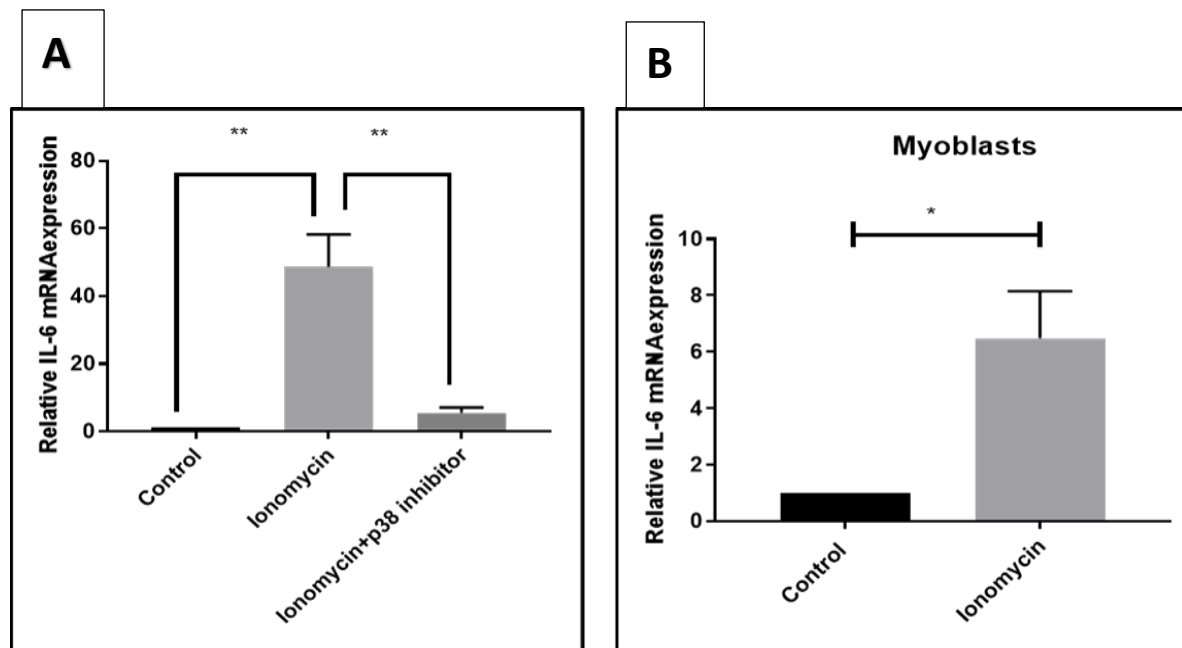


Figure 5.1. The effect of ionomycin and p38 MAP kinase inhibition on IL-6 gene expression in L6-G8C5 myotubes and myoblasts.

A) In L6-G8C5 myotubes IL-6 mRNA was measured by RT-qPCR using a Rat IL-6 Taqman gene expression assay and TBP as a house-keeping gene. The expression of IL-6 was related to TBP expression as described in 2.12.3 (Pfaffl, 2001). The myotubes were cultured in a medium based on MEM at pH 7.4, containing 2mM L-glutamine with 2% dialysed foetal bovine serum. Then the myotubes were incubated for 6 hours with 0.5 μ M ionomycin and 5 μ M SB202190 (p38 inhibitor), and either no drugs as a baseline control, or 0.5 μ M ionomycin as a positive control. Pooled data are shown from n=3 independent experiments. ** Denotes a significant difference from the positive control ($P<0.01$). B) shows a similar experiment performed in L6-G8C5 myoblasts. Culture conditions were as described below in (Figure 5.7). * Denotes a significant difference from the control ($P<0.05$).

5.2.2 The effect of low pH on IL-6 mRNA and protein expression in L6-G8C5 myotubes

It was hypothesised (in Section 1.15) that IL-6 expression (especially IL-6 protein expression) might be impaired at low pH. This also seems likely in view of the strong p38 dependence of IL-6 expression that was seen in (Figure 5.1, and the observation that basal p38 activation was inhibited by low pH in Figure 3.4. The effect of low extracellular pH on the expression both of IL-6 mRNA (Figure 5.2) and of IL-6 protein (Figure 5.3) was therefore tested. The predicted decrease of IL-6 mRNA expression was not observed (Figure 5.2) on the contrary when cells were stimulated at low pH in the presence of ionomycin, a surprising significant increase was observed in the IL-6 mRNA expression (Figure 5.2) and a similar fractional increase with low pH was also observed in the absence of ionomycin but fell short of statistical significance.

However, in contrast there was no significant effect of ionomycin or pH on IL-6 protein secretion into the culture medium measured by ELISA (Figure 5.3) even though the IL-6 positive control provided with the assay was clearly detected.

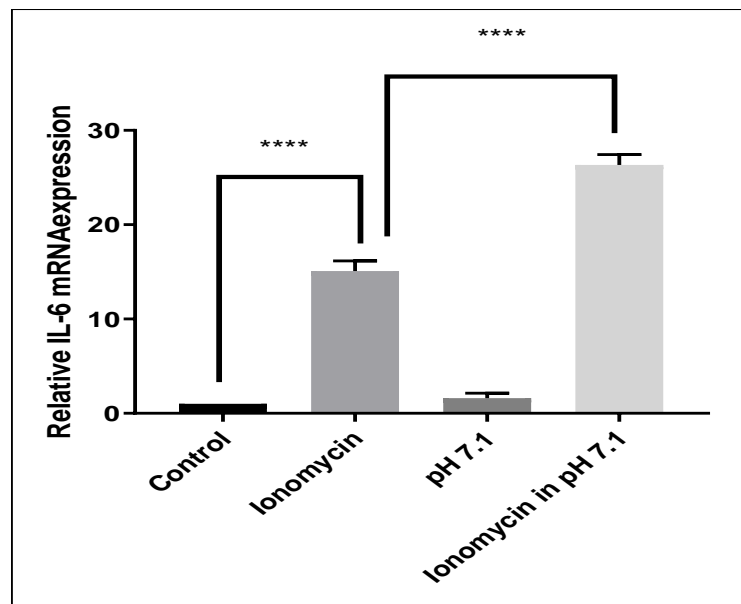


Figure 5.2. The effect of low pH on the stimulation by ionomycin of IL-6 gene expression in L6-G8C5 myotubes.

IL-6 mRNA was measured by RT-qPCR using Rat IL-6 Taqman gene expression assay and TBP as a house-keeping gene. The expression of IL-6 was related to TBP expression (Pfaffl, 2001). The myotubes were cultured in a medium that was based on MEM at a control pH of 7.4, or pH 7.1 which contained 2mM L-glutamine with 2% dialysed foetal bovine serum. The myotubes were then incubated for 6 hours either with no drug as a baseline control or with 0.5 μ M ionomycin at pH 7.4 or pH 7.1. Pooled data are shown from n=3 independent experiments. **** Denotes significant difference between two conditions ($P < 0.0001$).

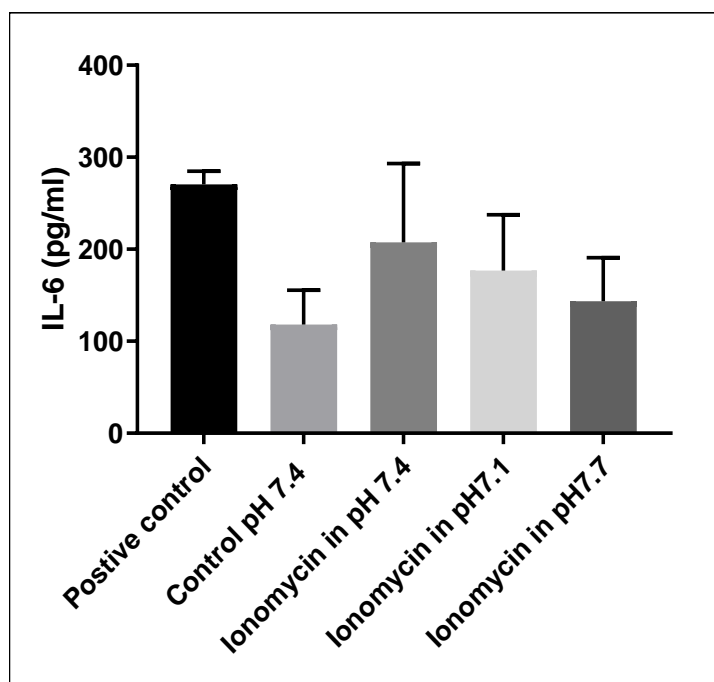


Figure 5.3. The effect of low pH and of ionomycin on IL-6 protein secretion in L6-G8C5 myotubes.

Myotubes were cultured in a medium that was based on MEM at pH 7.4 or pH 7.1 with 2mM L-glutamine with 2% dialysed foetal bovine serum. The myotubes were then incubated for 6 hours either with no drug as a baseline control or with 0.5 μ M ionomycin at pH 7.4 or pH 7.1 or pH 7.7 and supernatants was taken for assay as described in Section 2.7. Data pooled from 3 independent experiments.

5.2.3 The effect of p38 inhibitor, JNK inhibitor and MeAIB on the stimulatory effect of ionomycin on IL-6 gene expression in L6-G8C5 myotubes

It was hypothesised (in Section 1.15) that inhibition of System A/SNAT2 might lead to inhibition of IL-6 expression. In view of Chan *et al.*'s (Chan et al., 2004b) observation (confirmed in Figure 5.1A) of p38 inhibition suppressing IL-6 mRNA expression; and in view of the observation (in Figure 3.1A) that p38 inhibition inhibited System A / SNAT2 activity, it is also possible that p38 inhibition may be inhibiting IL-6 mRNA expression at least partly through inhibiting System A / SNAT2. In Figure 3.1A, it was observed that inhibition of JNK also inhibited System A/SNAT2 activity. JNK has also been reported in a number of cell types to be activated by Ca^{2+} (Sun et al., 2017, Brnjic et al., 2010, Kim and Sharma, 2004, Saxena et al., 2011, Arthur et al., 2000, Dhanasekaran and Reddy, 2017, Huang et al., 2014), suggesting that it might play a role in the stimulatory effect of ionomycin that was observed in Figure 5.1A. Therefore, the aim of this experiment was to see the effect of a JNK inhibitor, and direct competitive inhibition of System A / SNAT2 amino acid transport activity with a saturating

dose (10mM) of MeAIB, on IL-6 expression. In spite of the predicted roles of JNK and System A / SNAT2, it was found that only p38 inhibitor inhibited ionomycin-induced IL-6 expression (Figure 5.4), indeed MeAIB may have further increased expression, although this fell short of statistical significance ($P = 0.0754$), and JNK inhibitor may also have had a weak stimulatory effect.

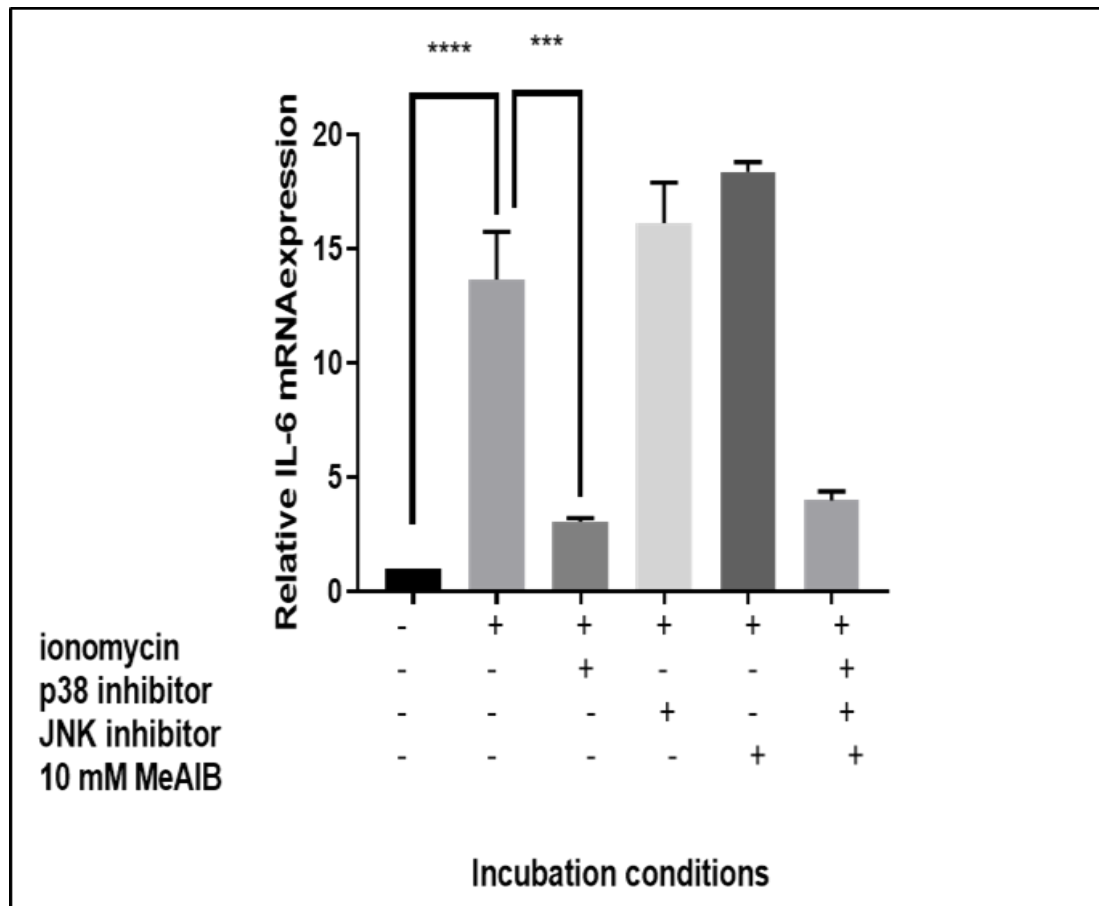


Figure 5.4. The effect of JNK inhibition and MeAIB on the stimulation by ionomycin of IL-6 gene expression in L6-G8C5 myotubes.

IL-6 mRNA was measured by RT-qPCR using Rat IL-6 Taqman gene expression assay and TBP as a house-keeping gene. The expression of IL-6 was related to TBP expression (Pfaffl, 2001). The myotubes were cultured in a medium that was based on MEM at pH 7.4, and which contained 2mM L-glutamine with 2% dialysed foetal bovine serum. The myotubes were then incubated for 6 hours either with no drugs as a baseline control or with 0.5 μ M ionomycin with and without drugs at pH 7.4. These drugs include 10 μ M JNK inhibitor (SP600125) and 10mM MeAIB. Pooled data are shown from $n=3$ independent experiments. *** Denotes significant difference between two conditions ($P < 0.001$), **** ($P < 0.0001$).

5.2.4 The effect of low pH with JNK inhibitor and MeAIB on the stimulation by ionomycin of IL-6 gene expression in L6-G8C5 myotubes

Even though JNK inhibitor and MeAIB failed to inhibit ionomycin-induced IL-6 expression at pH 7.4 (Figure 5.4), the acid-induced stimulation of IL-6 mRNA expression that was observed in Figure 5.2 showed a completely different response to these agents (Figure 5.5). The data show that IL-6 expression at pH 7.1 with ionomycin was significantly inhibited by JNK inhibitor and a marginally significant inhibition ($P=0.052$) was also observed with MeAIB. This observation of a marked JNK dependence at pH 7.1 but not at pH 7.4 was unexpected in view of the significant inhibition of basal JNK activation by low pH that had previously been observed in Chapter 3 (Figure 3.3) – see Discussion Section 5.3.

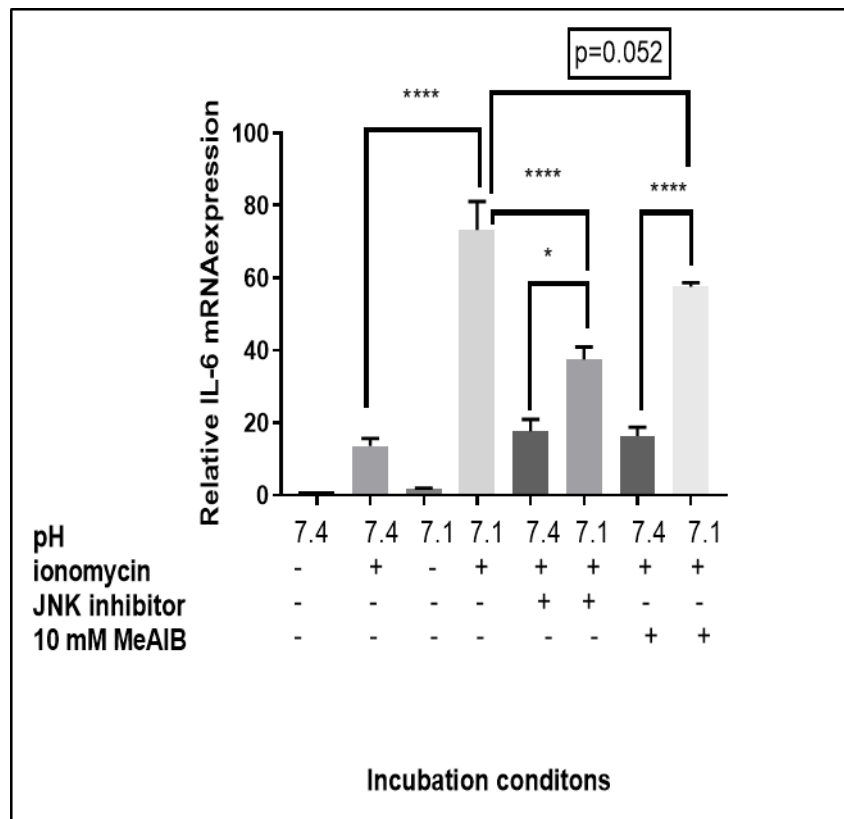


Figure 5.5. The effect of JNK inhibition and MeAIB on the stimulatory effect of low pH and ionomycin on IL-6 gene expression in L6-G8C5 myotubes.

IL-6 mRNA was measured by RT-qPCR using Rat IL-6 Taqman gene expression assay and TBP as a house-keeping gene. The expression of IL-6 was related to TBP expression (Pfaffl, 2001). The myotubes were cultured in a medium that was based on MEM at pH 7.4 or pH 7.1 which contained 2mM- glutamine with 2% dialysed foetal bovine serum. The myotubes were then incubated for 6 hours either with no drugs as a baseline control or with 0.5 μ M ionomycin with and without drugs either at pH 7.4 or pH 7.1. These drugs included 10 μ M JNK inhibitor (SP600125) and 10 mM MeAIB. Pooled data are shown from n=3 independent experiments. * Denotes significant difference between two conditions ($P<0.05$), **** ($P<0.0001$).

5.2.5 Measurement of intracellular Ca^{2+}

A possible explanation for the unexpected stimulation of IL-6 mRNA expression by low pH in Figures 5.2 and 5.5, and for the suppression of this effect by a JNK inhibitor at low pH (Figure 5.5) but not at pH 7.4 (Figures 5.4 and 5.5) is that low pH is increasing intracellular Ca^{2+} which could further enhance the effect shown in Figure 5.1 and also activate JNK (Sun et al., 2017, Brnjic et al., 2010, Kim and Sharma, 2004, Saxena et al., 2011, Arthur et al., 2000, Dhanasekaran and Reddy, 2017, Huang et al., 2014). As low pH had only a relatively small stimulatory effect on IL-6 expression in the absence of ionomycin (Figure 5.2) this might arise because low pH increases the ability of ionomycin to carry Ca^{2+} into the cell. However, direct measurements of the pH dependence of ionomycin's effect as an ionophore have shown that this does not occur: in fact ionomycin is reported to become more active as pH rises (Stiles et al., 1991). Furthermore direct measurement of intracellular Ca^{2+} in L6-G8C5 myoblasts using the fluorescent indicator Fluo-4 (Figure 5.6) failed to detect any significant change in response to low pH or to inhibition of System A / SNAT2 transporter flux with a saturating dose of MeAIB. Even though the Fluo-4 AM ester had entered the cells and undergone de-esterification to the fluorescent dye (Figure 5.6) and even though this fluorescence was clearly responsive to Ca^{2+} depletion with EGTA and to Ca^{2+} loading with high dose ionomycin during calibration (Figure 5.6), all other stimuli had no apparent effect on the Ca^{2+} concentration (Figure 5.6).

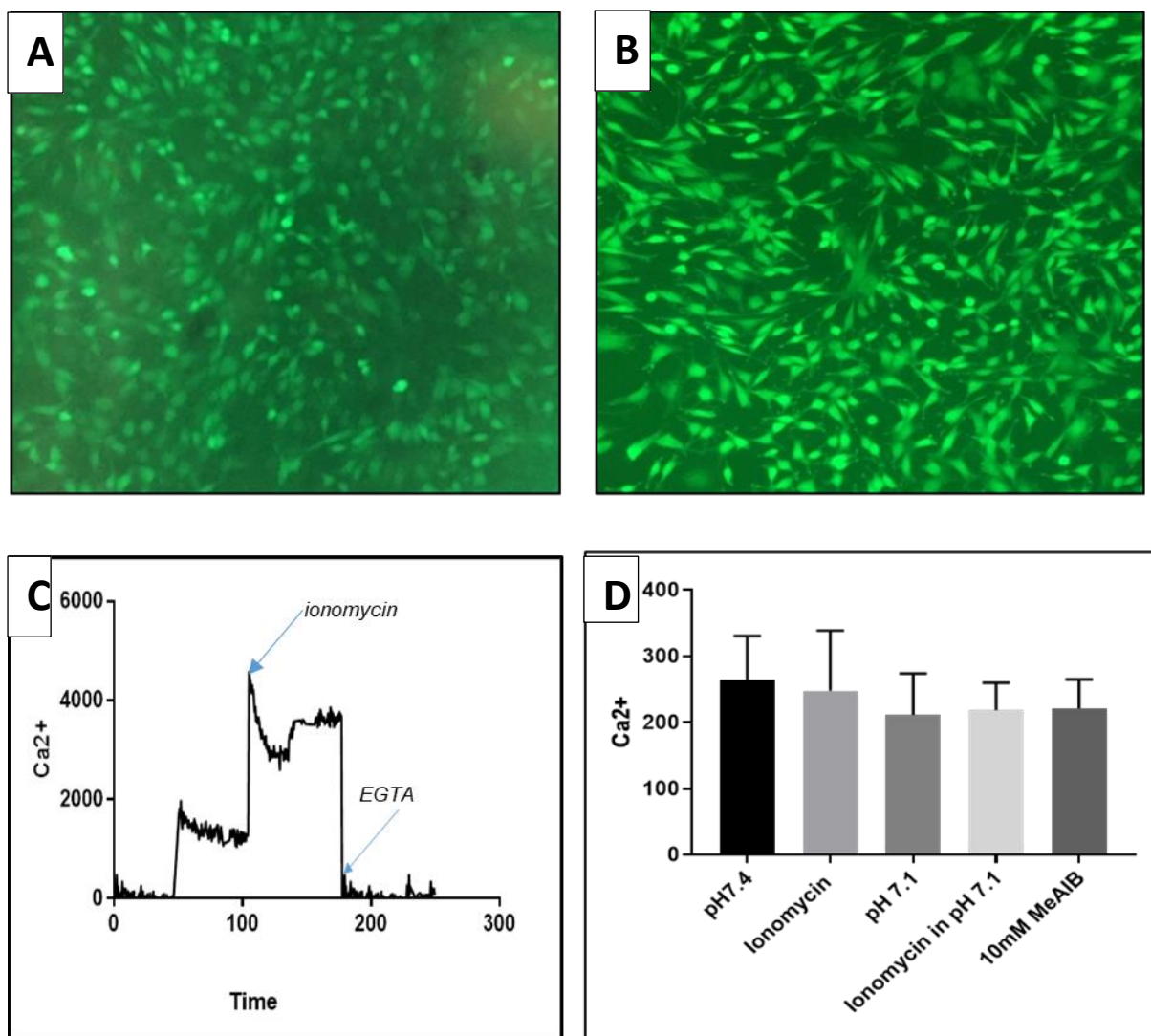


Figure 5.6. The effect of pH and MeAIB with or without ionomycin on intracellular calcium levels of L6 myoblasts.

A) Negative control image of cells without FLuo-4 showing auto-fluorescence. B) An image of the Fluo-4 loaded cells showing their enhanced fluorescence. C) Typical calibration data showing the effect on the fluorescence signal of adding high dose ionomycin and EGTA. D) L6 myoblasts were cultured in DMEM Growth Medium for 18h as described in Section 2.13. Then, the Growth Medium was gently aspirated from each well, which was then rinsed with 200 μ l of PSS. Then, the cells were loaded with fluo-4-AM ester (Fisher-11504786) for 45 minutes at 37°C under a 5% CO₂ atmosphere. After that, the wells were rinsed three times with 200 μ l of PSS-BSA, and then 200 μ l of fresh PSS-BSA was added to each well and cells were incubated again in a humidified incubator at 37°C to allow time for the Fluo-4 AM to be de-esterified by the cells to generate the free Fluo-4 dye. Then the fluorescence intensity was read on a NOVOstar plate-reader at an excitation wavelength of 488nm, and detecting at >500nm at 37°C. Pooled data are shown from $n = 3$ independent experiments. The ionomycin concentrations that was used in the experiment was 0.5 μ M and the higher concentration of ionomycin that was used in the calibration was 1 μ M.

5.2.6 The effect of siRNA silencing of SNAT2 on the stimulation of IL-6 gene expression in L6-G8C5 myoblasts

The aforementioned results (Figure 5.5) suggest that the stimulation of IL-6 mRNA expression by ionomycin in L6-G8C5 myotubes is more effective at pH 7.1 than at pH 7.4. This is not what would be expected if, as originally postulated (Section 1.15), System A / SNAT2 promotes IL-6 expression and is inhibited by low pH. However, a saturating dose of the System A substrate MeAIB did seem to suppress IL-6 expression in Figure 5.5. Therefore, to clarify further the role of System A / SNAT2 in regulation of IL-6 expression, silencing of the expression of SNAT2 with anti-SNAT2 siRNA was performed, to see whether it mimicked the enhancing effect of low pH on ionomycin-induced IL6 expression in L6-G8C5 cells, or (in contrast) mimicked the inhibitory effect of MeAIB.

In this experiment, it was necessary to use myoblasts rather than myotubes, because myoblasts allow more efficient siRNA transfection and hence more efficient siRNA silencing of SNAT2 (Evans et al., 2007a, Evans et al., 2008a). Silencing of SNAT2 with siRNA is measurable in myotubes (Evans et al., 2008b) but is less marked than in myoblasts. However, myotubes (Figure 5.1A) and myoblasts (Figure 5.1B) both show a strong increase in IL-6 mRNA expression in response to ionomycin, thus allowing the effect of SNAT2 silencing on IL-6 expression to be studied in myoblasts.

The experiment aimed to test whether the level of SNAT2 expression can influence IL-6 expression. In myoblasts SNAT2 was silenced successfully using the silencing siRNA (Figure 5.7). However, in studying cytokine expression, it is important to control for non-specific effects of siRNAs on cells, because of evidence that uncapped RNA is sensed by mammalian cells as a sign of viral infection, and can induce some aspects of an inflammatory response (Kanasty et al., 2012). In studying IL-6 expression, it is important therefore to compare the effect of SNAT2 silencing siRNA with an irrelevant scrambled control sequence rather than with transfection reagent alone. Compared with transfection reagent alone, scrambled siRNA led to an apparent increase in IL-6 expression both without (Figure 5.8A) and with (Figure 5.8B) ionomycin, and this reached statistical significance when no ionomycin was present. However, relative to this elevated baseline, the same concentration of SNAT2 silencing siRNA gave an apparent decrease in IL-6 mRNA. In the presence of ionomycin (Figure 5.8B), this reached statistical significance – apparently consistent with the marginal inhibition of IL-6 mRNA expression induced by MeAIB at low pH in Figure 5.4.

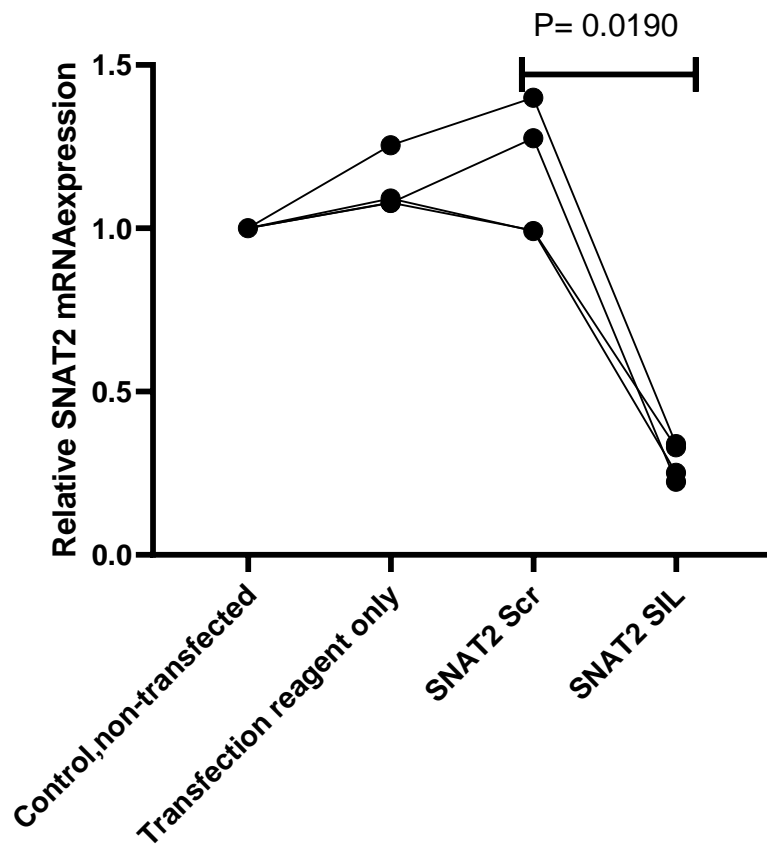


Figure 5.7. Testing the effect of anti-SNAT2 siRNA reagent on SNAT2 mRNA expression.

L6 myoblasts were cultured in DMEM growth medium for 24h then the medium was aspirated and replaced with half of the usual volume of growth medium and treated with 30nM scrambled control siRNA (Scr) (Evans et al., 2007b), silencing anti-SNAT2 siRNA (SIL). The cells were left with the transfection mix for 16h then the medium with the transfection mix was aspirated and replaced with double the normal volume of the usual growth medium for another 24h before commencing the experiment. The myoblasts were then incubated for 6 hours in the test media. The medium that was used was based on MEM at pH 7.4 and contained 2mM L-Gln with 2% dialysed foetal bovine serum. The non-transfected cells were used as an additional negative control in the experiment. SNAT2 mRNA was measured by RT-qPCR using rat SNAT2 Taqman gene expression assay and TBP as a house-keeping gene. The expression of SNAT2 was related to TBP expression (Pfaffl, 2001). Pooled data are shown from n=4 independent experiments. (Friedman's ANOVA with Dunn's multiple comparison post hoc test).

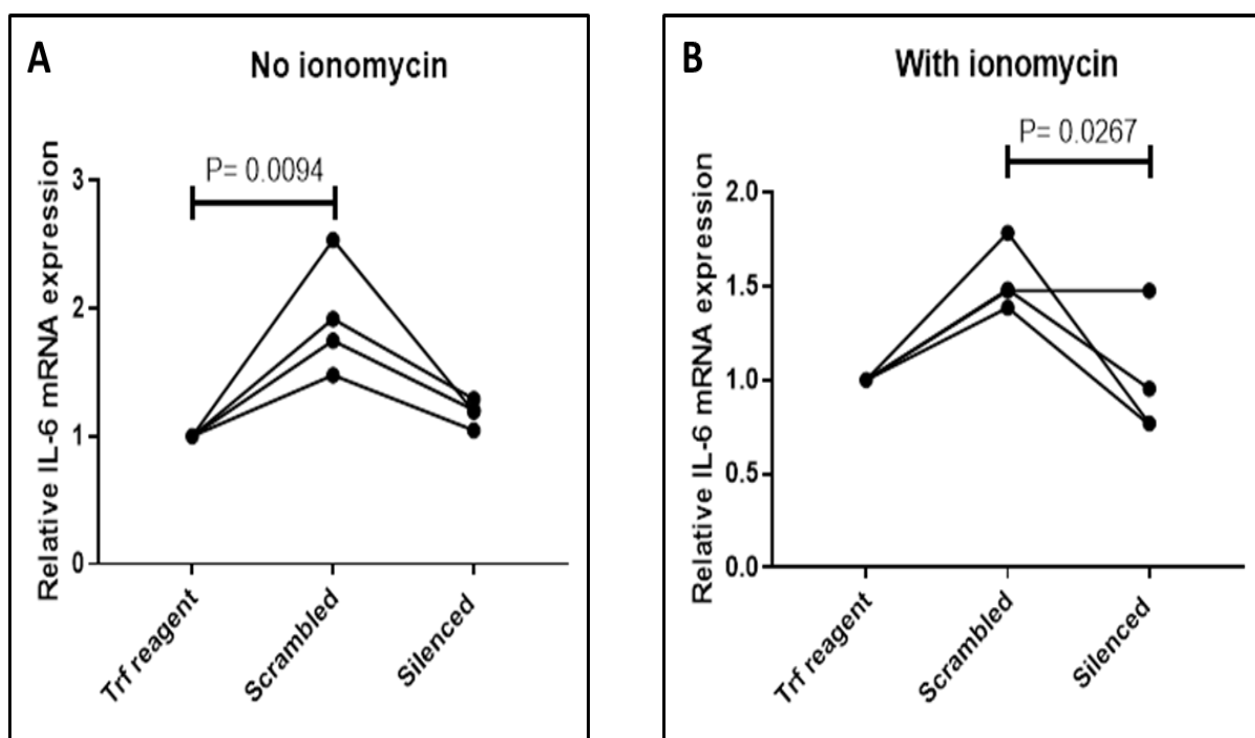


Figure 5.8. Effect SNAT2 silencing on the expression of IL-6 mRNA in absence of ionomycin.

L6 myoblasts were cultured in DMEM growth medium for 24h then the medium was aspirated and replaced with half of the usual volume of growth medium and treated with 30nM scrambled control siRNA (Scr) (Evans et al., 2007b), or silencing anti-SNAT2 siRNA (SIL). The cells were left with the transfection mix for 16h then the medium with the transfection mix was aspirated and replaced with double the normal volume of the usual growth medium for another 24h before commencing the experiment. The myoblasts were then incubated for 6 hours in the test media A) in absence of ionomycin, B) with 0.5 μ M ionomycin. The medium that was used was based on MEM at pH 7.4 and contained 2mM L-Gln with 2% dialysed foetal bovine serum. IL-6 mRNA was measured by RT-qPCR using a rat IL-6 Taqman gene expression assay and TBP as a house-keeping gene. The expression of IL-6 was related to TBP (Pfaffl, 2001). Pooled data are shown from n=4 independent experiments. (Friedman's ANOVA with Dunn's multiple comparison post hoc test).

5.2.7 A revised model for regulation of IL-6 expression

The results presented above do not support the hypothesis in Section 1.15 that a low extracellular pH would decrease IL-6 expression by inhibiting the amino acid transport rate through System A/SNAT2 transporters and by inhibiting MAPK (p38) activation. However, even though there was no clear evidence that the System A amino acid transporter activity of SNAT2 affected IL-6 expression, it is possible that indirect effects of the SNAT2 protein occur through the proposed “transceptor” function of SNAT2 in sensing extracellular signals (Hyde et al., 2007). Additionally, System A transporters like SNAT2 may associate with integrins in the plasma membrane (McCormick and Johnstone, 1995). Integrins and their associated tyrosine kinases (for example Focal Adhesion Kinase, FAK) are thought to play an important role in the mechanotransduction signals by which mechanical stretch can activate MAPKs

(Hanke et al., 2010). It has also been shown using L6-G8C5 myoblasts that siRNA silencing of SNAT2 can impair phospho-activation of JNK (Blbas, 2018). A revised model that may explain the links observed between mechanical stretching, SNAT2 and JNK activation is illustrated below in Figure 5.14 (see Discussion Section 5.3).

If the proposed link between System A / SNAT2, integrins (McCormick and Johnstone, 1995) and possibly FAK occurs in L6G8C5 myotubes, it would be predicted that:

1. Mechanotransduction through this complex by stretching the cells should increase IL-6 mRNA.
2. As the proposed effect in (1) is not directly Ca^{2+} - dependent, it should occur without ionomycin.
3. As pH sensitive System A transport is not involved, the effect in (1) may not be strongly pH sensitive.
4. The effect in (1) may be inhibited by a selective inhibitor of FAK

5.2.8 The effect of short periods of cyclic stretching on IL-6 mRNA expression in L6-G8C5 myotubes

The only previously reported study of the effect of stretch on IL-6 expression in myotubes stretched the cells up to 1 hour (Juffer et al., 2014). Therefore, this study sought to evaluate the effect of short duration (30 minutes) stretching on the expression of mRNA of IL-6 in L6-G8C5 myotubes, using a vacuum FX-4000 mechanical stretcher exactly as described in Chapter 4. A significant increase was found in the expression of IL-6 mRNA after the L6 myotubes were stretched. This was observed in the absence of ionomycin and in all pH conditions studied – from pH 7.1 to pH 7.7 (Figure 5.9). Unlike the myotubes treated with ionomycin (Figures 5.2 and 5.5), no statistically significant pH dependence of the IL-6 mRNA expression was seen, either in stretched or unstretched cells (Figure 5.9).

However, in the same experiments there was no corresponding effect on IL-6 protein secretion when the same conditions were applied (Figure 5.10). This could be due a defective step in post-translation modification of the IL-6 protein (see Discussion) or a decline in cell viability owing to myotubes rupture induced by stretch. However, L6 myotubes that were stretched for 30 minutes showed no sign of cell damage judged from release of the intracellular marker enzyme CPK into the medium, except at pH 7.7. This condition had slightly higher CPK levels,

as can be seen in Figure 5.11. For this reason, the apparent (but statistically insignificant) increase in IL-6 mRNA observed at pH 7.7 in Figure 5.9 should be treated with caution, as it may be a consequence of cell damage.

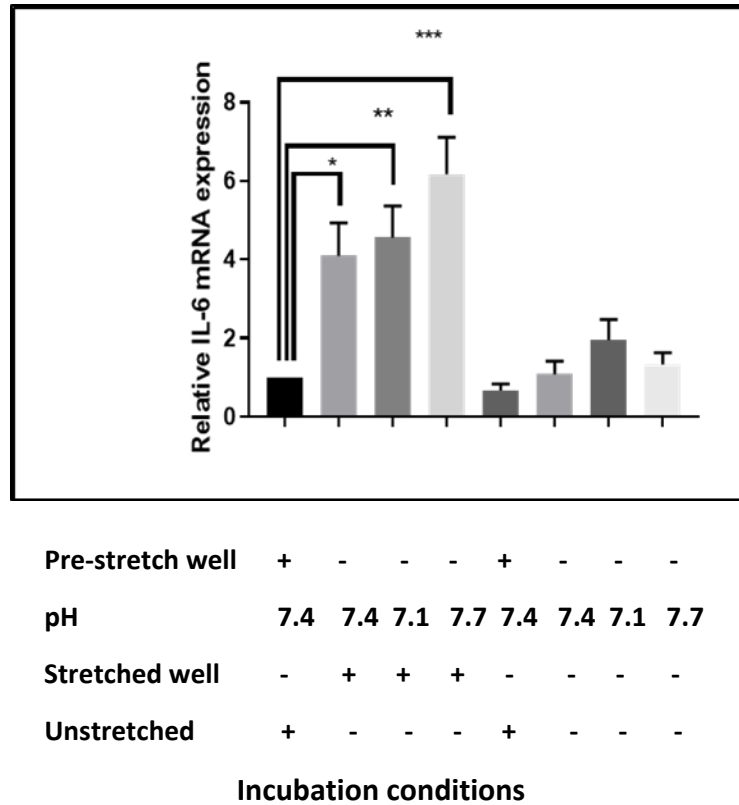
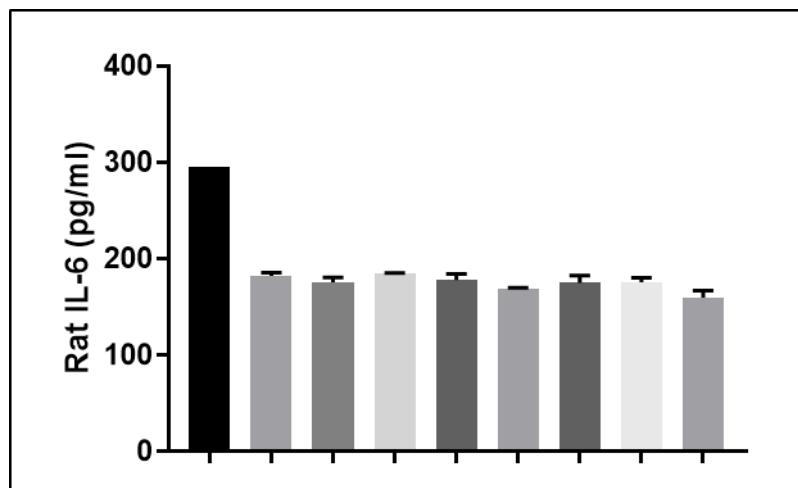


Figure 5.9. Effect of 30 minutes of cyclic stretch on the expression of IL-6 mRNA.

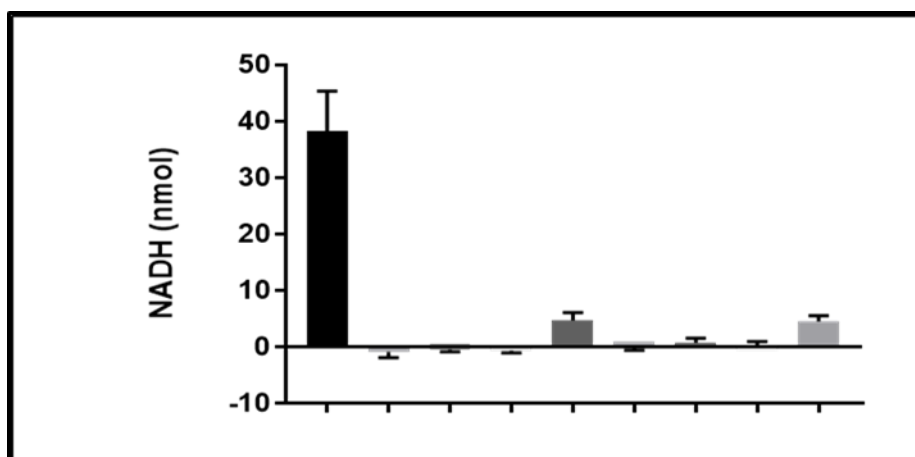
*L6-G8C5 myotubes were cultured on collagen-coated Flexcell silicone-based culture wells. The medium used was based on MEM at pH 7.4 and contained 2mM L-Gln with 2% dialysed foetal bovine serum. Myotubes were stretched using an FX-4000 system as described in Section 2.4 (Goto et al., 2003). IL-6 mRNA was measured by RT-qPCR using a rat IL-6 Taqman gene expression assay and TBP (TATA-box binding protein) as a house-keeping gene. The expression of IL-6 was related to TBP expression (Pfaffl, 2001). Pooled data are shown from n=3 independent experiments. * Denotes significant difference from Pre-stretch Control ($P<0.05$), ** ($P<0.01$), *** ($P<0.001$).*



Positive control	+	-	-	-	-	-	-	-	-
Pre-stretch well	-	+	-	-	-	+	-	-	-
pH	7.4	7.4	7.4	7.1	7.7	7.4	7.4	7.1	7.7
Stretched well	-	-	+	+	+	-	-	-	-
unstretched	+	+	-	-	-	+	-	-	-
Incubation conditions									

Figure 5.10. Effect of 30 minutes of cyclic stretch on the secretion of IL-6 protein.

L6-G8C5 myotubes were cultured on collagen-coated Flexcell silicone-based culture wells. Myotubes were stretched for 30 minutes using a FX-4000 system as described in Section 2.4 (Goto et al., 2003) under the different conditions shown on the figure and supernatants were taken and assayed for rat IL-6 by ELISA as described in Section 2.8. Data pooled from 3 independent experiments are shown.



Positive control	+	-	-	-	-	-	-	-	-
Pre-stretch well	-	+	-	-	-	+	-	-	-
pH	7.4	7.4	7.4	7.1	7.7	7.4	7.4	7.1	7.7
Stretched well	-	-	+	+	+	-	-	-	-
unstretched	+	+	-	-	-	+	-	-	-
Incubation conditions									

Figure 5.11. The effect of 30 minutes of cyclic stretch on creatine phosphokinase (CPK) released into the medium from L6-G8C5 myotubes.

L6-G8C5 myotubes were cultured on collagen-coated Flexcell silicone-based culture wells. Myotubes were stretched for 30 minutes using the FX-4000 system as described in Section 2.4 (Goto et al., 2003) under the conditions shown on the figure and supernatants were taken and assayed for CPK as described in Section 2.9. Data pooled from 3 independent experiments are shown.

5.2.9 The effect of blockade of Focal Adhesion Kinase (FAK) with selective inhibitor (PF-573228) and p38 inhibitor (SB202190) on the effect of mechanical stretch on IL-6 expression in L6-G8C5 myotubes

The model shown in Section 5.3, Figure 5.14 suggests that integrins and FAK may play a role in regulation of MAPKs (and hence IL-6 gene expression). Therefore, the aim of this experiment was to measure the effect of a selective FAK Inhibitor (PF-573228) (Slack-Davis et al., 2007) and of a p38 inhibitor (SB202190) on the apparent stimulation of IL-6 mRNA expression that was induced in L6 myotubes by mechanical stretching as described in Figure 5.9. First, FAK inhibitor (PF-573228) was tested to confirm its efficacy by pre-incubating it

with L6-G8C5 myotubes for 4 hours and measuring the FAK-phosphorylation using an anti-phospho-FAK (Tyr576/577) antibody. To ensure optimum selectivity of this FAK inhibitor, the minimum dose was used that gave a clearly measurable inhibition of the phosphorylation of FAK (Figure 5.12). Then, L6 myotubes were stretched for 30 minutes with FAK and p38 inhibitors and IL-6 expression were measured. Interestingly, both inhibitors detectably inhibited the increased IL-6 expression that was induced by stretching (Figure 5.13).

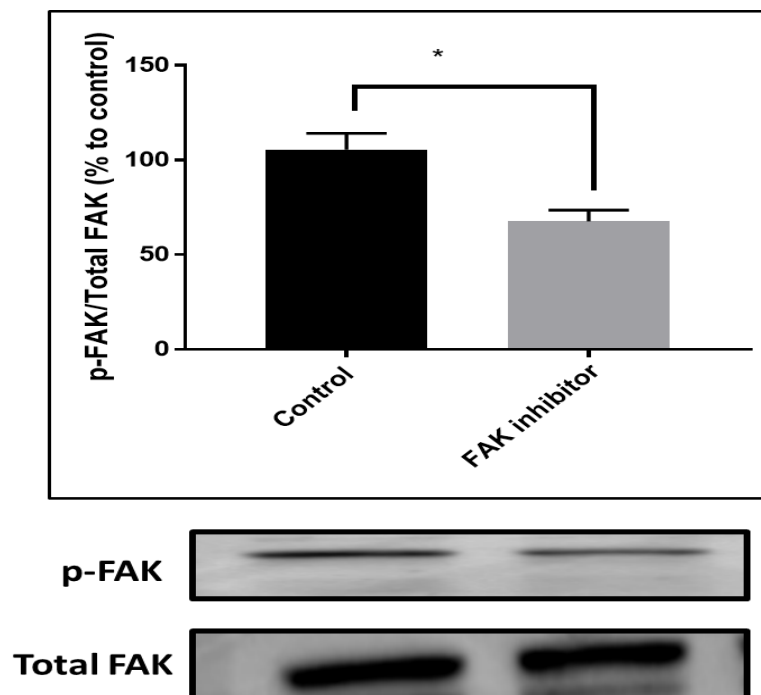


Figure 5.12. Testing the effectiveness of FAK inhibitor (PF-573228) on phosphorylation of phospho-FAK (Tyr576/577) in L6-G8C5 myotubes.

Cells were pre-incubated at pH 7.4 in MEM/2% DFBS with FAK inhibitor (1 μ M PF573228) for 4 hours. After 4 hours incubation in the test media, the plates were immediately placed on a tray of crushed ice. The media were then rapidly aspirated and each well immediately scraped in 200ul of Lysis Buffer. Immunoblots of proteins were separated by SDS-PAGE; probing with anti-p-FAK antibody and the bands (125 kDa) were quantified by densitometry using the ChemiDoc Touch Imaging System. Pooled data are shown from n=3 independent experiments, with at least 2 replicate culture wells in each experiment. * Denotes significant difference from Control (P<0.05).

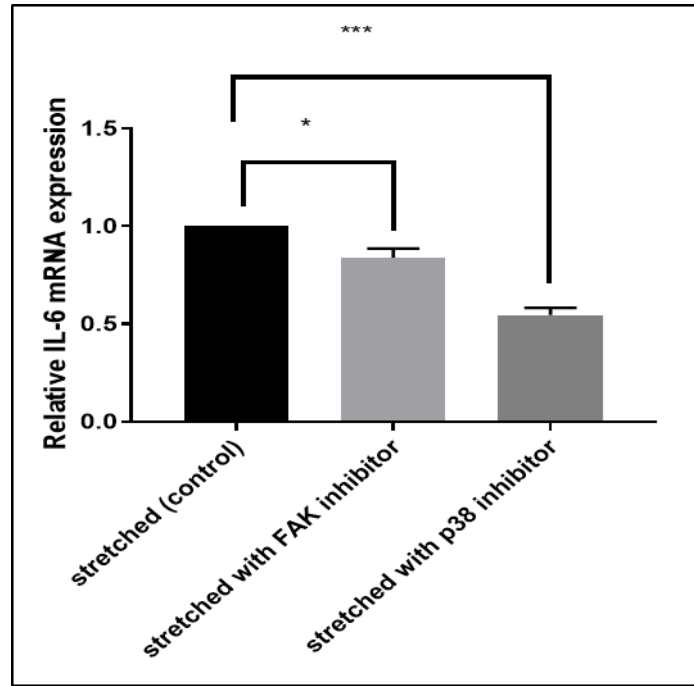


Figure 5.13. The effect of blockade of Focal Adhesion Kinase (FAK) with selective inhibitor (PF-573228) and p38 inhibitor (SB202190) on the effect of mechanical stretch on IL-6 Expression in L6-G8C5 myotubes.

L6-G8C5 myotubes were cultured on collagen-coated Flexcell silicone-based culture wells. The medium used was based on MEM at pH 7.4 and contained 2mM L-Gln with 2% dialysed foetal bovine serum. Myotubes were stretched using an FX-4000 system as described in Section 2.4 (Goto, Okuyama et al. 2003). IL-6 mRNA was measured by RT-qPCR using a rat IL-6 Taqman gene expression assay and TBP as a house-keeping gene. The expression of IL-6 was related to TBP expression (Pfaffl 2001). Pooled data are shown from $n=3$ independent experiments. * Denotes significant difference between stretched control cells and stretched cells with FAK inhibitor ($1\mu\text{M}$ PF573228) ($P<0.05$). *** Denotes significant difference between stretched control cells and stretched cells with p38 inhibitor ($5\mu\text{M}$ SB202190) ($P<0.001$).

5.3 Discussion

5.3.1 Ionomycin or cyclic stretch increase expression of IL-6 mRNA but not IL-6 protein

The reason for the failure of the stimulatory effects of ionomycin and low pH on IL-6 mRNA to be translated into similar effects on the secreted IL-6 protein is unknown. In principle an effect may have been missed here because of a possible time lag between the rise in IL-6 mRNA and secretion of a mature IL-6 protein for which rate-limiting processing steps such as glycosylation (Santhanam et al., 1989) may be required. Sampling the culture medium at later time points might therefore have detected stimulation of release of IL-6 protein. However it should be noted that such stimulation of IL-6 protein expression *in vitro* has also not been reported elsewhere (for example in (Chan et al., 2004b)), possibly indicating some form of defect in post-translational processing of the IL-6 protein or a defect in its secretion from L6-G8C5 cells. As the protein was assayed here only in the medium and not in the cell layer, the present experiments give no information on the efficiency of IL-6 secretion from the cells, and this would be worth investigating in future experiments.

5.3.2 Low pH exerts an unexpected stimulatory effect on ionomycin-induced IL-6 mRNA expression

An important paradox that was observed in these experiments was that the acid-induced rise in IL-6 mRNA (at pH 7.1 with ionomycin) was partly blocked by JNK inhibitor even though JNK inhibitor had no effect on IL-6 mRNA at pH 7.4 (Figure 5.5). This effect of JNK inhibitor at low pH was unexpected, because directly measured phospho-activation of JNK was lower at pH 7.1 than at pH 7.4 (Figure 3.3). However, an important difference between the Chapter 3 data and the data in Figure 5.5 is that Figure 3.3 shows the effect of pH on JNK activation under basal conditions, whereas Figure 5.5 shows the effect of pH in Ca^{2+} - loaded cells. As Ca^{2+} has been reported to activate JNK (Sun et al., 2017, Brnjic et al., 2010, Kim and Sharma, 2004, Saxena et al., 2011, Arthur et al., 2000, Dhanasekaran and Reddy, 2017, Huang et al., 2014), it is possible that the overall pH dependence of JNK activation is significantly different in Ca^{2+} loaded cells. In the presence of Ca^{2+} it seems that a JNK-dependent pathway has been activated by low pH, possibly indicating that the decline in JNK phospho-activation that was observed in Figure 3.3 is reversed in Ca^{2+} loaded cells, resulting in a rise in JNK activation at low pH. This could be tested by direct measurement of the pH dependence of JNK activation in ionomycin-treated cells.

The acid-induced rise in IL-6 mRNA at pH 7.1 with ionomycin could not be explained by an effect on low pH on System A transporters. The molecule(s) that sense this pH change and signal to IL-6 gene expression (possibly via JNK) are still unknown. The findings of the current study might be attributable to an effect of low pH on intracellular calcium signalling to the induction of IL-6 expression. However, direct measurement of cytosolic Ca^{2+} under different conditions (including pH 7.4, and pH 7.1 with and without ionomycin) did not detect a significant change of cytosolic Ca^{2+} in Figure 5.6. This does not completely rule out a role for intracellular calcium levels in L6 myoblasts however, because it is possible that low pH is acting on the cells through some other intracellular calcium pool – for example in the nucleus where a nuclear p38 pool is thought to be acting on IL-6 gene expression (Chan et al., 2004b). The occurrence of such large non-cytosolic calcium pools in L6-G8C5 cells, buffering the cytosolic pool, might explain why the measured cytosolic Ca^{2+} pool was so resistant to ionomycin in Figure 5.6.

5.3.3 Coupling between System A/SNAT2 and IL-6 expression

Even though attempted inhibition of System A transporters with a saturating dose of MEAIB (Figure 5.5) or silencing of SNAT2 gene expression with siRNA (Figures 5.7 and 5.8) may have had some partial blunting effect on the stimulation of IL-6 mRNA expression by ionomycin with or without low pH, no evidence was found in this chapter for a tight or obligatory coupling between System A / SNAT2 transporters and the amount of IL-6 mRNA. MeAIB had no detectable effect on IL-6 mRNA with ionomycin at the control pH of 7.4 (Figure 5.4); and mechanical stretching clearly stimulated IL-6 mRNA expression, even though stretch had no effect on System A / SNAT2 activity in Chapter 4 under the same conditions.

Even though the scrambled siRNA control that was used here in Figures 5.7 and 5.8 has previously been validated in L6 myoblasts (Evans 2007, 2008), in future work on IL-6 expression in these cells it would be useful to examine other scrambled control sequences to confirm that these give similar results and that the scrambled sequence used here is not exerting an indirect off-target stimulatory effect on SNAT2 or IL-6 expression.

5.3.4 A revised model for regulation of IL-6 expression in L6G8-C5 myotubes

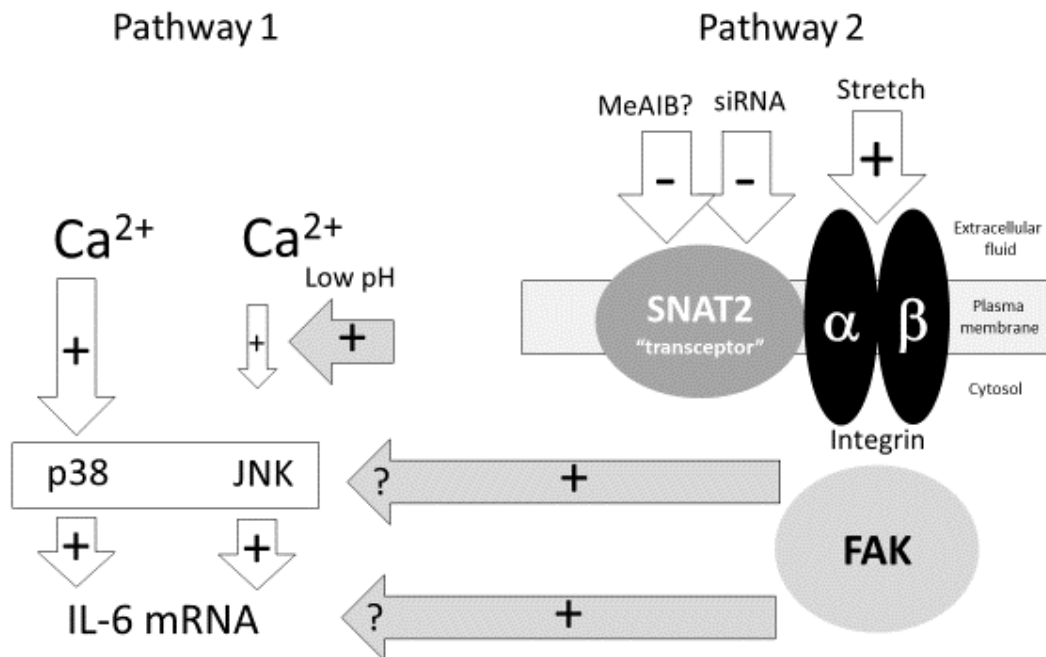


Figure 5.14. Schematic diagram showing pathways investigated in this chapter that may contribute to increased IL-6 mRNA expression in L6-G8C5 cells.

A number of observations in this study seem consistent with the revised model that is shown in schematic form in Figure 5.14 and as outlined in Section 5.2.7. Stretching L6 myotubes for short periods significantly increased levels of IL-6 mRNA gene expression, even at low pH. This outcome would not be expected if the amino acid transport rate through System A / SNAT2 was a dominant factor controlling IL-6 expression as was originally postulated in Section 1.15. However, this does not exclude a possible involvement of the SNAT2 protein as a “transceptor” – sensing extracellular signals or, through its reported complex with alpha 3 , beta 1 integrins (McCormick and Johnstone, 1995), possibly sending stretch signals to FAK. At least a partial involvement of FAK was detected here in the inhibitor experiment in Figure 5.14.

In addition to competitively blocking amino acid influx into cells through System A / SNAT2 transporters, a saturating dose of MeAIB has also been reported to down-regulate SNAT2 protein expression in L6 myotubes, apparently through sensing extracellular MeAIB and signalling as a transceptor in these cells (Hyde et al., 2007). This may explain the apparent blunting effect of MeAIB on IL-6 mRNA that was observed in (Figure 5.5). Such transceptor signals from SNAT2 have also been reported to be blocked by a JNK inhibitor (Hyde et al.,

2007) which might contribute to the inhibitory effect of JNK inhibition on the rise in IL-6 mRNA in response to ionomycin and low pH in Figure 5.5.

In contrast to the marked effect of pH on ionomycin-induced IL-6 expression in Figure 5.5, no significant pH dependence of the effect of mechanical stretch on IL-6 mRNA expression was observed. This seems consistent with the idea that pH sensitive System A amino acid transport is not directly involved in this process. A transport-independent System A/integrin/FAK complex might have a role (Figure 5.14) and might be insensitive to pH. FAK itself has been reported to respond to pH (Ilic et al., 2007, Choi et al., 2013, Paradise et al., 2011), but it is not yet known whether FAK in L6-G8C5 myotubes is able to respond to the relatively narrow range of pH values that were applied in this study.

5.3.5 Conclusion from the experimental work

In spite of the importance of System A / SNAT2 amino acid transporters in the supply of neutral amino acids and regulation of mTORC1 and global protein synthesis in L6-G8C5 cells (Evans et al., 2007b, Evans et al., 2008b), and in spite of the inhibition of System A / SNAT2 and of basal MAPK activation (including p38) by low pH; applying a low pH to these cells was found to enhance significantly the p38-dependent stimulation of IL-6 mRNA expression that was induced by ionomycin. Discussion of the possible physiological relevance of this result in the response of muscle to exercise and in the response of muscle to acidosis is the subject of the next chapter.

Chapter 6 General Discussion and Future Work

6.1 General discussion

6.1.1 The physiological significance of the findings in this thesis

Previously in Section 1.15 and Figure 1.7 of this thesis, the hypothesis to be tested was stated to be that in L6-G8C5 rat skeletal muscle cells the expression and biosynthesis of IL-6 would be:

- c) Stimulated by FAK and MAP kinases (p38 and JNK) and dependent on the System A/SNAT2 amino acid transporter, and
- d) Inhibited by low extracellular pH acting through an inhibitory effect on MAP kinase activation and on System A/SNAT2 transporters (Evans et al., 2007b, Evans et al., 2008b, Blbas, 2018).

The data presented in Chapters 3, 4 and 5 of this thesis do not support part (b) of this hypothesis. In particular, in Chapter 5 the effect of low extracellular pH on the expression of IL-6 at mRNA level (in the presence of Ca^{2+} loading with ionomycin) was found to be the opposite of what was predicted. A significant enhancement of IL-6 expression was observed at low pH. Even though the model in Figure 1.7 cannot fully explain the data, neither can the previously accepted model of IL-6 transcriptional regulation in muscle proposed by Febbraio and Pedersen in 2002 (Febbraio and Pedersen, 2002) (Figure 6.1) explain this significant pH sensitivity.

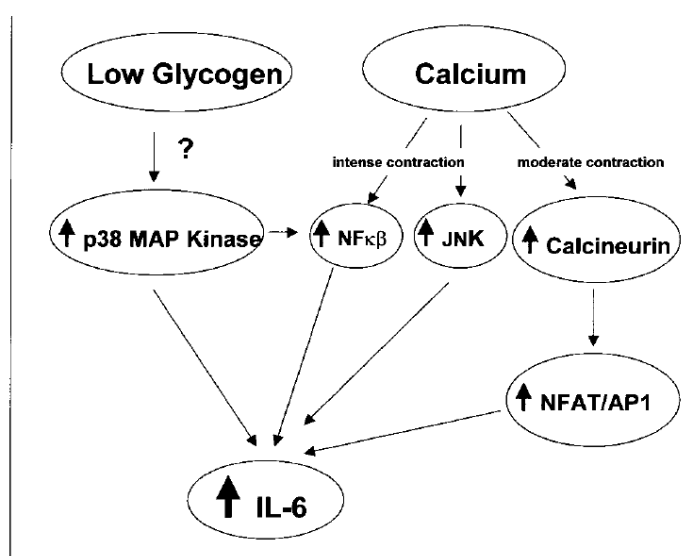


Figure 6.1 The 2002 model proposed for the transcriptional regulation of IL-6 in skeletal muscle in Febbraio, MA and Pedersen, BK (Febbraio and Pedersen, 2002).

The idea that low pH and lactic acidosis might play a part in the IL-6 myokine response to exercise is not new however. It was suggested 20 years ago that lactate or lactic acid generated by exercise might have an important role in mediating the increased expression and secretion of IL-6 in muscle (Ostrowski et al., 1998a), because the circulating IL-6 response to exercise was found to correlate tightly with the peak lactate response. However this idea was abandoned when it was found that in mitochondrial myopathy patients the opposite response was observed (Steensberg et al., 2001b). IL-6 production was measured in exercising patients who had mitochondrial myopathy and consequently high levels of plasma lactate (Steensberg et al., 2001b). The patients who exercised and received treatment with dichloroacetate to suppress their lactic acidosis produced more IL-6 than the patients who did not have treatment (Steensberg et al., 2001b) which may indicate that lactate or low pH could inhibit IL-6 production. This observation was in part the basis of part (b) of the hypothesis underlying the present project (Section 1.15).

The principal finding in the present study (that low pH enhances ionomycin-induced IL-6 mRNA expression) seems more consistent with the original observation by Ostrowski *et al* (Ostrowski et al., 1998a). A possible flaw with the study that implied suppression of the IL-6 response by lactate (Steensberg et al., 2001b) was that mitochondrial myopathy, or the dichloroacetate drug that was used in that study, might have had confounding effect(s) on the lactate or acidosis dependence of IL-6 expression.

The possible role of lactic acidosis has recently been investigated again, but without such confounding factors (Hojman et al., 2019). This again showed a tight positive correlation between the circulating concentration of the IL-6 protein and the serum concentration of lactate; following interval-based cycling exercise in healthy men. Such a correlation was also shown in electrically stimulated human myotubes, and in non-exercising mice in which lactic acid was directly injected into their muscles (Hojman et al., 2019). However, unlike the effect of low pH described in this thesis, the lactic acid effect was attributed to a post-translational mechanism in which proteolysis caused by activation of matrix metalloproteases 2 and 9 stimulated release of a vesicular pool of IL-6 protein stored within myocytes. It is interesting to note however that, in the same study (Hojman et al., 2019), injecting lactic acid into the skeletal muscle of non-exercising mice *in vivo* led to a 5.4-fold increase in IL-6 mRNA – apparently resembling the response to low pH in Chapter 5 of this thesis. A role for acidosis

was also implied in the Hojman *et al* study by the observation that the IL-6 myokine response to exercise in mice was abolished by pre-treating the animals with bicarbonate (- although that part of the study did not reach statistical significance (Hojman et al., 2019)).

It therefore seems both from (Hojman et al., 2019) and from the data in Chapter 5, that low pH may enhance the IL-6 response to exercise, and the data in the present study are the first direct demonstration of this effect *in vitro* without the presence of lactate, suggesting that this is a direct effect of pH rather than lactic acid itself. However, in neither study was it possible to identify the pH sensing mechanism, and no convincing evidence was found in this thesis that the rise in IL-6 mRNA expression at low pH was linked to the pH sensitive System A / SNAT2 transporter. A possible missing factor, which was not considered in either study, is extracellular ATP which is released from stimulated skeletal muscle cells through pannexin-1 hemichannels and has been suggested as a mediator of the increase in IL-6 expression in electrically stimulated myotubes (Bustamante et al., 2014). Such hemichannels are reported to be pH sensitive but, as low pH closes rather than opens such channels (Trexler et al., 1999), it is unlikely that this explains the enhancement of IL-6 expression by low pH.

It was also observed in the present study that stretching L6-G8C5 myotubes for up to 30 minutes led to an increase in IL-6 mRNA (Figure 5.9). A further unsolved question about pH-sensing in these cells is why does this response to stretch show no significant pH sensitivity? Surprisingly, stretched L6 myotubes showed a significant increase in the expression of mRNA of IL-6 in all pH conditions tested, including pH 7.1 (Figure 5.9).

6.1.2 The complex relationships between MAPKs, SNAT2, IL-6 and pH

Part (a) of the hypothesis that was stated in Section 1.15 (and again at the start of Section 6.1 above) suggests that MAP kinases (p38 and JNK) and the System A/SNAT2 amino acid transporter may be important factors in the expression and biosynthesis of IL-6. Low pH can inhibit System A / SNAT2 transport activity (Christensen et al., 1965, Evans et al., 2007b) and inhibition of this transporter can inhibit global protein synthesis through inhibition of mTORC1 (Evans et al., 2008a). It was also demonstrated here that both JNK and p38 were inhibited at low pH (Figures 3.3 and 3.4). MAPKs especially p38 and JNK were demonstrated to have some ability to control the activity of System A / SNAT2 transporters (Figure 3.1a). On the basis of these observations it might be expected that p38, JNK and System A /SNAT2 would promote IL-6 expression and biosynthesis in L6-G8C5 myotubes, and this pathway was hypothesised to be blunted in the acidic condition at pH 7.1. It is therefore interesting that, in

spite of the properties of p38, JNK and SNAT2 that were clearly demonstrated above, low pH *in vitro* (Chapter 5) and lactic acidosis *in vivo* (Hojman et al., 2019) significantly promoted (rather than suppressed) the expression and secretion of IL-6.

6.1.3 The physiological significance of System A/SNAT2 during exercise

Chapter 4 of this study investigated whether mechanical loading can increase System A / SNAT2 transporter activity. Even though stretching of L6-G8C5 myotubes led to a clear increase in the phospho-activation of p38 and JNK, stretching for up to 17 or even 48 hours did not lead to reproducible activation of System A / SNAT2, although a possible increase of SNAT2 activity was transiently observed as a result of short periods of stretching (1 minute) (Figure 4.4B). This contrasts with the *ex vivo* experiments on muscle obtained from exercising rats (King, 1994, Henriksen et al., 1992, Henriksen et al., 1993) which showed that System A can be activated and that this effect persists in the isolated muscle. Possible technical reasons for this discrepancy between stretched L6-G8C5 myotubes and *ex vivo* muscle preparations were discussed at the end of Chapter 4. This may merit further investigation because understanding up-regulation of an important amino acid transporter during exercise may be of value in promoting the effect of nutrient supplementation in parallel with exercise (Nelson et al., 2019). The factors controlling success or failure of such feeding are poorly understood (Nelson et al., 2019), but success could potentially increase muscle protein mass and biosynthesis of IL-6.

6.1.4 The role of ionomycin in IL-6 expression *in vitro*

The original *in vitro* modelling of the effect of ionomycin on IL-6 gene expression in L6 myotubes (Chan et al., 2004b) was made on the assumption that cytosolic Ca^{2+} was a key regulator of IL-6 expression (Febbraio and Pedersen, 2002). However, cytosolic Ca^{2+} was not measured directly in that study. Measurement of this parameter in the present study using the fluorescent Ca^{2+} indicator Fluo-4 suggested that the pH dependence of expression of IL-6 mRNA under pH 7.1 to pH 7.7 conditions could not be explained by variation in this Ca^{2+} pool (Figure 5.6). This pool showed clear changes in response to the high dose of ionomycin that was used to calibrate the assay (Figure 5.6). However, the cytosolic Ca^{2+} pool detected in this way did not show any significant changes in response to the lower dose of ionomycin that clearly gave a p38 dependent activation of IL-6 mRNA expression (Figures 5.1 and 5.6). The reason for this is unknown, but possibly arises because ionomycin is acting through some other (non-cytosolic) Ca^{2+} pool, for example in the nucleus where p38 is thought to be acting (Chan

et al., 2004b). Alternatively, the effect of ionomycin could be off-target and might be altering some parameter(s) other than the size of Ca^{2+} pools. For example it has been suggested that ionomycin may also be able to induce intracellular alkalinisation (Anwer, 1993), although there is no evidence at present that such a rise in pH could promote p38-dependent IL-6 expression.

6.2 Future work

In view of the questions raised above, it would be of interest to perform the following future work to extend the findings in this thesis:

To extend the work from Chapter 3, other ways of inhibiting MAPKs would be of interest, for example:

- Using alternative small molecule inhibitors, such as the p38 inhibitor used in the original study reported in (Chan et al., 2004b).
- Transfecting with cDNA constructs encoding mutant “dominant negative” MAP kinases (as described for example for p38 inhibition (López-Fontanals et al., 2003)).
- Silencing of MAPKs by transfection with siRNAs.

A problem with the latter two transfection-based approaches is that they require transfection of L6 myotubes, which is difficult to achieve. An alternative approach would be to perform stable transfection of myoblasts with short-hairpin (sh) RNAs which would give stable MAPK silencing in myoblasts which could then be fused to form myotubes. However, this could be problematic because long-term silencing of these functionally important MAP kinases could in principle impair cell proliferation, survival or differentiation.

In Chapter 4, it was observed that a possible transient stimulation of System A activity was observed after only 1 minute of cyclic stretch. However, it was also observed that *basal* System A transport activity was strongly dependent on the time elapsed since the addition of fresh culture medium (Figure 4.8). In future investigations of this apparent transient effect of stretch, careful timing of the incubations would therefore be needed to eliminate such artifactual basal effects. (Alternatively changing of the medium about an hour before attempting stretching might yield a more stable baseline). It would then also be of interest to search for transient stretch effects in related experimental systems. For example:

- In cyclically stretched mouse C2C12 or human myotubes.

- In cyclically stretched bundles of isolated mouse skeletal muscle fibres (Wendowski et al., 2017).
- In passively stretched muscles (e.g. EDL (Chambers et al., 2009b)).
- In electrically stimulated skeletal muscle or myotubes (Yano et al., 2011, Hojman et al., 2019).

To test the idea (from the discussion section of Chapter 4) that a key protein phosphorylation signal (e.g. from MAPKs – Chapter 3) or from FAK (Chapter 5) is being turned off by a phosphoprotein phosphatase during stretch, the effect of pharmacological inhibition of phosphoprotein phosphatases (Abbasian et al., 2015) or loading of myotubes with the physiological inhibitor Pi (Abbasian et al., 2015) could be tested. Loading of the culture medium with physiologically attainable Pi concentrations may be sufficient to give functionally important effects, because effects on global protein metabolism have been observed in these cells in such Pi-loaded medium (Zhang et al., 2018).

In Chapter 5, SNAT2 silencing in L6-G8C5 cells seemed capable of inhibiting the expression of IL-6 mRNA (Figure 5.8) and this may indicate the potential influence of this transporter on IL-6. It was observed that siRNA silencing of SNAT2 inhibited IL-6 mRNA expression, whereas competitive inhibition of all System A transport with MeAIB gave a more complex result: no effect was observed at control pH (Figure 5.4) but a borderline significant inhibition was seen at low pH (Figure 5.5). Therefore, to extend the work of Chapter 5, other ways of manipulating SNAT2 expression or activity could be tested. For example:

- Testing of alternative scrambled siRNA sequences as controls for non-specific effects of siRNA transfection on IL-6 expression
- Stable transfection of myoblasts with short-hairpin (sh) RNAs to give stable SNAT2 silencing followed by fusion to form myotubes.
- Transfection with SNAT2 cDNA constructs (Blbas, 2018) to determine the effect of over-expression of functionally active SNAT2 transporters on IL-6 expression.
- Transfection with SNAT2 cDNA constructs following site-directed mutagenesis (Chen et al., 2016, Zhang and Grewer, 2007, Zhang et al., 2008) to determine the effect on IL-6 expression of mutated SNAT2 e.g. SNAT2 mutated to suppress its ability to transport amino acids (Zhang et al., 2008). Such mutation would be of interest to determine whether the apparent effect of siRNA silencing in (Figure 5.8) arises from a transport

effect of SNAT2 or a transport-independent “transceptor” signalling (Hyde et al., 2007) effect of the SNAT2 protein.

As no significant effects on IL-6 protein expression or secretion were detected in Chapter 5, the work could also be extended by increasing the duration of the experiments to determine whether effects reflecting those on mRNA could also be obtained for IL-6 protein at later time points. This seems feasible because effects of ROS and NF-kappa-B signalling have been reported on IL-6 protein release from C2C12 myotubes in 24h incubations (Kosmidou et al., 2002). It would also be of interest to extend the measurements to other inflammatory (TNF-alpha) or anti-inflammatory (IL-10) cytokines.

Finally, as it was observed in Chapter 5 that the acid-induced increment in IL-6 mRNA expression was sensitive to inhibition by JNK, it would be of interest in future exercise studies in experimental animals, or in human muscle biopsies from exercising volunteers or acidotic CKD patients, to test for the predicted JNK-dependent stimulation of IL-6 expression by acidosis. It would be predicted that IL-6 expression (both at mRNA level and at protein level) and phospho-activation of JNK and c-Jun would be strongly observed following exercise, but suppressed in individuals who had received oral bicarbonate supplementation as in (Watson et al., 2013a).

6.2 Conclusion

Exercise-induced IL-6 production is regarded as physiologically important as an anti-inflammatory stimulus (Petersen and Pedersen, 2005a), as a measure to promote muscle growth and suppress cachexia (Munoz-Canoves et al., 2013) and, from recent systems biology analysis (Morettini et al., 2017), as a regulator of glucose homeostasis and insulin sensitivity via the action of IL-6 on Glucagon-like Peptide-1 (GLP-1) (Morettini et al., 2017). The key observation from this thesis of direct pH dependence of ionomycin-induced IL-6 mRNA expression in L6-G8C6 myotubes seems likely to be of physiological value in optimising the effect of exercise on IL-6 release – strongly supported by recent studies on the effect of lactic acid on IL-6 expression and secretion *in vitro* and *in vivo* (Hojman et al., 2019).

Appendixes

Appendix A: Culture medium and Test medium

A.1 DMEM (Invitrogen 11880-028)

Components	Molecular Weight	Concentration (mg/L)	mM
Amino Acids			
Glycine	75.0	30.0	0.4
L-Arginine hydrochloride	211.0	84.0	0.39810428
L-Cystine 2HCl	313.0	63.0	0.20127796
L-Histidine hydrochloride-H ₂ O	210.0	42.0	0.2
L-Isoleucine	131.0	105.0	0.8015267
L-Leucine	131.0	105.0	0.8015267
L-Lysine hydrochloride	183.0	146.0	0.7978142
L-Methionine	149.0	30.0	0.20134228
L-Phenylalanine	165.0	66.0	0.4
L-Serine	105.0	42.0	0.4
L-Threonine	119.0	95.0	0.79831934
L-Tryptophan	204.0	16.0	0.078431375
L-Tyrosine	181.0	72.0	0.39779004
L-Valine	117.0	94.0	0.8034188
Vitamins			
	140.0	4.0	0.028571429
D-Calcium pantothenate	477.0	4.0	0.008385744
Folic Acid	441.0	4.0	0.009070295
Niacinamide	122.0	4.0	0.032786883
Pyridoxine hydrochloride	206.0	4.0	0.019417476
Riboflavin	376.0	0.4	0.0010638298
Thiamine hydrochloride	337.0	4.0	0.011869436
i-Inositol	180.0	7.2	0.04
Inorganic Salts			
Calcium Chloride (CaCl ₂ ·2H ₂ O)	147.0	264.0	1.7959183
Ferric Nitrate (Fe(NO ₃) ₃ ·9H ₂ O)	404.0	0.1	2.4752476E-4
Magnesium Sulfate (MgSO ₄ ·7H ₂ O)	246.0	200.0	0.8130081
Potassium Chloride (KCl)	75.0	400.0	5.3333335
Sodium Bicarbonate (NaHCO ₃)	84.0	3700.0	44.04762
Sodium Chloride (NaCl)	58.0	6400.0	110.344826
Sodium Phosphate monobasic (NaH ₂ PO ₄ ·2H ₂ O)	154.0	141.0	0.91558444
Other Components			
D-Glucose (Dextrose)	180.0	1000.0	5.5555553
Sodium Pyruvate	110.0	110.0	1.0

<https://www.thermofisher.com/order/catalog/product/11880028?SID=srch-hj-11880-028#/11880028?SID=srch-hj-11880-028>

A.2 MEM (Invitrogen 21090-022)

Components	Molecular Weight	Concentration (mg/L)	mM
Amino Acids			
L-Arginine hydrochloride	211.0	126.0	0.5971564
L-Cystine	240.0	24.0	0.1
L-Histidine hydrochloride-H ₂ O	210.0	42.0	0.2
L-Isoleucine	131.0	52.0	0.39694658
L-Leucine	131.0	52.0	0.39694658
L-Lysine hydrochloride	183.0	73.0	0.3989071
L-Methionine	149.0	15.0	0.10067114
L-Phenylalanine	165.0	32.0	0.19393939
L-Threonine	119.0	48.0	0.40336135
L-Tryptophan	204.0	10.0	0.04901961
L-Tyrosine	181.0	36.0	0.19889502
L-Valine	117.0	46.0	0.3931624
Vitamins			
Choline chloride	140.0	1.0	0.007142857
D-Calcium pantothenate	477.0	1.0	0.002096436
Folic Acid	441.0	1.0	0.0022675737
Niacinamide	122.0	1.0	0.008196721
Pyridoxal hydrochloride	204.0	1.0	0.004901961
Riboflavin	376.0	0.1	2.6595744E-4
Thiamine hydrochloride	337.0	1.0	0.002967359
i-Inositol	180.0	2.0	0.011111111
Inorganic Salts			
Calcium Chloride (CaCl ₂ ·2H ₂ O)	147.0	264.0	1.7959183
Magnesium Sulfate (MgSO ₄ ·7H ₂ O)	246.0	200.0	0.8130081
Potassium Chloride (KCl)	75.0	400.0	5.3333335
Sodium Bicarbonate (NaHCO ₃)	84.0	2200.0	26.190475
Sodium Chloride (NaCl)	58.0	6800.0	117.24138
Sodium Phosphate monobasic (NaH ₂ PO ₄ ·2H ₂ O)	156.0	158.0	1.0128205
Other Components			
D-Glucose (Dextrose)	180.0	1000.0	5.5555553
Phenol Red	376.4	10.0	0.026567481

<https://www.thermofisher.com/uk/en/home/technical-resources/media-formulation.197.html>

A.3 HBSS (Invitrogen 24020-133/500ml)

Components	Molecular Weight	Concentration (mg/L)	mM
Inorganic Salts			
Calcium Chloride (CaCl ₂) (anhyd.)	111.0	140.0	1.2612612
Magnesium Chloride (MgCl ₂ ·6H ₂ O)	203.0	100.0	0.49261084
Magnesium Sulfate (MgSO ₄ ·7H ₂ O)	246.0	100.0	0.40650406
Potassium Chloride (KCl)	75.0	400.0	5.3333335
Potassium Phosphate monobasic (KH ₂ PO ₄)	136.0	60.0	0.44117647
Sodium Bicarbonate (NaHCO ₃)	84.0	350.0	4.1666665
Sodium Chloride (NaCl)	58.0	8000.0	137.93103
Sodium Phosphate dibasic (Na ₂ HPO ₄) anhydrous	142.0	48.0	0.33802816
Other Components			
D-Glucose (Dextrose)	180.0	1000.0	5.5555553
Phenol Red	376.4	10.0	0.026567481

<https://www.thermofisher.com/uk/en/home/technical-resources/media-formulation.152.html>

A.4 Hepes Buffered Saline (HBS) (1Litre)

Component	Formula Weight	Weight (g)	Concentration (mM/L)
NaCl	58.44	8.1816	140
Hepes Acid	238.3	4.7660	20
MgSO ₄ ·7H ₂ O	246.5	0.6163	2.5
KCl	74.55	0.3728	5.0
CaCl ₂ ·2H ₂ O	147.02	0.1470	1.0
Phenol Red	-----	0.010g	10mg/L

The above components were dissolved in about 750ml of freshly drawn ultra-pure water by stirring to dissolve with a magnetic stirrer bar. The pH was adjusted to 7.4 at room temperature

by titrating about 18-20ml of 0.5M NaOH into the solution. The volume made up to 1 L and stored it at +4°C.

A.5 Physiological Salt Solution (PSS) (1Litre)

Component	Formula Weight	Weight (g)	Concentration (mM/L)
NaCl	58.44	8.4738	145
Hepes Acid	238.3	2.383	10
MgSO₄.7H₂O	246.5	0.2465	1.0
KCl	74.55	0.2237	3.0
CaCl₂.2H₂O	147.02	0.2940	2.0
D-glucose	180.16	1.8016	10.0

The above components were dissolved in about 750ml of freshly drawn ultra-pure water by stirring to dissolve with a magnetic stirrer bar. The pH was adjusted to 7.4 at room temperature by titrating about 18-20ml of 0.5M NaOH into the solution. The volume made up to 1 L and stored it at +4°C.

Appendix B (Buffers and Reagents)

B.1 0.5 M Sodium Hydroxide (NaOH)

To prepare 500 ml of 0.5M NaOH, dissolve 10g of pellets (Sigma S-8045 FW: 40.00) in nearly 250 ml of ultra-pure water then bring up the volume to 500 ml by using volumetric flask and store in room temperature.

B.2 Lowry (Folin) Reagent A (L)

Dissolve the following composition in 500 ml ultra-pure water:

- 20.00 g Sodium Carbonate “Anhydrous” (Sigma S-2127 FW 106.0)
- 4.00 g Sodium hydroxide (Sigma S-8045 FW: 40.00)
- 0.2 g Potassium Sodium (+)-tartrate.4H₂O (BDH AR 10219 FW: 282.22)

Then make up to 1L in a volumetric flask and store in 4°C.

B.3 Lowry (Folin) Reagent B (L)

Dissolve 5g of Cupric Sulphate (BDH AR 10091 FW: 249.68) in 500 ml ultra-pure water and make up the volume to 1L in a volumetric flask then store 4°C.

B.4 Lowry (Folin) standards

Make up a stock solution (S) first, weigh out 0.05 g of Bovine Serum Albumin (BSA: Sigma A-7638) and add 20 ml of 0.5M NaOH. Dissolve it with magnetic stirrer then make the standards as follows:

Final BSA(μg/ml)	0	50	100	150	200	300	400	500
Volume of Stock (S) (μl)	0	50	100	150	200	300	400	500
Volume of 0.5M NaOH (ml)	2.5	2.45	2.4	2.35	2.3	2.2	2.1	2.0

B.5 Immunoblotting buffers

B.5.1 Reducing Lysis buffer

Stock Solutions				For 10ml	Final concentration
1M	pH	7.4	beta	100ul	10mM
glycerophosphate					
0.5M pH 8 EDTA				20ul	1mM
40mM EGTA				250ul	1mM
1M pH 7.5 Tris-HCl				500ul	50mM
100mM Na Orthovanadate				100ul	1mM
1M Benzamidine				10ul	1mM
100mM PMSF				20ul	0.2mM
5mg/ml Pepstatin A				10ul	
5mg/ml Leupeptin				10ul	
Beta-Mercaptoethanol				10ul	0.1%
10% Triton X-100				1ml	1%
500mM Na Fluoride				1ml	50mM
Nano-pure water				6.97ml	

B.5.2 Sample Buffer

Component	Volume (ml)
Water	4.00
0.5m TRIS HCl pH6.8	1.00
Glycerol	0.80
10% (w/v) SDS	1.60
2-β-mercaptoethanol	0.40
0.05% (w/v) bromophenol blue	0.20

B.5.3 Resolving and Stacking Gel for Immunoblotting (×1 gel)

Stock solutions	12% Resolving gel	10% Resolving gel	12% Stacking gel
Water (Nano-pure)	3.35 ml	3.1 ml	3.03 ml
Acrylamide ¹ (30 w/v)	4 ml	2.5 ml	0.65 ml
1.5M Tris HCl (pH:8.8)	2.5 ml	1.875	---
0.5M Tris HCl(pH:6.8)	---	---	1.25 ml
SDS(10% w/v)	100 µl	75 µl	50 µl
APS ²	50 µl	37.5 µl	25 µl
TEMED ³	5 µl	10 µl	5 µl

1 Acrylamide: Sigma A3699-100ml

2 APS: Ammonium persulphate

3 N,N,N',N'- Tetramethylene diamine (Sigma T9281-25ml)

B.5.4 Immunoblotting Transfer buffer (1litre)

3.03g Tris-base

14.4g Glycine

200ml Methanol

B.5.5 SDS-PAGE Running buffer (1litre)

3.03g Tris-base

14.4g glycine

50ml 20% w/v SDS

B.5.6 Tris-buffered saline 10 X (TBS) (1 litre)

6.055g Trizma Base

8.766g NaCl

Adjust to pH 7.6 with HCl

B.5.7 TBS-Tween 1 X (1 litre)

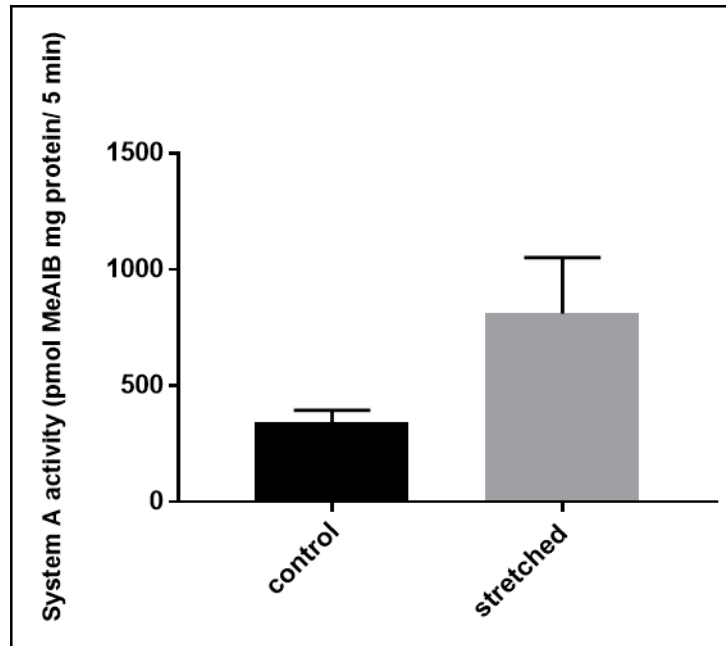
100ml 10X TBS

900ml De-ionised H₂O

1ml Tween 20

Appendix C

C.1. Artifactual effect of 5 minutes of vacuum-induced cyclic stretch on System A (SNAT2) transporter activity accompanied by cell detachment in L6-G8C5 myotubes.



L6-G8C5 myotubes cultured on collagen-coated Flexcell silicone-based culture wells were subjected to cyclic stretching using a Flexcell FX-4000 system as described in Section 2.4 (Goto et al., 2003) and stretched for 5 minutes. The medium used was MEM at pH 7.4 and contained 2mM L-Gln with 2% dialysed foetal bovine serum. Data compiled from 3 independent experiments are presented, with 4 replicate culture wells in each experiment.

Appendix D

D.1. An example of how RNA concentration was quantified

RNA extraction calculations

No.	Sample Name	OD 1 (ng/μl)	OD 2 (ng/μl)	Mean	260/280	260/280	Mean
1	1.0	1432.9	1421.8	1427.4	2.0	2.0	2.0
2	2.0	1854.6	1808.3	1831.5	1.9	1.9	1.9
3	3.0	1352.9	1363.7	1358.3	1.9	1.9	1.9
4	4.0	1422.2	1388.1	1405.2	1.9	1.9	1.9
5	5.0	1315.6	1290.2	1302.9	2.0	1.9	1.9
6	6.0	1156.7	1146.9	1151.8	1.9	1.9	1.9

No.	Sample Name	RNA ng/μl Reading	RNA μg/μl	μl of DEPC H ₂ O to 1μl of RNA (to make it 0.5 μg/μl)	amount of water for 5ul RNA
1	1.0	1427.4	1.42735	1.8547	9.2735
2	2.0	1831.5	1.83145	2.6629	13.3145
3	3.0	1358.3	1.3583	1.7166	8.583
4	4.0	1405.2	1.40515	1.8103	9.0515
5	5.0	1302.9	1.3029	1.6058	8.029
6	6.0	1151.8	1.1518	1.3036	6.518

References

- AAS, V., BAKKE, S. S., FENG, Y. Z., KASE, E. T., JENSEN, J., BAJPEYI, S., THORESEN, G. H. & RUSTAN, A. C. 2013. Are cultured human myotubes far from home? *Cell and tissue research*, 354, 671-682.
- ABBASIAN, N., BURTON, J. O., HERBERT, K. E., TREGUNNA, B.-E., BROWN, J. R., GHADERI-NAJAFABADI, M., BRUNSKILL, N. J., GOODALL, A. H. & BEVINGTON, A. 2015. Hyperphosphatemia, phosphoprotein phosphatases, and microparticle release in vascular endothelial cells. *Journal of the American Society of Nephrology*, 26, 2152-2162.
- ABDUL-GHANI, M. A. & DEFRONZO, R. A. 2010. Pathogenesis of insulin resistance in skeletal muscle. *BioMed Research International*, 2010.
- ABRAMOWITZ, M. K., MELAMED, M. L., BAUER, C., RAFF, A. C. & HOSTETTER, T. H. 2013. Effects of oral sodium bicarbonate in patients with CKD. *Clinical Journal of the American Society of Nephrology*, CJN. 08340812.
- ANNARATONE, L., MARCHIÒ, C., RUSSO, R., CIARDO, L., RONDON-LAGOS, S. M., GOIA, M., SCALZO, M. S., BOLLA, S., CASTELLANO, I. & DI CANTOGNO, L. V. 2013. A collection of primary tissue cultures of tumors from vacuum packed and cooled surgical specimens: a feasibility study. *PLoS One*, 8, e75193.
- ANWER, M. S. 1993. Mechanism of ionomycin-induced intracellular alkalinization of rat hepatocytes. *Hepatology*, 18, 433-439.
- APPELL, H.-J. 1990. Muscular atrophy following immobilisation. *Sports Medicine*, 10, 42-58.
- ARNOLD, D., TAYLOR, D. & RADDA, G. 1985. Investigation of human mitochondrial myopathies by phosphorus magnetic resonance spectroscopy. *Annals of Neurology: Official Journal of the American Neurological Association and the Child Neurology Society*, 18, 189-196.
- ARONSON, D., VIOLAN, M. A., DUFRESNE, S. D., ZANGEN, D., FIELDING, R. A. & GOODYEAR, L. J. 1997. Exercise stimulates the mitogen-activated protein kinase pathway in human skeletal muscle. *Journal of Clinical Investigation*, 99, 1251.
- ARTHUR, J. M., LAWRENCE, M. S., PAYNE, C. R., RANE, M. J. & MCLEISH, K. R. 2000. The calcium-sensing receptor stimulates JNK in MDCK cells. *Biochemical and biophysical research communications*, 275, 538-541.
- ASTROM, M.-B., FEIGH, M. & PEDERSEN, B. K. 2010. Persistent low-grade inflammation and regular exercise. *Front Biosci*, 2, 96-105.
- ATHERTON, P., SZEWCZYK, N., SELBY, A., RANKIN, D., HILLIER, K., SMITH, K., RENNIE, M. & LOUGHNA, P. 2009a. Cyclic stretch reduces myofibrillar protein synthesis despite increases in FAK and anabolic signalling in L6 cells. *The Journal of physiology*, 587, 3719-3727.
- ATHERTON, P. J., SZEWCZYK, N. J., SELBY, A., RANKIN, D., HILLIER, K., SMITH, K., RENNIE, M. J. & LOUGHNA, P. T. 2009b. Cyclic stretch reduces myofibrillar protein synthesis despite increases in FAK and anabolic signalling in L6 cells. *J Physiol*, 587, 3719-27.
- AYE, I. L., JANSSON, T. & POWELL, T. L. 2015. TNF-alpha stimulates System A amino acid transport in primary human trophoblast cells mediated by p38 MAPK signaling. *Physiol Rep*, 3.
- BAAR, K. & ESSER, K. 1999. Phosphorylation of p70S6k correlates with increased skeletal muscle mass following resistance exercise. *American Journal of Physiology-Cell Physiology*, 276, C120-C127.
- BAILEY, J. L., ZHENG, B., HU, Z., PRICE, S. R. & MITCH, W. E. 2006. Chronic kidney disease causes defects in signaling through the insulin receptor substrate/phosphatidylinositol 3-kinase/Akt pathway: implications for muscle atrophy. *Journal of the American Society of Nephrology*, 17, 1388-1394.
- BAIRD, F. E., PINILLA-TENAS, J. J., OGILVIE, W. L., GANAPATHY, V., HUNDAL, H. S. & TAYLOR, P. M. 2006. Evidence for allosteric regulation of pH-sensitive System A (SNAT2) and System N

- (SNAT5) amino acid transporter activity involving a conserved histidine residue. *Biochemical Journal*, 397, 369-375.
- BALAKRISHNAN, V. S., RAO, M., MENON, V., GORDON, P. L., PILICHOWSKA, M., CASTANEDA, F. & CASTANEDA-SCEPPA, C. 2010. Resistance training increases muscle mitochondrial biogenesis in patients with chronic kidney disease. *Clinical Journal of the American Society of Nephrology*, 5, 996-1002.
- BEAVERS, K. M., BRINKLEY, T. E. & NICKLAS, B. J. 2010. Effect of exercise training on chronic inflammation. *Clin Chim Acta*, 411, 785-93.
- BEVINGTON, A., BROWN, J., BUTLER, H., GOVINDJI, S., SHERIDAN, K. & WALLS, J. 2002. Impaired system A amino acid transport mimics the catabolic effects of acid in L6 cells. *European journal of clinical investigation*, 32, 590-602.
- BEVINGTON, A., BROWN, J., PRATT, A., MESSER, J. & WALLS, J. 1998a. Impaired glycolysis and protein catabolism induced by acid in L6 rat muscle cells. *European journal of clinical investigation*, 28, 908-917.
- BEVINGTON, A., BROWN, J. & WALLS, J. 2001. Leucine suppresses acid-induced protein wasting in L6 rat muscle cells. *European journal of clinical investigation*, 31, 497-503.
- BEVINGTON, A., POULTER, C., BROWN, J. & WALLS, J. 1998b. Inhibition of protein synthesis by acid in L6 skeletal muscle cells: analogies with the acute starvation response. *Mineral and electrolyte metabolism*, 24, 261-266.
- BLAIR, S. N., CHENG, Y. & HOLDER, J. S. 2001. Is physical activity or physical fitness more important in defining health benefits? *Medicine and science in sports and exercise*, 33, S379-S399.
- BLBAS, S. S. I. 2018. *The role of acidosis sensing in the regulation of chronic inflammation by skeletal muscle*. PhD thesis, University of Leicester.
- BLOCK, G. A., KLASSEN, P. S., LAZARUS, J. M., OFSTHUN, N., LOWRIE, E. G. & CHERTOW, G. M. 2004. Mineral metabolism, mortality, and morbidity in maintenance hemodialysis. *Journal of the American Society of Nephrology*, 15, 2208-2218.
- BODINE, S. C., STITT, T. N., GONZALEZ, M., KLINE, W. O., STOVER, G. L., BAUERLEIN, R., ZLOTCHENKO, E., SCRIMGEOUR, A., LAWRENCE, J. C. & GLASS, D. J. 2001. Akt/mTOR pathway is a crucial regulator of skeletal muscle hypertrophy and can prevent muscle atrophy in vivo. *Nature cell biology*, 3, 1014.
- BOPPART, M. D., ARONSON, D., GIBSON, L., ROUBENOFF, R., ABAD, L. W., BEAN, J., GOODYEAR, L. J. & FIELDING, R. A. 1999. Eccentric exercise markedly increases c-Jun NH2-terminal kinase activity in human skeletal muscle. *Journal of applied physiology*, 87, 1668-1673.
- BOPPART, M. D., HIRSHMAN, M. F., SAKAMOTO, K., FIELDING, R. A. & GOODYEAR, L. J. 2001. Static stretch increases c-Jun NH2-terminal kinase activity and p38 phosphorylation in rat skeletal muscle. *American Journal of Physiology-Cell Physiology*, 280, C352-C358.
- BOULÉ, N. G., HADDAD, E., KENNY, G. P., WELLS, G. A. & SIGAL, R. J. 2001. Effects of exercise on glycemic control and body mass in type 2 diabetes mellitus: a meta-analysis of controlled clinical trials. *Jama*, 286, 1218-1227.
- BRNJIC, S., OLOFSSON, M. H., HAVELKA, A. M. & LINDER, S. 2010. Chemical biology suggests a role for calcium signaling in mediating sustained JNK activation during apoptosis. *Molecular BioSystems*, 6, 767-774.
- BROER, S. 2014. The SLC38 family of sodium-amino acid co-transporters. *Pflugers Arch*, 466, 155-72.
- BURNS, C. P. & ROZENGURT, E. 1983. Serum, platelet-derived growth factor, vasopressin and phorbol esters increase intracellular pH in Swiss 3T3 cells. *Biochemical and biophysical research communications*, 116, 931-938.
- BUSTAMANTE, M., FERNÁNDEZ-VERDEJO, R., JAIMOVICH, E. & BUVINIC, S. 2014. Electrical stimulation induces IL-6 in skeletal muscle through extracellular ATP by activating Ca²⁺ signals and an IL-6 autocrine loop. *American Journal of Physiology-Endocrinology and Metabolism*, 306, E869-E882.
- CAIRNS, S. P. 2006. Lactic acid and exercise performance. *Sports medicine*, 36, 279-291.

- CAREY, A. L., STEINBERG, G. R., MACAULAY, S. L., THOMAS, W. G., HOLMES, A. G., RAMM, G., PRELOVSEK, O., HOHNEN-BEHRENS, C., WATT, M. J., JAMES, D. E., KEMP, B. E., PEDERSEN, B. K. & FEBBRAIO, M. A. 2006. Interleukin-6 increases insulin-stimulated glucose disposal in humans and glucose uptake and fatty acid oxidation in vitro via AMP-activated protein kinase. *Diabetes*, 55, 2688-97.
- CARGNELLO, M. & ROUX, P. P. 2011a. Activation and function of the MAPKs and their substrates, the MAPK-activated protein kinases. *Microbiol Mol Biol Rev*, 75, 50-83.
- CARGNELLO, M. & ROUX, P. P. 2011b. Activation and function of the MAPKs and their substrates, the MAPK-activated protein kinases. *Microbiol. Mol. Biol. Rev.*, 75, 50-83.
- CARRERO, J. J., STENVINKEL, P., CUPPARI, L., IKIZLER, T. A., KALANTAR-ZADEH, K., KAYSEN, G., MITCH, W. E., PRICE, S. R., WANNER, C. & WANG, A. Y. 2013. Etiology of the protein-energy wasting syndrome in chronic kidney disease: a consensus statement from the International Society of Renal Nutrition and Metabolism (ISRNM). *Journal of Renal Nutrition*, 23, 77-90.
- CASTANEDA, C., GORDON, P. L., PARKER, R. C., UHLIN, K. L., ROUBENOFF, R. & LEVEY, A. S. 2004. Resistance training to reduce the malnutrition-inflammation complex syndrome of chronic kidney disease. *American Journal of Kidney Diseases*, 43, 607-616.
- CHAILLOU, T., LEE, J. D., ENGLAND, J. H., ESSER, K. A. & MCCARTHY, J. J. 2013. Time course of gene expression during mouse skeletal muscle hypertrophy. *Journal of applied physiology*, 115, 1065-1074.
- CHAMBERS, M. A., MOYLAN, J. S., SMITH, J. D., GOODYEAR, L. J. & REID, M. B. 2009a. Stretch-stimulated glucose uptake in skeletal muscle is mediated by reactive oxygen species and p38 MAP-kinase. *J Physiol*, 587, 3363-73.
- CHAMBERS, M. A., MOYLAN, J. S., SMITH, J. D., GOODYEAR, L. J. & REID, M. B. 2009b. Stretch-stimulated glucose uptake in skeletal muscle is mediated by reactive oxygen species and p38 MAP-kinase. *The Journal of physiology*, 587, 3363-3373.
- CHAN, M. H., MCGEE, S. L., WATT, M. J., HARGREAVES, M. & FEBBRAIO, M. A. 2004a. Altering dietary nutrient intake that reduces glycogen content leads to phosphorylation of nuclear p38 MAP kinase in human skeletal muscle: association with IL-6 gene transcription during contraction. *Faseb J*, 18, 1785-7.
- CHAN, M. S., MCGEE, S. L., WATT, M. J., HARGREAVES, M. & FEBBRAIO, M. A. 2004b. Altering dietary nutrient intake that reduces glycogen content leads to phosphorylation of nuclear p38 MAP kinase in human skeletal muscle: association with IL-6 gene transcription during contraction. *The FASEB journal*, 18, 1785-1787.
- CHANG, L. & KARIN, M. 2001. Mammalian MAP kinase signalling cascades. *Nature*, 410, 37-40.
- CHEEMA, U., YANG, S. Y., MUDERA, V., GOLDSPIK, G. & BROWN, R. 2003. 3-D in vitro model of early skeletal muscle development. *Cell motility and the cytoskeleton*, 54, 226-236.
- CHEN, C., WANG, J., CAI, R., YUAN, Y., GUO, Z., GREWER, C. & ZHANG, Z. 2016. Identification of a Disulfide Bridge in Sodium-Coupled Neutral Amino Acid Transporter 2 (SNAT2) by Chemical Modification. *PloS one*, 11, e0158319.
- CHENG, Z., PANG, T., GU, M., GAO, A.-H., XIE, C.-M., LI, J.-Y., NAN, F.-J. & LI, J. 2006. Berberine-stimulated glucose uptake in L6 myotubes involves both AMPK and p38 MAPK. *Biochimica et Biophysica Acta (BBA)-General Subjects*, 1760, 1682-1689.
- CHEUNG, W. W., PAIK, K. H. & MAK, R. H. 2010. Inflammation and cachexia in chronic kidney disease. *Pediatric nephrology*, 25, 711-724.
- CHIEN, H.-C., ZUR, A. A., MAURER, T. S., YEE, S. W., TOLSMA, J., JASPER, P., SCOTT, D. O. & GIACOMINI, K. M. 2016. Rapid Method To Determine Intracellular Drug Concentrations in Cellular Uptake Assays: Application to Metformin in Organic Cation Transporter 1–Transfected Human Embryonic Kidney 293 Cells. *Drug Metabolism and Disposition*, 44, 356-364.
- CHIU, Y.-W., KOPPLE, J. D. & MEHROTRA, R. Correction of metabolic acidosis to ameliorate wasting in chronic kidney disease: goals and strategies. *Seminars in nephrology*, 2009. Elsevier, 67-74.

- CHOI, C. H., WEBB, B. A., CHIMENTI, M. S., JACOBSON, M. P. & BARBER, D. L. 2013. pH sensing by FAK-His58 regulates focal adhesion remodeling. *J Cell Biol*, 202, 849-59.
- CHOMCZYNSKI, P. & SACCHI, N. 1987. Single-step method of RNA isolation by acid guanidinium thiocyanate-phenol-chloroform extraction. *Analytical biochemistry*, 162, 156-159.
- CHRISTENSEN, H. N., OXENDER, D. L., LIANG, M. & VATZ, K. A. 1965. The use of N-methylation to direct the route of mediated transport of amino acids. *Journal of Biological Chemistry*, 240, 3609-3616.
- CLAPP, E. L. 2010. *The effect of therapeutic exercise and metabolic acidosis on skeletal muscle metabolism in chronic kidney disease*. PhD thesis, Loughborough University.
- CROSSLAND, H., KAZI, A. A., LANG, C. H., TIMMONS, J. A., PIERRE, P., WILKINSON, D. J., SMITH, K., SZEWCZYK, N. J. & ATHERTON, P. J. 2013. Focal adhesion kinase is required for IGF-I-mediated growth of skeletal muscle cells via a TSC2/mTOR/S6K1-associated pathway. *American Journal of Physiology-Endocrinology and Metabolism*, 305, E183-E193.
- CUENDA, A. & COHEN, P. 1999. Stress-activated protein kinase-2/p38 and a rapamycin-sensitive pathway are required for C2C12 myogenesis. *Journal of Biological Chemistry*, 274, 4341-4346.
- CUENDA, A. & ROUSSEAU, S. 2007. p38 MAP-kinases pathway regulation, function and role in human diseases. *Biochim Biophys Acta*, 1773, 1358-75.
- DANDONA, P., ALJADA, A. & BANDYOPADHYAY, A. 2004. Inflammation: the link between insulin resistance, obesity and diabetes. *Trends in immunology*, 25, 4-7.
- DE-GRAFT AIKINS, A. 2007. Ghana's neglected chronic disease epidemic: a developmental challenge. *Ghana Med J*, 41, 154-9.
- DEGER, S. M., HUNG, A. M., GAMBOA, J. L., SIEW, E. D., ELLIS, C. D., BOOKER, C., SHA, F., LI, H., BIAN, A. & STEWART, T. G. 2017. Systemic inflammation is associated with exaggerated skeletal muscle protein catabolism in maintenance hemodialysis patients. *JCI insight*, 2.
- DESCAMPS-LATSCHA, B., ATRICE, E., JUNGERS, P., WITKO-SARSAT, V. & RONIQUÉ, E. 2002. Immune system dysregulation in uremia: role of oxidative stress. *Blood purification*, 20, 481-484.
- DHANASEKARAN, D. N. & REDDY, E. P. 2017. JNK-signaling: a multiplexing hub in programmed cell death. *Genes & cancer*, 8, 682.
- DI MEO, S., NAPOLITANO, G. & VENDITTI, P. 2019. Mediators of Physical Activity Protection against ROS-Linked Skeletal Muscle Damage. *International journal of molecular sciences*, 20, 3024.
- DREYER, H. C., FUJITA, S., CADENAS, J. G., CHINKES, D. L., VOLPI, E. & RASMUSSEN, B. B. 2006. Resistance exercise increases AMPK activity and reduces 4E-BP1 phosphorylation and protein synthesis in human skeletal muscle. *The Journal of physiology*, 576, 613-624.
- DREYER, H. C., FUJITA, S., GLYNN, E. L., DRUMMOND, M. J., VOLPI, E. & RASMUSSEN, B. B. 2010. Resistance exercise increases leg muscle protein synthesis and mTOR signalling independent of sex. *Acta Physiol (Oxf)*, 199, 71-81.
- DRUMMOND, M. J., FRY, C. S., GLYNN, E. L., DREYER, H. C., DHANANI, S., TIMMERMAN, K. L., VOLPI, E. & RASMUSSEN, B. B. 2009. Rapamycin administration in humans blocks the contraction-induced increase in skeletal muscle protein synthesis. *J Physiol*, 587, 1535-46.
- DUPONT, S., MORSUT, L., ARAGONA, M., ENZO, E., GIULITTI, S., CORDENONSI, M., ZANCONATO, F., LE DIGABEL, J., FORCATO, M. & BICCIATO, S. 2011. Role of YAP/TAZ in mechanotransduction. *Nature*, 474, 179.
- ELSNER, P., QUISTORFF, B., HERMANN, T. S., DICH, J. & GRUNNET, N. 1998. Regulation of glycogen accumulation in L6 myotubes cultured under optimized differentiation conditions. *American Journal of Physiology-Endocrinology and Metabolism*, 275, E925-E933.
- EVANS, K., NASIM, Z., BROWN, J., BUTLER, H., KAUSER, S., VAROQUI, H., ERICKSON, J. D., HERBERT, T. P. & BEVINGTON, A. 2007a. Acidosis-sensing glutamine pump SNAT2 determines amino acid levels and mammalian target of rapamycin signalling to protein synthesis in L6 muscle cells. *J Am Soc Nephrol*, 18, 1426-36.

- EVANS, K., NASIM, Z., BROWN, J., BUTLER, H., KAUSER, S., VAROQUI, H., ERICKSON, J. D., HERBERT, T. P. & BEVINGTON, A. 2007b. Acidosis-sensing glutamine pump SNAT2 determines amino acid levels and mammalian target of rapamycin signalling to protein synthesis in L6 muscle cells. *Journal of the American Society of Nephrology*, 18, 1426-1436.
- EVANS, K., NASIM, Z., BROWN, J., CLAPP, E., AMIN, A., YANG, B., HERBERT, T. P. & BEVINGTON, A. 2008a. Inhibition of SNAT2 by metabolic acidosis enhances proteolysis in skeletal muscle. *J Am Soc Nephrol*, 19, 2119-29.
- EVANS, K., NASIM, Z., BROWN, J., CLAPP, E., AMIN, A., YANG, B., HERBERT, T. P. & BEVINGTON, A. 2008b. Inhibition of SNAT2 by metabolic acidosis enhances proteolysis in skeletal muscle. *Journal of the American Society of Nephrology*, 19, 2119-2129.
- EVANS, K. F. 2009. *The effects of acidosis, glutamine starvation and inhibition of the pH sensitive SNAT 2 amino acid transporter on protein metabolism in L6 muscle cells*. PhD thesis, University of Leicester.
- FANTUZZI, G. 2005. Adipose tissue, adipokines, and inflammation. *J Allergy Clin Immunol*, 115, 911-9; quiz 920.
- FARUP, J., DE PAOLI, F., BJERG, K., RIIS, S., RINGGARD, S. & VISSING, K. 2015. Blood flow restricted and traditional resistance training performed to fatigue produce equal muscle hypertrophy. *Scandinavian journal of medicine & science in sports*, 25, 754-763.
- FEBBRAIO, M. A. & PEDERSEN, B. K. 2002. Muscle-derived interleukin-6: mechanisms for activation and possible biological roles. *The FASEB Journal*, 16, 1335-1347.
- FIUZA-LUCES, C., SANTOS-LOZANO, A., JOYNER, M., CARRERA-BASTOS, P., PICAZO, O., ZUGAZA, J. L., IZQUIERDO, M., RUILOPE, L. M. & LUCIA, A. 2018. Exercise benefits in cardiovascular disease: beyond attenuation of traditional risk factors. *Nature Reviews Cardiology*, 15, 731-743.
- FLETCHER, G. F., LANDOLFO, C., NIEBAUER, J., OZEMEK, C., ARENA, R. & LAVIE, C. J. 2018. Promoting physical activity and exercise: JACC health promotion series. *Journal of the American College of Cardiology*, 72, 1622-1639.
- FRANCHI-GAZZOLA, R., DALL'ASTA, V., SALA, R., VISIGALLI, R., BEVILACQUA, E., GACCIOLI, F., GAZZOLA, G. C. & BUSSOLATI, O. 2006. The role of the neutral amino acid transporter SNAT2 in cell volume regulation. *Acta Physiol (Oxf)*, 187, 273-83.
- FRANCHI-GAZZOLA, R., DALL'ASTA, V., SALA, R., VISIGALLI, R., BEVILACQUA, E., GACCIOLI, F., GAZZOLA, G. & BUSSOLATI, O. 2006. The role of the neutral amino acid transporter SNAT2 in cell volume regulation. *Acta physiologica*, 187, 273-283.
- FRANCHI, M., RUOSS, S., VALDIVIESO, P., MITCHELL, K., SMITH, K., ATHERTON, P., NARICI, M. & FLÜCK, M. 2018. Regional regulation of focal adhesion kinase after concentric and eccentric loading is related to remodelling of human skeletal muscle. *Acta Physiologica*, 223, e13056.
- FU, S., YIN, L., LIN, X., LU, J. & WANG, X. 2018. Effects of Cyclic Mechanical Stretch on the Proliferation of L6 Myoblasts and Its Mechanisms: PI3K/Akt and MAPK Signal Pathways Regulated by IGF-1 Receptor. *Int J Mol Sci*, 19.
- GABRIEL, B. M., HAMILTON, D. L., TREMBLAY, A. M. & WACKERHAGE, H. 2016. The Hippo signal transduction network for exercise physiologists. *Journal of Applied Physiology*, 120, 1105-1117.
- GINGRAS, A.-C., RAUGHT, B. & SONENBERG, N. 1999. eIF4 initiation factors: effectors of mRNA recruitment to ribosomes and regulators of translation. *Annual review of biochemistry*, 68, 913-963.
- GLOVER, E. I., OATES, B. R., TANG, J. E., MOORE, D. R., TARNOPOLSKY, M. A. & PHILLIPS, S. M. 2008. Resistance exercise decreases eIF2Bε phosphorylation and potentiates the feeding-induced stimulation of p70S6K1 and rpS6 in young men. *American Journal of Physiology-Regulatory, Integrative and Comparative Physiology*, 295, R604-R610.
- GOLDBERG, A. L., ETLINGER, J. D., GOLDSPIK, D. F. & JABLECKI, C. 1975. Mechanism of work-induced hypertrophy of skeletal muscle. *Medicine and science in sports*, 7, 185-198.

- GOODMAN, C. A., DIETZ, J. M., JACOBS, B. L., MCNALLY, R. M., YOU, J.-S. & HORNBERGER, T. A. 2015. Yes-Associated Protein is up-regulated by mechanical overload and is sufficient to induce skeletal muscle hypertrophy. *FEBS letters*, 589, 1491-1497.
- GOODMAN, C. A., FREY, J. W., MABREY, D. M., JACOBS, B. L., LINCOLN, H. C., YOU, J. S. & HORNBERGER, T. A. 2011. The role of skeletal muscle mTOR in the regulation of mechanical load-induced growth. *J Physiol*, 589, 5485-501.
- GOTO, K., OKUYAMA, R., SUGIYAMA, H., HONDA, M., KOBAYASHI, T., UEHARA, K., AKEMA, T., SUGIURA, T., YAMADA, S. & OHIRA, Y. 2003. Effects of heat stress and mechanical stretch on protein expression in cultured skeletal muscle cells. *Pflügers Archiv*, 447, 247-253.
- GRAHAM, Z. A., GALLAGHER, P. M. & CARDOZO, C. P. 2015. Focal adhesion kinase and its role in skeletal muscle. *Journal of muscle research and cell motility*, 36, 305-315.
- GUO, X., GREENE, K., AKANDA, N., SMITH, A. S., STANCESCU, M., LAMBERT, S., VANDENBURGH, H. & HICKMAN, J. J. 2014. In vitro differentiation of functional human skeletal myotubes in a defined system. *Biomaterials science*, 2, 131-138.
- GUPTA, J., MITRA, N., KANETSKY, P. A., DEVANEY, J., WING, M. R., REILLY, M., SHAH, V. O., BALAKRISHNAN, V. S., GUZMAN, N. J. & GIRNDT, M. 2012. Association between albuminuria, kidney function, and inflammatory biomarker profile in CKD in CRIC. *Clinical journal of the American Society of Nephrology*, 7, 1938-1946.
- HAMEED, M., ORRELL, R., COBBOLD, M., GOLDSPINK, G. & HARRIDGE, S. 2003. Expression of IGF-I splice variants in young and old human skeletal muscle after high resistance exercise. *The Journal of physiology*, 547, 247-254.
- HANKE, N., KUBIS, H. P., SCHEIBE, R. J., BERTHOLD-LOSLEBEN, M., HUSING, O., MEISSNER, J. D. & GROS, G. 2010. Passive mechanical forces upregulate the fast myosin heavy chain IIId/x via integrin and p38 MAP kinase activation in a primary muscle cell culture. *Am J Physiol Cell Physiol*, 298, C910-20.
- HANSEN, C. G., NG, Y. L. D., LAM, W.-L. M., PLOUFFE, S. W. & GUAN, K.-L. 2015. The Hippo pathway effectors YAP and TAZ promote cell growth by modulating amino acid signaling to mTORC1. *Cell research*, 25, 1299.
- HANSSON, G. K., LIBBY, P., SCHÖNBECK, U. & YAN, Z.-Q. 2002. Innate and adaptive immunity in the pathogenesis of atherosclerosis. *Circulation research*, 91, 281-291.
- HATFALUDY, S., SHANSKY, J. & VANDENBURGH, H. H. 1989. Metabolic alterations induced in cultured skeletal muscle by stretch-relaxation activity. *American Journal of Physiology-Cell Physiology*, 256, C175-C181.
- HAUSER, A. B., STINGHEN, A. E., KATO, S., BUCHARLES, S., AITA, C., YUZAWA, Y. & PECOITS-FILHO, R. 2008. Characteristics and causes of immune dysfunction related to uremia and dialysis. *Peritoneal Dialysis International*, 28, S183-S187.
- HEDING, A., ELLING, C. & SCHWARTZ, T. 2002. Novel method for the study of receptor Ca²⁺ signalling exemplified by the NK1 receptor. *Journal of Receptors and Signal Transduction*, 22, 241-252.
- HENRIKSEN, E. J., LOUTERS, L. L., STUMP, C. S. & TIPTON, C. M. 1992. Effects of prior exercise on the action of insulin-like growth factor I in skeletal muscle. *American Journal of Physiology-Endocrinology And Metabolism*, 263, E340-E344.
- HENRIKSEN, E. J., SCHNEIDER, M. C. & RITTER, L. S. 1993. Regulation of contraction-stimulated system A amino acid uptake in skeletal muscle: role of vicinal sulfhydryls. *Metabolism*, 42, 440-445.
- HIBI, M., LIN, A., SMEAL, T., MINDEN, A. & KARIN, M. 1993. Identification of an oncoprotein-and UV-responsive protein kinase that binds and potentiates the c-Jun activation domain. *Genes & development*, 7, 2135-2148.
- HISCOCK, N., CHAN, M. S., BISUCCI, T., DARBY, I. A. & FEBBRAIO, M. A. 2004. Skeletal myocytes are a source of interleukin-6 mRNA expression and protein release during contraction: evidence of fiber type specificity. *The FASEB journal*, 18, 992-994.

- HOJMAN, P., BROLIN, C., NØRGAARD-CHRISTENSEN, N., DETHLEFSEN, C., LAUENBORG, B., OLSEN, C. K., ÅBOM, M. M., KRAG, T., GEHL, J. & PEDERSEN, B. K. 2019. IL-6 release from muscles during exercise is stimulated by lactate-dependent protease activity. *American Journal of Physiology-Endocrinology and Metabolism*, 316, E940-E947.
- HORNBERGER, T., CHU, W., MAK, Y., HSIUNG, J., HUANG, S. & CHIEN, S. 2006a. The role of phospholipase D and phosphatidic acid in the mechanical activation of mTOR signaling in skeletal muscle. *Proceedings of the National Academy of Sciences*, 103, 4741-4746.
- HORNBERGER, T. A. & CHIEN, S. 2006. Mechanical stimuli and nutrients regulate rapamycin-sensitive signaling through distinct mechanisms in skeletal muscle. *J Cell Biochem*, 97, 1207-16.
- HORNBERGER, T. A., STUPPARD, R., CONLEY, K. E., FEDELE, M. J., FIOROTTO, M. L. & ESSER, K. A. 2004. Mechanical stimuli regulate rapamycin-sensitive signalling by a phosphoinositide 3-kinase-, protein kinase B-and growth factor-independent mechanism. *Biochemical Journal*, 380, 795-804.
- HORNBERGER, T. A., SUKHIJA, K. B. & CHIEN, S. 2006b. Regulation of mTOR by mechanically induced signaling events in skeletal muscle. *Cell cycle*, 5, 1391-1396.
- HOTOKEZAKA, H., SAKAI, E., KANAOKA, K., SAITO, K., MATSUO, K.-I., KITaura, H., YOSHIDA, N. & NAKAYAMA, K. 2002. U0126 and PD98059, specific inhibitors of MEK, accelerate differentiation of RAW264. 7 cells into osteoclast-like cells. *Journal of Biological Chemistry*, 277, 47366-47372.
- HUANG, Y., LI, X., WANG, Y., WANG, H., HUANG, C. & LI, J. 2014. Endoplasmic reticulum stress-induced hepatic stellate cell apoptosis through calcium-mediated JNK/P38 MAPK and Calpain/Caspase-12 pathways. *Molecular and cellular biochemistry*, 394, 1-12.
- HUNDAL, H. S. & TAYLOR, P. M. 2009. Amino acid transceptors: gate keepers of nutrient exchange and regulators of nutrient signaling. *Am J Physiol Endocrinol Metab*, 296, E603-13.
- HYDE, R., CWIKLINSKI, E. L., MACAULAY, K., TAYLOR, P. M. & HUNDAL, H. S. 2007. Distinct sensor pathways in the hierarchical control of SNAT2, a putative amino acid transceptor, by amino acid availability. *J Biol Chem*, 282, 19788-98.
- HYDE, R., PEYROLLIER, K. & HUNDAL, H. S. 2002. Insulin promotes the cell surface recruitment of the SAT2/ATA2 system A amino acid transporter from an endosomal compartment in skeletal muscle cells. *Journal of Biological Chemistry*, 277, 13628-13634.
- ILIC, D., MAO-QIANG, M., CRUMRINE, D., DOLGANOV, G., LAROCQUE, N., XU, P., DEMERJIAN, M., BROWN, B. E., LIM, S.-T. & OSSOVSKAYA, V. 2007. Focal adhesion kinase controls pH-dependent epidermal barrier homeostasis by regulating actin-directed Na⁺/H⁺ exchanger 1 plasma membrane localization. *The American journal of pathology*, 170, 2055-2067.
- ISKRATSCHE, T., WOLFENSON, H. & SHEETZ, M. P. 2014. Appreciating force and shape—the rise of mechanotransduction in cell biology. *Nature Reviews Molecular Cell Biology*, 15, 825.
- IWATA, M., HAYAKAWA, K., MURAKAMI, T., NARUSE, K., KAWAKAMI, K., INOUE-MIYAZU, M., YUGE, L. & SUZUKI, S. 2007. Uniaxial cyclic stretch-stimulated glucose transport is mediated by a Ca²⁺-dependent mechanism in cultured skeletal muscle cells. *Pathobiology*, 74, 159-168.
- JAKA, O., CASAS-FRAILE, L., DE MUNAIN, A. L. & SÁENZ, A. 2015. Costamere proteins and their involvement in myopathic processes. *Expert reviews in molecular medicine*, 17.
- JOHANSEN, K. L. & PAINTER, P. 2012. Exercise in individuals with CKD. *American Journal of Kidney Diseases*, 59, 126-134.
- JOHNSON, G. L. & LAPADAT, R. 2002. Mitogen-activated protein kinase pathways mediated by ERK, JNK, and p38 protein kinases. *Science*, 298, 1911-1912.
- JOHNSON, G. L. & NAKAMURA, K. 2007. The c-jun kinase/stress-activated pathway: regulation, function and role in human disease. *Biochim Biophys Acta*, 1773, 1341-8.
- JUFFER, P., BAKKER, A. D., KLEIN-NULEND, J. & JASPERS, R. T. 2014. Mechanical loading by fluid shear stress of myotube glycocalyx stimulates growth factor expression and nitric oxide production. *Cell biochemistry and biophysics*, 69, 411-419.

- JUNG, T., SCHAUER, U., HEUSSER, C., NEUMANN, C. & RIEGER, C. 1993. Detection of intracellular cytokines by flow cytometry. *Journal of immunological methods*, 159, 197-207.
- KAHN, B. B., ALQUIER, T., CARLING, D. & HARDIE, D. G. 2005. AMP-activated protein kinase: ancient energy gauge provides clues to modern understanding of metabolism. *Cell metabolism*, 1, 15-25.
- KAMIMURA, D., ISHIHARA, K. & HIRANO, T. 2003. IL-6 signal transduction and its physiological roles: the signal orchestration model. *Reviews of physiology, biochemistry and pharmacology*. Springer.
- KANASTY, R. L., WHITEHEAD, K. A., VEGAS, A. J. & ANDERSON, D. G. 2012. Action and reaction: the biological response to siRNA and its delivery vehicles. *Molecular Therapy*, 20, 513-524.
- KATO, S., CHMIELEWSKI, M., HONDA, H., PECOITS-FILHO, R., MATSUO, S., YUZAWA, Y., TRANAEUS, A., STENVINKEL, P. & LINDHOLM, B. 2008. Aspects of immune dysfunction in end-stage renal disease. *Clinical Journal of the American Society of Nephrology*, 3, 1526-1533.
- KELLEHER, A. R., GORDON, B. S., KIMBALL, S. R. & JEFFERSON, L. S. 2014. Changes in REDD1, REDD2, and atroгене mRNA expression are prevented in skeletal muscle fixed in a stretched position during hindlimb immobilization. *Physiological reports*, 2, e00246.
- KELLER, C., STEENSBERG, A., PILEGAARD, H., OSADA, T., SALTIN, B., PEDERSEN, B. K. & NEUFER, P. D. 2001. Transcriptional activation of the IL-6 gene in human contracting skeletal muscle: influence of muscle glycogen content. *The FASEB Journal*, 15, 2748-2750.
- KELLER, P., PENKOWA, M., KELLER, C., STEENSBERG, A., FISCHER, C. P., GIRALT, M., HIDALGO, J. & PEDERSEN, B. K. 2005. Interleukin-6 receptor expression in contracting human skeletal muscle: regulating role of IL-6. *The FASEB Journal*, 19, 1181-1183.
- KELLY, M., KELLER, C., AVILUCEA, P. R., KELLER, P., LUO, Z., XIANG, X., GIRALT, M., HIDALGO, J., SAHA, A. K. & PEDERSEN, B. K. 2004. AMPK activity is diminished in tissues of IL-6 knockout mice: the effect of exercise. *Biochemical and biophysical research communications*, 320, 449-454.
- KEMP, G. 2007. Muscle cell volume and pH changes due to glycolytic ATP synthesis. *The Journal of physiology*, 582, 461.
- KIM, J. & SHARMA, R. P. 2004. Calcium-mediated activation of c-Jun NH2-terminal kinase (JNK) and apoptosis in response to cadmium in murine macrophages. *Toxicological sciences*, 81, 518-527.
- KING, P. A. 1994. Effects of insulin and exercise on amino acid transport in rat skeletal muscle. *American Journal of Physiology-Cell Physiology*, 266, C524-C530.
- KLETZIEN, R. F., PARIZA, M. W., BECKER, J. E. & POTTER, V. R. 1975. A method using 3-O-methyl-D-glucose and phloretin for the determination of intracellular water space of cells in monolayer culture. *Analytical biochemistry*, 68, 537-544.
- KOOK, S.-H., LEE, H.-J., CHUNG, W.-T., HWANG, I.-H., LEE, S.-A., KIM, B.-S. & LEE, J.-C. 2008. Cyclic mechanical stretch stimulates the proliferation of C2C12 myoblasts and inhibits their differentiation via prolonged activation of p38 MAPK. *Molecules and cells*, 25, 479-486.
- KOSMADAKIS, G. C., JOHN, S. G., CLAPP, E. L., VIANA, J. L., SMITH, A. C., BISHOP, N. C., BEVINGTON, A., OWEN, P. J., MCINTYRE, C. W. & FEEHALLY, J. 2012. Benefits of regular walking exercise in advanced pre-dialysis chronic kidney disease. *Nephrol Dial Transplant*, 27, 997-1004.
- KOSMIDOU, I., VASSILAKOPOULOS, T., XAGORARI, A., ZAKYNTHINOS, S., PAPAPETROPOULOS, A. & ROUSSOS, C. 2002. Production of interleukin-6 by skeletal myotubes: role of reactive oxygen species. *American journal of respiratory cell and molecular biology*, 26, 587-593.
- KUBICA, N., KIMBALL, S. R., JEFFERSON, L. S. & FARRELL, P. A. 2004. Alterations in the expression of mRNAs and proteins that code for species relevant to eIF2B activity after an acute bout of resistance exercise. *Journal of applied physiology*, 96, 679-687.
- KYRIAKIS, J., BRAUTIGAN, D., INGEBRITSEN, T. & AVRUCH, J. 1991. pp54 microtubule-associated protein-2 kinase requires both tyrosine and serine/threonine phosphorylation for activity. *Journal of Biological Chemistry*, 266, 10043-10046.

- KYRIAKIS, J. M. & AVRUCH, J. 1990. pp54 microtubule-associated protein 2 kinase. A novel serine/threonine protein kinase regulated by phosphorylation and stimulated by poly-L-lysine. *Journal of Biological Chemistry*, 265, 17355-17363.
- KYRIAKIS, J. M. & AVRUCH, J. 1996. Sounding the alarm: protein kinase cascades activated by stress and inflammation. *Journal of Biological Chemistry*, 271, 24313-24316.
- LACASSE, Y., BROSEAU, L., MILNE, S., MARTIN, S., WONG, E., GUYATT, G., GOLDSTEIN, R. & WHITE, J. 2001. Pulmonary rehabilitation for chronic obstructive pulmonary disease. *The Cochrane Library*.
- LAEMMLI, U. K. 1970. Cleavage of structural proteins during the assembly of the head of bacteriophage T4. *nature*, 227, 680.
- LANCET, T. 2017. Worldwide trends in body-mass index, underweight, overweight, and obesity from 1975 to 2016: a pooled analysis of 2416 population-based measurement studies in 128.9 million children, adolescents, and adults. *Lancet*, 390, 2627-2642.
- LANG, F. 2007. Mechanisms and significance of cell volume regulation. *Journal of the American college of nutrition*, 26, 613S-623S.
- LIEBERTHAL, W. & LEVINE, J. S. 2009a. The role of the mammalian target of rapamycin (mTOR) in renal disease. *J Am Soc Nephrol*, 20, 2493-502.
- LIEBERTHAL, W. & LEVINE, J. S. 2009b. The role of the mammalian target of rapamycin (mTOR) in renal disease. *Journal of the American Society of Nephrology*, ASN. 2008111186.
- LIU, A., YANG, J., GONZALEZ, F. J., CHENG, G. Q. & DAI, R. 2010. Biphasic regulation of intracellular calcium by gemfibrozil contributes to inhibiting L6 myoblast differentiation: implications for clinical myotoxicity. *Chemical research in toxicology*, 24, 229-237.
- LIU, J., LIU, J., MAO, J., YUAN, X., LIN, Z. & LI, Y. 2009. Caspase-3-mediated cyclic stretch-induced myoblast apoptosis via a Fas/FasL-independent signaling pathway during myogenesis. *Journal of cellular biochemistry*, 107, 834-844.
- LÓPEZ-FONTANALS, M., RODRÍGUEZ-MULERO, S., CASADO, F. J., DÉRIJARD, B. & PASTOR-ANGLADA, M. 2003. The osmoregulatory and the amino acid-regulated responses of system A are mediated by different signal transduction pathways. *The Journal of general physiology*, 122, 5-16.
- LOW, S. Y. & TAYLOR, P. M. 1998. Integrin and cytoskeletal involvement in signalling cell volume changes to glutamine transport in rat skeletal muscle. *The Journal of physiology*, 512, 481.
- LOWRY, O. H., ROSEBROUGH, N. J., FARR, A. L. & RANDALL, R. J. 1951. Protein measurement with the Folin phenol reagent. *J biol Chem*, 193, 265-275.
- LUO, Y. & ZHENG, S. G. 2016. Hall of fame among pro-inflammatory cytokines: interleukin-6 gene and its transcriptional regulation mechanisms. *Frontiers in immunology*, 7, 604.
- MACKENZIE, B. & ERICKSON, J. D. 2004. Sodium-coupled neutral amino acid (System N/A) transporters of the SLC38 gene family. *Pflugers Arch*, 447, 784-95.
- MACKENZIE, M. G., HAMILTON, D. L., MURRAY, J. T., TAYLOR, P. M. & BAAR, K. 2009. mVps34 is activated following high-resistance contractions. *The Journal of physiology*, 587, 253-260.
- MAK, R. H. 2008. Insulin and its role in chronic kidney disease. *Pediatric Nephrology*, 23, 355-362.
- MALLAT, Z., BESNARD, S., DURIEZ, M., DELEUZE, V., EMMANUEL, F., BUREAU, M. F., SOUBRIER, F., ESPOSITO, B., DUEZ, H. & FIEVET, C. 1999. Protective role of interleukin-10 in atherosclerosis. *Circulation research*, 85, e17-e24.
- MARCOTTE, G. R., WEST, D. W. & BAAR, K. 2015. The molecular basis for load-induced skeletal muscle hypertrophy. *Calcified tissue international*, 96, 196-210.
- MAY, L. T., GHAYEB, J., SANTHANAM, U., TATTER, S., STHOEGER, Z., HELFGOTT, D., CHIORAZZI, N., GRIENINGER, G. & SEHGAL, P. 1988a. Synthesis and secretion of multiple forms of beta 2-interferon/B-cell differentiation factor 2/hepatocyte-stimulating factor by human fibroblasts and monocytes. *Journal of Biological Chemistry*, 263, 7760-7766.

- MAY, L. T., SANTHANAM, U., TATTER, S. B., BHARDWAJ, N., GHRAYEB, J. & SEHGAL, P. B. 1988b. Phosphorylation of secreted forms of human $\beta 2$ -interferon/hepatocyte stimulating factor/interleukin-6. *Biochemical and biophysical research communications*, 152, 1144-1150.
- MAY, R., KELLY, R. & MITCH, W. 1987. Mechanisms for defects in muscle protein metabolism in rats with chronic uremia. Influence of metabolic acidosis. *Journal of Clinical Investigation*, 79, 1099.
- MCCORMICK, J. & JOHNSTONE, R. 1995. Identification of the integrin $\alpha 3 \beta 1$ as a component of a partially purified A-system amino acid transporter from Ehrlich cell plasma membranes. *Biochemical Journal*, 311, 743-751.
- MEDICINE, A. C. O. S. 2009. American College of Sports Medicine position stand. Progression models in resistance training for healthy adults. *Medicine and science in sports and exercise*, 41, 687.
- MENG, Z., QIU, Y., LIN, K. C., KUMAR, A., PLACONE, J. K., FANG, C., WANG, K.-C., LU, S., PAN, M. & HONG, A. W. 2018. RAP2 mediates mechanoresponses of the Hippo pathway. *Nature*, 560, 655.
- MERRICK, W. C. 1992. Mechanism and regulation of eukaryotic protein synthesis. *Microbiological reviews*, 56, 291-315.
- MILLER, B. F., OLESEN, J. L., HANSEN, M., DØSSING, S., CRAMERI, R. M., WELLING, R. J., LANGBERG, H., FLYVBJERG, A., KJAER, M. & BABRAJ, J. A. 2005. Coordinated collagen and muscle protein synthesis in human patella tendon and quadriceps muscle after exercise. *The Journal of physiology*, 567, 1021-1033.
- MITCH, W. E. 1998. Robert H Herman Memorial Award in Clinical Nutrition Lecture, 1997. Mechanisms causing loss of lean body mass in kidney disease. *The American journal of clinical nutrition*, 67, 359-366.
- MITCH, W. E., MEDINA, R., GRIEBER, S., MAY, R. C., ENGLAND, B. K., PRICE, S. R., BAILEY, J. L. & GOLDBERG, A. L. 1994. Metabolic acidosis stimulates muscle protein degradation by activating the adenosine triphosphate-dependent pathway involving ubiquitin and proteasomes. *Journal of Clinical Investigation*, 93, 2127.
- MITCHELL, S. F. & LORSCH, J. R. 2008. Should I stay or should I go? Eukaryotic translation initiation factors 1 and 1A control start codon recognition. *Journal of Biological Chemistry*, 283, 27345-27349.
- MORETTINI, M., PALUMBO, M. C., SACCHETTI, M., CASTIGLIONE, F. & MAZZÀ, C. 2017. A system model of the effects of exercise on plasma Interleukin-6 dynamics in healthy individuals: Role of skeletal muscle and adipose tissue. *PloS one*, 12, e0181224.
- MUNOZ-CANOVES, P., SCHEELE, C., PEDERSEN, B. K. & SERRANO, A. L. 2013. Interleukin-6 myokine signaling in skeletal muscle: a double-edged sword? *FEBS J*, 280, 4131-48.
- NAKAYAMA, A., AOI, W., TAKAMI, M., HIRANO, N., OGAYA, Y., WADA, S. & HIGASHI, A. 2019. Effect of downhill walking on next-day muscle damage and glucose metabolism in healthy young subjects. *The Journal of Physiological Sciences*, 69, 31-38.
- NELSON, A., CAMIC, C. L., FOSTER, C., ZAJAC, B., HOECHERL, K., ERICKSON, J. & JAGIM, A. R. 2019. Supplementation with a Multi-ingredient Pre-workout Supplement does not Augment Resistance Training Adaptations in Females. *International journal of exercise science*, 12, 187.
- NICKLIN, P., BERGMAN, P., ZHANG, B., TRIANTAFELLOW, E., WANG, H., NYFELER, B., YANG, H., HILD, M., KUNG, C. & WILSON, C. 2009. Bidirectional transport of amino acids regulates mTOR and autophagy. *Cell*, 136, 521-534.
- NIEMINEN, R., LAHTI, A., JALONEN, U., KANKAANRANTA, H. & MOILANEN, E. 2006. JNK inhibitor SP600125 reduces COX-2 expression by attenuating mRNA in activated murine J774 macrophages. *International immunopharmacology*, 6, 987-996.
- NYATI, K. K., MASUDA, K., ZAMAN, M. M.-U., DUBEY, P. K., MILLRINE, D., CHALISE, J. P., HIGA, M., LI, S., STANDLEY, D. M. & SAITO, K. 2017. TLR4-induced NF- κ B and MAPK signaling regulate the IL-6 mRNA stabilizing protein Arid5a. *Nucleic acids research*, 45, 2687-2703.

- O'NEIL, T. K., DUFFY, L., FREY, J. & HORNBERGER, T. 2009. The role of phosphoinositide 3-kinase and phosphatidic acid in the regulation of mammalian target of rapamycin following eccentric contractions. *The Journal of physiology*, 587, 3691-3701.
- OSTROWSKI, K., HERMANN, C., BANGASH, A., SCHJERLING, P., NIELSEN, J. N. & PEDERSEN, B. K. 1998a. A trauma-like elevation of plasma cytokines in humans in response to treadmill running. *The Journal of physiology*, 513, 889-894.
- OSTROWSKI, K., ROHDE, T., ASP, S., SCHJERLING, P. & PEDERSEN, B. K. 1999. Pro-and anti-inflammatory cytokine balance in strenuous exercise in humans. *The Journal of physiology*, 515, 287-291.
- OSTROWSKI, K., ROHDE, T., ZACHO, M., ASP, S. & PEDERSEN, B. 1998b. Evidence that interleukin-6 is produced in human skeletal muscle during prolonged running. *The Journal of physiology*, 508, 949-953.
- OSTROWSKI, K., SCHJERLING, P. & PEDERSEN, B. K. 2000. Physical activity and plasma interleukin-6 in humans—effect of intensity of exercise. *European journal of applied physiology*, 83, 512-515.
- PAPADOYANNAKIS, N., STEFANIDIS, C. & MCGEOWN, M. 1984. The effect of the correction of metabolic acidosis on nitrogen and potassium balance of patients with chronic renal failure. *The American journal of clinical nutrition*, 40, 623-627.
- PARADISE, R. K., LAUFFENBURGER, D. A. & VAN VLIET, K. J. 2011. Acidic extracellular pH promotes activation of integrin $\alpha\beta3$. *PloS one*, 6, e15746.
- PASSEY, S., MARTIN, N., PLAYER, D. & LEWIS, M. 2011. Stretching skeletal muscle in vitro: does it replicate in vivo physiology? *Biotechnology letters*, 33, 1513-1521.
- PEAKE, J. M., NEUBAUER, O., DELLA GATTA, P. A. & NOSAKA, K. 2016. Muscle damage and inflammation during recovery from exercise. *Journal of applied physiology*, 122, 559-570.
- PEDERSEN, B. & SALTIN, B. 2015a. Exercise as medicine—evidence for prescribing exercise as therapy in 26 different chronic diseases. *Scandinavian journal of medicine & science in sports*, 25, 1-72.
- PEDERSEN, B. K., AKERSTROM, T. C., NIELSEN, A. R. & FISCHER, C. P. 2007. Role of myokines in exercise and metabolism. *Journal of applied physiology*, 103, 1093-1098.
- PEDERSEN, B. K. & FEBBRAIO, M. A. 2008a. Muscle as an endocrine organ: focus on muscle-derived interleukin-6. *Physiol Rev*, 88, 1379-406.
- PEDERSEN, B. K. & FEBBRAIO, M. A. 2008b. Muscle as an endocrine organ: focus on muscle-derived interleukin-6. *Physiological reviews*, 88, 1379-1406.
- PEDERSEN, B. K. & SALTIN, B. 2006. Evidence for prescribing exercise as therapy in chronic disease. *Scandinavian journal of medicine & science in sports*, 16, 3-63.
- PEDERSEN, B. K. & SALTIN, B. 2015b. Exercise as medicine - evidence for prescribing exercise as therapy in 26 different chronic diseases. *Scand J Med Sci Sports*, 25 Suppl 3, 1-72.
- PEREIRA, M. G., DYAR, K. A., NOGARA, L., SOLAGNA, F., MARABITA, M., BARALDO, M., CHEMELLO, F., GERMINARIO, E., ROMANELLO, V. & NOLTE, H. 2017. Comparative analysis of muscle hypertrophy models reveals divergent gene transcription profiles and points to translational regulation of muscle growth through increased mTOR signaling. *Frontiers in physiology*, 8, 968.
- PERRONE, C. E., FENWICK-SMITH, D. & VANDENBURGH, H. H. 1995. Collagen and stretch modulate autocrine secretion of insulin-like growth factor-1 and insulin-like growth factor binding proteins from differentiated skeletal muscle cells. *Journal of Biological Chemistry*, 270, 2099-2106.
- PETERSEN, A. M. & PEDERSEN, B. K. 2005a. The anti-inflammatory effect of exercise. *J Appl Physiol (1985)*, 98, 1154-62.
- PETERSEN, A. M. W. & PEDERSEN, B. K. 2005b. The anti-inflammatory effect of exercise. *Journal of applied physiology*, 98, 1154-1162.
- PFÄFFL, M. W. 2001. A new mathematical model for relative quantification in real-time RT-PCR. *Nucleic acids research*, 29, e45-e45.

- PHILP, A., BELEW, M. Y., EVANS, A., PHAM, D., SIVIA, I., CHEN, A., SCHENK, S. & BAAR, K. 2011. The PGC-1 α -related coactivator promotes mitochondrial and myogenic adaptations in C2C12 myotubes. *American Journal of Physiology-Regulatory, Integrative and Comparative Physiology*, 301, R864-R872.
- PHILP, A., PEREZ-SCHINDLER, J., GREEN, C., HAMILTON, D. L. & BAAR, K. 2010. Pyruvate suppresses PGC1 α expression and substrate utilization despite increased respiratory chain content in C2C12 myotubes. *American Journal of Physiology-Cell Physiology*, 299, C240-C250.
- PICKERING, W., CHENG, M.-K., BROWN, J., BUTLER, H., WALLS, J. & BEVINGTON, A. 2003. Stimulation of protein degradation by low pH in L6G8C5 skeletal muscle cells is independent of apoptosis but dependent on differentiation state. *Nephrology Dialysis Transplantation*, 18, 1466-1474.
- PINILLA, J., ALEDO, J. C., CWIKLINSKI, E., HYDE, R., TAYLOR, P. M. & HUNDAL, H. S. 2011. SNAT2 transceptor signalling via mTOR: a role in cell growth and proliferation. *Front Biosci (Elite Ed)*, 3, 1289-1299.
- POCHINI, L., SCALISE, M., GALLUCCIO, M. & INDIVERI, C. 2014. Membrane transporters for the special amino acid glutamine: structure/function relationships and relevance to human health. *Front Chem*, 2, 61.
- POWELL, C. A., SMILEY, B. L., MILLS, J. & VANDENBURGH, H. H. 2002. Mechanical stimulation improves tissue-engineered human skeletal muscle. *American Journal of Physiology-Cell Physiology*, 283, C1557-C1565.
- PRICE, S. & MITCH, W. Acidification-Induced Metabolic Responses Muscle-Cells-Stimulation of Stress-Activated Protein-Kinase Activity. JOURNAL OF THE AMERICAN SOCIETY OF NEPHROLOGY, 1995. WILLIAMS & WILKINS 351 WEST CAMDEN ST, BALTIMORE, MD 21201-2436, 1028-1028.
- PROUD, C. 2006. Regulation of protein synthesis by insulin. *Biochemical Society Transactions*, 34, 213-216.
- PSATHA, M., WU, Z., GAMMIE, F. M., RATKEVICIUS, A., WACKERHAGE, H., LEE, J. H., REDPATH, T. W., GILBERT, F. J., ASHCROFT, G. P. & MEAKIN, J. R. 2012. A longitudinal MRI study of muscle atrophy during lower leg immobilization following ankle fracture. *Journal of Magnetic Resonance Imaging*, 35, 686-695.
- RAMOS, J. W. 2008. The regulation of extracellular signal-regulated kinase (ERK) in mammalian cells. *Int J Biochem Cell Biol*, 40, 2707-19.
- RAPHAEL, K. L. 2018. Metabolic acidosis and subclinical metabolic acidosis in CKD. *Journal of the American Society of Nephrology*, 29, 376-382.
- RAUCH, C. & LOUGHNA, P. T. 2005a. Static stretch promotes MEF2A nuclear translocation and expression of neonatal myosin heavy chain in C2C12 myocytes in a calcineurin- and p38-dependent manner. *Am J Physiol Cell Physiol*, 288, C593-605.
- RAUCH, C. & LOUGHNA, P. T. 2005b. Static stretch promotes MEF2A nuclear translocation and expression of neonatal myosin heavy chain in C2C12 myocytes in a calcineurin-and p38-dependent manner. *American Journal of Physiology-Cell Physiology*, 288, C593-C605.
- RAUCH, C. & LOUGHNA, P. T. 2008a. Stretch-induced activation of ERK in myocytes is p38 and calcineurin-dependent. *Cell Biochem Funct*, 26, 866-9.
- RAUCH, C. & LOUGHNA, P. T. 2008b. Stretch-induced activation of ERK in myocytes is p38 and calcineurin-dependent. *Cell Biochemistry and Function: Cellular biochemistry and its modulation by active agents or disease*, 26, 866-869.
- REACH, D., CHANNON, S., SCRIMGEOUR, C., DALEY, S., WILKINSON, R. & GOODSHIP, T. 1993. Correction of acidosis in humans with CRF decreases protein degradation and amino acid oxidation. *American Journal of Physiology-Endocrinology And Metabolism*, 265, E230-E235.
- RINDOM, E., KRISTENSEN, A. M., OVERGAARD, K., VISSING, K. & DE PAOLI, F. V. 2019. Activation of mTORC 1 signaling in rat skeletal muscle is independent of the EC-coupling sequence but dependent on tension per se in a dose-response relationship. *Acta Physiologica*, e13336.

- RODWELL, V., BENDER, D., BOTHAM, K. M., KENNELLY, P. J. & WEIL, P. A. 2015. *Harpers Illustrated Biochemistry 30th Edition*, McGraw-Hill Education.
- ROSE, A. J. & RICHTER, E. A. 2005. Skeletal muscle glucose uptake during exercise: how is it regulated? *Physiology*, 20, 260-270.
- ROSKOSKI, R., JR. 2012. ERK1/2 MAP kinases: structure, function, and regulation. *Pharmacol Res*, 66, 105-43.
- SAKAMOTO, K. & GOODYEAR, L. J. 2002. Invited review: intracellular signaling in contracting skeletal muscle. *Journal of applied physiology*, 93, 369-383.
- SANTHANAM, U., GHAYEB, J., SEHGAL, P. B. & MAY, L. T. 1989. Post-translational modifications of human interleukin-6. *Archives of biochemistry and biophysics*, 274, 161-170.
- SANTOS, J., RIBEIRO, S., GAYA, A., APPELL, H. & DUARTE, J. 2008. Skeletal muscle pathways of contraction-enhanced glucose uptake. *International journal of sports medicine*, 29, 785-794.
- SAXENA, M., PANDEY, S., KRYWORUCHKO, M. & KUMAR, A. 2011. CpG Protects Human Monocytic Cells against HIV-Vpr-Induced Apoptosis by Cellular Inhibitor of Apoptosis-2 through the Calcium-Activated JNK Pathway in a TLR9-Independent Manner. *The Journal of Immunology*, 187, 5865-5878.
- SCHELLER, J., CHALARIS, A., SCHMIDT-ARRAS, D. & ROSE-JOHN, S. 2011. The pro-and anti-inflammatory properties of the cytokine interleukin-6. *Biochimica et Biophysica Acta (BBA)-Molecular Cell Research*, 1813, 878-888.
- SCHOENFELD, B. J. & CONTRERAS, B. 2014. The muscle pump: potential mechanisms and applications for enhancing hypertrophic adaptations. *Strength & Conditioning Journal*, 36, 21-25.
- SCHULTZ, E. & MCCORMICK, K. M. 1994. Skeletal muscle satellite cells. *Reviews of Physiology, Biochemistry and Pharmacology, Volume 123*. Springer.
- SEHGAL, S. Sirolimus: its discovery, biological properties, and mechanism of action. Transplantation proceedings, 2003. Elsevier, S7-S14.
- SEN, C. K., HANNINEN, O. & ORLOV, S. N. 1995. Unidirectional sodium and potassium flux in myogenic L6 cells: mechanisms and volume-dependent regulation. *Journal of Applied Physiology*, 78, 272-281.
- SHRESTHA, M. M. 2017. *Phosphorylation of tropomodulin3 by AMPK regulates GLUT4 translocation and glucose uptake in L6 myoblasts*. National University of Singapore (Singapore).
- SIMARD, F. A., CLOUTIER, A., EAR, T., VARDHAN, H. & MCDONALD, P. P. 2015. MEK-independent ERK activation in human neutrophils and its impact on functional responses. *Journal of leukocyte biology*, 98, 565-573.
- SLACK-DAVIS, J. K., MARTIN, K. H., TILGHMAN, R. W., IWANICKI, M., UNG, E. J., AUTRY, C., LUZZIO, M. J., COOPER, B., KATH, J. C. & ROBERTS, W. G. 2007. Cellular characterization of a novel focal adhesion kinase inhibitor. *Journal of Biological Chemistry*, 282, 14845-14852.
- SPANGENBURG, E. E. 2009. Changes in muscle mass with mechanical load: possible cellular mechanisms This paper is one of a selection of papers published in this Special Issue, entitled 14th International Biochemistry of Exercise Conference-Muscles as Molecular and Metabolic Machines, and has undergone the Journal's usual peer review process. *Applied Physiology, Nutrition, and Metabolism*, 34, 328-335.
- STARKIE, R., OSTROWSKI, S. R., JAUFFRED, S., FEBBRAIO, M. & PEDERSEN, B. K. 2003. Exercise and IL-6 infusion inhibit endotoxin-induced TNF- α production in humans. *The FASEB Journal*, 17, 884-886.
- STEENSBERG, A., FEBBRAIO, M. A., OSADA, T., SCHJERLING, P., HALL, G., SALTIN, B. & PEDERSEN, B. K. 2001a. Interleukin-6 production in contracting human skeletal muscle is influenced by pre-exercise muscle glycogen content. *The Journal of Physiology*, 537, 633-639.
- STEENSBERG, A., FISCHER, C. P., KELLER, C., MØLLER, K. & PEDERSEN, B. K. 2003. IL-6 enhances plasma IL-1ra, IL-10, and cortisol in humans. *American Journal of Physiology-Endocrinology And Metabolism*, 285, E433-E437.

- STEENSBERG, A., KELLER, C., STARKIE, R. L., OSADA, T., FEBBRAIO, M. A. & PEDERSEN, B. K. 2002. IL-6 and TNF- α expression in, and release from, contracting human skeletal muscle. *American Journal of Physiology-Endocrinology and Metabolism*, 283, E1272-E1278.
- STEENSBERG, A., VAN HALL, G., OSADA, T., SACCHETTI, M., SALTIN, B. & PEDERSEN, B. K. 2000. Production of interleukin-6 in contracting human skeletal muscles can account for the exercise-induced increase in plasma interleukin-6. *The Journal of physiology*, 529, 237-242.
- STEENSBERG, A., VISSING, J. & PEDERSEN, B. K. 2001b. Lack of IL-6 production during exercise in patients with mitochondrial myopathy. *European journal of applied physiology*, 84, 155-157.
- STILES, M. K., CRAIG, M. E., GUNNELL, S., PFEIFFER, D. & TAYLOR, R. 1991. The formation constants of ionomycin with divalent cations in 80% methanol/water. *Journal of Biological Chemistry*, 266, 8336-8342.
- STOCKDALE, F. E. & MILLER, J. B. 1987. The cellular basis of myosin heavy chain isoform expression during development of avian skeletal muscles. *Developmental biology*, 123, 1-9.
- STRETTON, C., LIPINA, C., HYDE, R., Cwiklinski, E., Hoffmann, T. M., Taylor, P. M. & HUNDAL, H. S. 2019. CDK7 is a component of the integrated stress response regulating SNAT2 (SLC38A2)/System A adaptation in response to cellular amino acid deprivation. *Biochimica et Biophysica Acta (BBA)-Molecular Cell Research*, 1866, 978-991.
- SUN, W., WU, X., GAO, H., YU, J., ZHAO, W., LU, J.-J., WANG, J., DU, G. & CHEN, X. 2017. Cytosolic calcium mediates RIP1/RIP3 complex-dependent necroptosis through JNK activation and mitochondrial ROS production in human colon cancer cells. *Free Radical Biology and Medicine*, 108, 433-444.
- SUN, Z., GUO, S. S. & FÄSSLER, R. 2016. Integrin-mediated mechanotransduction. *J Cell Biol*, 215, 445-456.
- SUZUKI, K., NAKAJI, S., YAMADA, M., TOTSUKA, M., SATO, K. & SUGAWARA, K. 2002. Systemic inflammatory response to exhaustive exercise. Cytokine kinetics. *Exercise immunology review*, 8, 6-48.
- SWEDBERG, K., CLELAND, J., DARGIE, H., DREXLER, H., FOLLATH, F., KOMAJDA, M., TAVAZZI, L., SMISETH, O. A., GAVAZZI, A. & HAVERICH, A. 2005. Guidelines for the diagnosis and treatment of chronic heart failure: executive summary (update 2005). *European heart journal*, 26, 1115-1140.
- TAYLOR, R. S., BROWN, A., EBRAHIM, S., JOLLIFFE, J., NOORANI, H., REES, K., SKIDMORE, B., STONE, J. A., THOMPSON, D. R. & OLDRIDGE, N. 2004. Exercise-based rehabilitation for patients with coronary heart disease: systematic review and meta-analysis of randomized controlled trials. *The American journal of medicine*, 116, 682-692.
- THALHAMER, T., MCGRATH, M. A. & HARNETT, M. M. 2008. MAPKs and their relevance to arthritis and inflammation. *Rheumatology (Oxford)*, 47, 409-14.
- TILLY, B. C., GAESTEL, M., ENGEL, K., EDIXHOVEN, M. J. & DE JONGE, H. R. 1996. Hypo-osmotic cell swelling activates the p38 MAP kinase signalling cascade. *Febs Letters*, 395, 133-136.
- TREXLER, E. B., BUKAUSKAS, F. F., BENNETT, M. V., BARGIELLO, T. A. & VERSELIS, V. K. 1999. Rapid and direct effects of pH on connexins revealed by the connexin46 hemichannel preparation. *The Journal of general physiology*, 113, 721-742.
- TSUZUKI, T., YOSHIHARA, T., ICHINOSEKI-SEKINE, N., KAKIGI, R., TAKAMINE, Y., KOBAYASHI, H. & NAITO, H. 2018. Body temperature elevation during exercise is essential for activating the Akt signaling pathway in the skeletal muscle of type 2 diabetic rats. *PloS one*, 13, e0205456.
- TUMANENG, K., SCHLEGELMILCH, K., RUSSELL, R. C., YIMLAMAI, D., BASNET, H., MAHADEVAN, N., FITAMANT, J., BARDEESY, N., CAMARGO, F. D. & GUAN, K.-L. 2012. YAP mediates crosstalk between the Hippo and PI (3) K-TOR pathways by suppressing PTEN via miR-29. *Nature cell biology*, 14, 1322.
- TZUR, A., MOORE, J. K., JORGENSEN, P., SHAPIRO, H. M. & KIRSCHNER, M. W. 2011. Optimizing optical flow cytometry for cell volume-based sorting and analysis. *PloS one*, 6, e16053.

- USHER-SMITH, J. A., FRASER, J. A., BAILEY, P. S., GRIFFIN, J. L. & HUANG, C. L. H. 2006. The influence of intracellular lactate and H⁺ on cell volume in amphibian skeletal muscle. *The Journal of physiology*, 573, 799-818.
- VANDENBURGH, H. H., HATFALUDY, S., KARLISCH, P. & SHANSKY, J. 1989. Skeletal muscle growth is stimulated by intermittent stretch-relaxation in tissue culture. *American Journal of Physiology-Cell Physiology*, 256, C674-C682.
- VERBRUGGE, S. A. J., WACKERHAGE, H., SCHÖNFELDER, M., NEZHAD, F. Y., BECKER, L. & HRABE DE ANGELIS, M. 2018. Genes whose gain or loss-of-function increases skeletal muscle mass in mice: a systematic literature review. *Frontiers in physiology*, 9, 553.
- VIANA, J. L., KOSMADAKIS, G. C., WATSON, E. L., BEVINGTON, A., FEEHALLY, J., BISHOP, N. C. & SMITH, A. C. 2014. Evidence for anti-inflammatory effects of exercise in CKD. *J Am Soc Nephrol*, 25, 2121-30.
- VISSING, K. & SCHJERLING, P. 2014. Simplified data access on human skeletal muscle transcriptome responses to differentiated exercise. *Scientific data*, 1, 140041.
- WACKERHAGE, H., DEL RE, D. P., JUDSON, R. N., SUDOL, M. & SADOSHIMA, J. 2014. The Hippo signal transduction network in skeletal and cardiac muscle. *Sci. Signal.*, 7, re4-re4.
- WACKERHAGE, H., SCHOENFELD, B. J., HAMILTON, D. L., LEHTI, M. & HULMI, J. J. 2018. Stimuli and sensors that initiate skeletal muscle hypertrophy following resistance exercise. *Journal of Applied Physiology*, 126, 30-43.
- WANG, Y. L., ZHANG, Y. Y., LU, C., ZHANG, W., DENG, H., WU, J. W., WANG, J. & WANG, Z. X. 2019. Kinetic and mechanistic studies of p38 α MAP kinase phosphorylation by MKK 6. *The FEBS journal*, 286, 1030-1052.
- WATSON, E. L., KOSMADAKIS, G. C., SMITH, A. C., VIANA, J. L., BROWN, J. R., MOLYNEUX, K., PAWLUCZYK, I. Z., MULHERAN, M., BISHOP, N. C. & SHIRREFFS, S. 2013a. Combined walking exercise and alkali therapy in patients with CKD4–5 regulates intramuscular free amino acid pools and ubiquitin E3 ligase expression. *European journal of applied physiology*, 113, 2111-2124.
- WATSON, E. L., KOSMADAKIS, G. C., SMITH, A. C., VIANA, J. L., BROWN, J. R., MOLYNEUX, K., PAWLUCZYK, I. Z., MULHERAN, M., BISHOP, N. C., SHIRREFFS, S., MAUGHAN, R. J., OWEN, P. J., JOHN, S. G., MCINTYRE, C. W., FEEHALLY, J. & BEVINGTON, A. 2013b. Combined walking exercise and alkali therapy in patients with CKD4-5 regulates intramuscular free amino acid pools and ubiquitin E3 ligase expression. *Eur J Appl Physiol*, 113, 2111-24.
- WATSON, K. & BAAR, K. mTOR and the health benefits of exercise. *Seminars in cell & developmental biology*, 2014a. Elsevier, 130-139.
- WATSON, K. & BAAR, K. 2014b. mTOR and the health benefits of exercise. *Semin Cell Dev Biol*, 36, 130-9.
- WATT, K. I., GOODMAN, C. A., HORNBERGER, T. A. & GREGOREVIC, P. 2018. The Hippo Signaling Pathway in the Regulation of Skeletal Muscle Mass and Function. *Exerc Sport Sci Rev*, 46, 92-96.
- WENDOWSKI, O., REDSHAW, Z. & MUTUNGI, G. 2017. Dihydrotestosterone treatment rescues the decline in protein synthesis as a result of sarcopenia in isolated mouse skeletal muscle fibres. *J Cachexia Sarcopenia Muscle*, 8, 48-56.
- WESTON, C. R. & DAVIS, R. J. 2007. The JNK signal transduction pathway. *Curr Opin Cell Biol*, 19, 142-9.
- WIDMANN, C., GIBSON, S., JARPE, M. B. & JOHNSON, G. L. 1999. Mitogen-activated protein kinase: conservation of a three-kinase module from yeast to human. *Physiological reviews*, 79, 143-180.
- WILLIAMSON, D., GALLAGHER, P., HARBER, M., HOLLON, C. & TRAPPE, S. 2003. Mitogen-activated protein kinase (MAPK) pathway activation: effects of age and acute exercise on human skeletal muscle. *J Physiol*, 547, 977-87.

- WING, M. R., RAJ, D. S. & VELASQUEZ, M. T. 2014. Protein Energy Metabolism in Chronic Kidney Disease. *Chronic Renal Disease*.
- WING, M. R., RAJ, D. S. & VELASQUEZ, M. T. 2015. Protein Energy Metabolism in Chronic Kidney Disease. *Chronic Renal Disease*. Elsevier.
- WINZER, E. B., WOITEK, F. & LINKE, A. 2018. Physical activity in the prevention and treatment of coronary artery disease. *Journal of the American Heart Association*, 7, e007725.
- WORLD HEALTH ORGANIZATION 2014. Global Burden of Disease
- YAFFE, D. 1968. Retention of differentiation potentialities during prolonged cultivation of myogenic cells. *Proceedings of the National Academy of Sciences*, 61, 477-483.
- YAMASAKI-MANN, M., DEMURO, A. & PARKER, I. 2009. cADPR stimulates SERCA activity in *Xenopus* oocytes. *Cell calcium*, 45, 293-299.
- YANO, S., MORINO-KOGA, S., KONDO, T., SUICO, M. A., KOGA, T., SHIMAUCHI, Y., MATSUYAMA, S., SHUTO, T., SATO, T. & ARAKI, E. 2011. Glucose uptake in rat skeletal muscle L6 cells is increased by low-intensity electrical current through the activation of the phosphatidylinositol-3-OH kinase (PI-3K)/Akt pathway. *Journal of pharmacological sciences*, 115, 94-98.
- YEO, E.-S., HWANG, J.-Y., PARK, J. E., CHOI, Y. J., HUH, K. B. & KIM, W. Y. 2010. Tumor necrosis factor (TNF- α) and C-reactive protein (CRP) are positively associated with the risk of chronic kidney disease in patients with type 2 diabetes. *Yonsei medical journal*, 51, 519-525.
- YOU, J.-S., LINCOLN, H. C., KIM, C.-R., FREY, J. W., GOODMAN, C. A., ZHONG, X.-P. & HORNBERGER, T. A. 2014. The role of diacylglycerol kinase ζ and phosphatidic acid in the mechanical activation of mammalian target of rapamycin (mTOR) signaling and skeletal muscle hypertrophy. *Journal of Biological Chemistry*, 289, 1551-1563.
- YU, J.-G., LIU, J.-X., CARLSSON, L., THORNELL, L.-E. & STÅL, P. S. 2013. Re-evaluation of sarcolemma injury and muscle swelling in human skeletal muscles after eccentric exercise. *PLoS one*, 8, e62056.
- ZHAN, M., JIN, B., CHEN, S. E., REECY, J. M. & LI, Y. P. 2007. TACE release of TNF- α mediates mechanotransduction-induced activation of p38 MAPK and myogenesis. *J Cell Sci*, 120, 692-701.
- ZHANG, Y. Y., YANG, M., BAO, J. F., GU, L. J., YU, H. L. & YUAN, W. J. 2018. Phosphate stimulates myotube atrophy through autophagy activation: evidence of hyperphosphatemia contributing to skeletal muscle wasting in chronic kidney disease. *BMC Nephrol*, 19, 45.
- ZHANG, Z., GAMEIRO, A. & GREWER, C. 2008. Highly conserved asparagine 82 controls the interaction of Na⁺ with the sodium-coupled neutral amino acid transporter SNAT2. *Journal of Biological Chemistry*, 283, 12284-12292.
- ZHANG, Z. & GREWER, C. 2007. The sodium-coupled neutral amino acid transporter SNAT2 mediates an anion leak conductance that is differentially inhibited by transported substrates. *Biophysical journal*, 92, 2621-2632.
- ZOU, K., MEADOR, B. M., JOHNSON, B., HUNTSMAN, H. D., MAHMASSANI, Z., VALERO, M. C., HUEY, K. A. & BOPPART, M. D. 2011. The $\alpha 7\beta 1$ -integrin increases muscle hypertrophy following multiple bouts of eccentric exercise. *Journal of Applied Physiology*, 111, 1134-1141.